

**Development of the biotechnological production
of (+)-zizaene: Enzymology, metabolic
engineering and in situ product recovery**

Von der Naturwissenschaftlichen Fakultät der
Gottfried Wilhelm Leibniz Universität Hannover

zur Erlangung des Grades

Doktor der Naturwissenschaften (Dr. rer. nat.)

genehmigte Dissertation

von

Francisco José Aguilar Cascante, M. Sc.

2019

Referent: Prof. Dr. rer. nat. Thomas Scheper

Korreferent: PD Dr. rer. nat. Sascha Beutel

Tag der Promotion: 11.12.2019

Acknowledgments

I would like to thank my *Doktor Vater*, Prof. Dr. Thomas Scheper for the opportunity to perform the doctoral study in the Institute of Technical Chemistry – TCI in such a fascinating and interesting research field. His advice and insights were very beneficial for this work.

A very special thanks to my supervisor PD. Dr. Sascha Beutel for the many hours used for the guidance, assistance and discussions provided in all the aspects surrounding this doctoral study. His support enhanced significantly the quality of the academic process, *Pura Vida Sascha!*

I thank PD. Dr. Ulrich Krings for his insights on many aspects of this investigation. Additional greetings to Daniel Sandner and the staff of the Institute of Food Chemistry – LCI for the assistance provided for the GC-MS measurements.

Special greetings to Martina Weiß for the training in chromatography and support in the daily issues in the laboratory. Additional thanks to Martin Pähler for the support in the molecular biology work. I would like to acknowledge the support from Ulrike Dreschel in the administrative processes and Dr. Ivo Havlik in the IT solving. Additional thanks to Friedbert Gellerman for his creativity in the construction of the expanded bed adsorption column. Special thanks to M.A. Zoë Vercelli from the FSZ for the peer review.

I would like to thank the colleges involved in the Terpene research group for the support and discussions from M.Sc. Kimia Ekramzadeh and Dr. Semra Alemdar. Additional thanks for the support in *Technikum* to Dr. Ingo de Vries and Dr. Bastian Quaas. Thanks to all the students who supported this investigation, especially to Kai Pandera, Daniela Santamaría, Lukas Koch and Samuel Edward Hakim. Special thanks to the TCI post-docs Dr. Christian Ude and Dr. Zhaopeng Li for providing advice in technical and protein-expression aspects involved in this study, it is greatly appreciated!

Thanks to Dr. Anibal Mora and the former members of the CENIBiot, Dr. Ginas Porras, Eng. Iray Mata and Eng. Luis Porras, as well as Prof. Dr. An-Ping Zeng and Prof. Dr. Andreas Liese from TUHH, for the support in the Terpene Project between CR-Germany.

I acknowledge the funding from the PINN program from the Ministry of Science, Technology and Telecommunications of Costa Rica – MICITT for the doctoral scholarship. I would like to thank Dr. Sergio Madrigal-Carballo for the support in the scholarship application process and his interest in the inter-institutional collaboration.

Thanks to the people of the TCI for all the support and the fun time during these years! Especially, for the group of my office Marcel, Daniel, Caro, Marc, Ferdi and Chris, as well as other TCItler`s Harsh, Basti, Nina, Basti B., Ingo, Tonya, Ileana, Florian, Jens and Tammi.

Very special thanks to my Costarrican friends in the distance Ronald, Allan, Shena, Nola, Pla, Monserat, Pablo and more in which one way or the other have contributed to my life.

Deepest thanks to my family for their constant support; my father Justo Aguilar for his constant advice; my mother Ana Cascante for her love and support; my brothers Andres, Paulo and Sergio for all the good times; my German family; and last but not least, my wife Linda for all her love, time and dedication, but overall, for embracing this journey with me called life!

Abstract

The sesquiterpene (+)-zizaene is the immediate precursor of khusimol, the main compound of the vetiver essential oil from the vetiver grass, which grants its characteristic woody scent. Among its distinct applications, this oil is relevant for the formulation of cosmetics and used in approximately 20% of all men's perfumery. The traditional supply of the vetiver essential oil had suffered shortages due to natural disasters. Consequently, the biotechnological production of khusimol is an alternative towards a more reliable supply. In this study, we provide new insights towards the microbial production of khusimol by characterizing the zizaene synthase, engineering the metabolic pathway of (+)-zizaene in *Escherichia coli* and analyzing the in situ recovery of (+)-zizaene from fermentation.

In the first chapter, the zizaene synthase, the critical enzyme for khusimol biosynthesis, was characterized. A SUMO-fused zizaene synthase variant was overexpressed in *E. coli*, and in vitro reactions yielded 90% (+)-zizaene. Furthermore, enzyme characterization comprised enzyme kinetics, optimal reaction conditions, substrate specificity and reaction mechanisms. The in vitro reactions showed high stability through varying pH and temperature values. By in silico docking model, this was explained due to the hydrophobicity of the surrounding loops, which stabilized the closed conformation of the active site.

The second chapter addressed the metabolic engineering of the (+)-zizaene biosynthetic pathway in *E. coli*. A systematic strategy was applied by modulating the substrate FDP and the zizaene synthase to improve the zizaene titers. The optimal (+)-zizaene production was reached by engineering the mevalonate pathway and two copies of the zizaene synthase into a multi-plasmid strain. Optimization of the fermentation conditions such as IPTG, media, pH and temperature improved the production further, achieving a (+)-zizaene titer of 25 mg L⁻¹.

In the third chapter, the in situ recovery of (+)-zizaene from fermentation was analyzed. Initially, liquid-liquid phase partitioning cultivation improved the (+)-zizaene recovery at shake flask scale. Subsequently, solid-liquid phase partitioning cultivation was evaluated by screening polymeric adsorbers, where Diaion HP20 obtained the highest recovery ratio. The bioprocess was scaled up to 2 L fed-batch bioreactors by integrating in situ recovery and fermentation. External and internal (with and without gas stripping) recovery configurations were tested, where the internal configuration obtained the highest (+)-zizaene recovery of all, achieving a (+)-zizaene titer of 211.13 mg L⁻¹ and a productivity of 3.2 mg L⁻¹ h⁻¹.

Key words: (+)-zizaene, zizaene synthase, khusimene, khusimol, vetiver essential oil, *Chrysopogon zizanioides*, in situ product recovery, polymeric adsorbers.

Kurzfassung

Das Sesquiterpen (+)-Zizaen ist der unmittelbare Vorläufer von Khusimol, der Hauptverbindung des ätherischen Öls aus dem Vetivergras, das seinen charakteristischen holzigen Geruch verleiht. Neben verschiedenen weiteren Anwendungen wird dieses Öl in ungefähr 20% aller Männerparfüme verwendet.

Die traditionelle Versorgung mit ätherischen Ölen litt aufgrund von Naturkatastrophen unter Engpässen. Folglich ist die biotechnologische Herstellung von Khusimol eine Alternative für eine zuverlässigere Versorgung. In dieser Studie wird die mikrobielle Produktion von Khusimol charakterisiert, indem die Zizaensynthase charakterisiert, der Stoffwechselweg von (+)-Zizaen in *E. coli* bestimmt und die in situ-Gewinnung von (+)-Zizaen aus der Fermentation analysiert wird.

Im ersten Kapitel wird die Zizaensynthase, das kritische Enzym für die Khusimol-Biosynthese, eingehend charakterisiert. Eine in *E. coli* überexprimierte SUMO-kondensierte Zizaensynthase-Variante und in-vitro-Reaktionen ergaben 90% (+)-Zizaen. Weiterhin wurden Enzymcharakterisierung, optimale Reaktionsbedingungen, Substratspezifität und Reaktionsmechanismen analysiert. Die in vitro-Reaktion zeigte eine hohe Stabilität bei unterschiedlichen pH- und Temperaturwerten. Im silico-Docking-Modell wurde dies aufgrund der Hydrophobizität der umgebenden Schleifen erklärt, die die geschlossene Konformation des aktiven Zentrums stabilisierten.

Das zweite Kapitel befasst sich mit dem metabolischen Engineering des (+)-Zizaen-Biosynthesewegs in *E. coli*. Eine systematische Strategie wurde angewendet, indem das Substrat FDP und die Zizaensynthase moduliert wurden, um den Zizaentiter zu verbessern. Die optimale (+)-Zizaen-Produktion wurde erreicht, indem der Mevalonat-Weg und zwei Kopien der Zizaen-Synthase in einen Multiplasmid-Stamm umgewandelt wurden. Eine weitere Optimierung der Fermentationsbedingungen wie IPTG, Medium, pH und Temperatur verbesserte die Produktion und erreichte einen (+)-Zizaen-Titer von 25 mg L⁻¹.

Im dritten Kapitel wurde die in situ-Gewinnung von (+)-Zizaen aus der Fermentation analysiert. Anfänglich wurde die Flüssig-Flüssig Extraktion für die (+)-Zizaen Gewinnung im Schüttelkolbenmaßstab untersucht. Anschließend wurde die Isolierung von (+)-Zizaene mit der Fest-Flüssig Extraktion untersucht, wofür polymere Adsorber gescreent wurden; Diaion HP20 erzielte bei die höchste Produktivität. Der Bioprozess wurde durch Integration von in situ Gewinnung und Fermentation auf 2 l Bioreaktoren skaliert. Die höchste (+)-Zizaen Gewinnung ergab in Ansatz mit direkter Adsorberrückgewinnung während des Fermentation mit einem (+)-Zizaen Titer von 211,13 mg L⁻¹ und einer Produktivität von 3,2 mg L⁻¹ h⁻¹.

Schlüsselwörter: (+)-Zizaen, Zizaensynthase, Khusimen, Khusimol, ätherisches Vetiveröl, *Chrysopogon zizanioides*, In-situ-Produktrückgewinnung, polymere Adsorber.

Contents

Acknowledgments	i
Abstract	iii
Kurzfassung.....	iv
Abbreviations	vi
1. INTRODUCTION	1
2. SCOPE OF THE INVESTIGATION.....	3
3. THEORETICAL BACKGROUND	4
3.1. General aspects of isoprenoids	4
3.2. Terpene biosynthesis	5
3.3. Biological roles of terpenes	8
3.4. Industrial application of terpenes	10
3.5. Essential oils in the cosmetic industry.....	10
3.6. Vetiver essential oil	11
3.7. The fragrant sesquiterpene Khusimol	13
3.8. The direct-precursor of khusimol, (+)-zizaene	14
3.9. Production of fragrant terpenes by metabolically engineered microorganisms	14
3.10. Downstreaming of terpenes.....	15
4. EXPERIMENTAL RESEARCH	17
CHAPTER 1	19
CHAPTER 2	33
CHAPTER 3	50
5. CONCLUDING REMARKS	72
6. OUTLOOK AND RECOMMENDATIONS.....	74
7. REFERENCES	76
APPENDIX.....	81
I. Publications and academic activities	81
II. Curriculum Vitae.....	83

Abbreviations

ADM	Aparicio defined media
Bp	Base pairs
BSA	Bovim serum albumina
DCW	Dry cell weight
DMAPP	Dimethylallyl diphosphate
DNB	Defined non-inducing broth
dNTP	Deoxynucleotide triphosphates
DTT	Dithiothreitol
EBA	Expanded bed adsorption
<i>E. coli</i>	<i>Escherichia coli</i>
ERC	External recovery configuration
FAD	Flavin adenine dinucleotide
FDP	Farnesyl diphosphate
FID	Flame ionization detector
FMN	Flavin mononucleotide
FPLC	Fast protein liquid chromatography
GC	Gas chromatography
GDP	Geranyl diphosphate
GGDP	Geranylgeranyl diphosphate
IF	Insoluble protein fraction
IMAC	Immobilized metal affinity chromatography
IPP	Isopentenyl diphosphate
IPTG	Isopropyl- β -D-1-thiogalactopyranoside
IRC	Internal recovery configuration
IRC+GS	Internal recovery configuration with gas stripping
IRES	Internal ribosome entry site
kDa	Kilo dalton
LB	Lysogeny broth
LLPPC	Liquid-liquid phase partitioning culture
M	Molecular marker
M9	Minimal 9 media
MEP	Methylerythritol phosphate
MEV	Mevalonate
MOPS	3-(N-morpholino) propanesulfonic acid
MS	Mass spectrometry
MW	Molecular weight
NDP	Neryl diphosphate

OD ₆₀₀	Optical density at 600 nm
PAGE	Polyacrylamide gel electrophoresis
PCR	Polymerase chain reaction
PI	Pearson coefficient
PP _i	Phosphate moiety
pO ₂	Dissolved oxygen
rpm	Revolutions per minute
RI	Retention index
SDS	Sodium dodecyl sulfate
SF	Soluble protein fraction
SLPPC	Solid-liquid phase partitioning culture
SUMO	Small ubiquitin-like modifier
STP	Sesquiterpene cyclase
TB	Terrific broth
TEMED	Tetramethylethylenediamin
TPS	Terpene synthase
UV	Ultraviolet
VEO	Vetiver essential oil
vvm	Vessel volume per minute
Y _{P/S}	Yield of product between substrate
Y _{P/X}	Yield of product between cells
Y _{X/S}	Yield of cells between substrate
ZS	Zizaene synthase

1. Introduction

The vetiver essential oil (VEO) extracted from the roots of the vetiver grass *Chrysopogon zizanioides*, also called “Ruh-Khus”, is a “Perfume of its own right” [1], due to its pleasant dark woody scent, defined by Morris as “the gift of India to the world of perfumes” [2].

The VEO is comprised by a complex mixture of components, mainly sesquiterpenes and their hydroxylated derivatives, which provides a viscous essential oil with a low volatilization rate, high solubility in alcohol, and is used for the formulation of the Majmua Indian perfume and in nearly 20% of men’s perfumes [1]. In the Western world, the VEO is the basis for many cosmetics such as Guerlain Vetiver, Chanel No. 5, Caleche and Parure.

The traditional production of VEO is by steam distillation of vetiver roots of 1–2 m in length and after 12–18 months of cultivation. Commonly, the extraction rate is roughly 0.2–3% by steam distillation and 4% by supercritical fluid extraction. The most important producers in the world are Haiti, Indonesia, India, China and Brazil with a world market size of 300–350 tons per year.

In recent years, the VEO supply has suffered shortages from its main producer, Haiti, due to earthquakes, floods and political unrest. Additionally, the extensive land use for the vetiver grass plantations has raised the environmental pressure due to the reduction of the natural forests. Consequently, the demand for VEO has risen considerably with an expected market of USD 169.5 million to be reached in 2022. To meet this demand, different alternatives are being considered to produce the aromatic compounds of VEO and mimic its woody smell. Among others, khusimol, α -vetivone and β -vetivone are the main fragrant sesquiterpenes which have not yet been produced successfully by traditional chemical synthesis. Therefore, the production of khusimol by metabolically engineered microorganisms has gained interest from the cosmetic and academic sector; this is especially because khusimol is the main constituent of VEO and it grants the characteristic woody vetiver note.

Recent advances in the engineering of the mevalonate (MEV) and methylerythritol phosphate (MEP) pathway, as well as current progress in the heterologous expression and characterization of terpene synthases have made possible the industrialized production of terpenes. As an example, the high-valued cosmetic oil squalane is produced by a semi-biotechnological process, through the microbial production of the precursor β -farnesene, which is further chemically hydrogenated to squalane. Such a strategy has proven valuable because the traditional source of squalane originates from shark livers, and it has raised great concern by environmental authorities.

1. Introduction

Similar to the squalane production strategy, the production of the direct precursor of khusimol, the tricyclic sesquiterpene (+)-zizaene, could also be achieved by a biotechnological process and then, further hydroxylated to khusimol. This process could be advantageous by reducing the production costs using an economical carbon source. Moreover, it could provide a reliable and sustainable supply of fragrant sesquiterpenes through all the seasons to the cosmetic industry from renewable resources.

2. Scope of the investigation

The main goal of this dissertation is to provide new insights from basic to applied research in the production of (+)-zizaene by a microbial platform towards the production of the fragrant sesquiterpene khusimol.

As a starting point, the first specific goal is to characterize the zizaene synthase by biochemical methods to build the basis towards the metabolic engineering of (+)-zizaene. This enzyme is crucial in the (+)-zizaene biosynthesis and the enzymology study will comprise the enzyme kinetics, reaction conditions, substrate specificity, reactions mechanisms and catalytical conformation changes.

The second goal is to engineer the metabolic pathway of (+)-zizaene in *E. coli* as host by optimizing the FDP and zizaene synthase pathway to improve the (+)-zizaene titers. Additionally, the study will optimize the fermentation conditions and evaluate distinct *E. coli* B strains to further improve the (+)-zizaene titers.

The last goal is to integrate the in situ product recovery and fermentation by different fed batch bioreactor configurations to enhance the microbial production of (+)-zizaene. For that, the loss of (+)-zizaene by volatilization will be initially studied, as well as the liquid-liquid phase partitioning cultivation. Moreover, distinct polymeric adsorbers will be screened and the (+)-zizaene recovery will be measured. Finally, distinct bioreactor configurations will be tested at 2 L stirred-tank bioreactor scale with integrated in situ product recovery.

3. Theoretical background

3.1. General aspects of isoprenoids

Isoprenoids are the largest family of natural products, consisting of more than 40,000 molecules, structured as hydrocarbon skeletons and their oxygenated derivatives as alcohols, lactones, aldehydes and ketones [3,4]. The term “terpene” originates from the studies of Otto Wallach (1847-1931), who studied the components of pine tree resins from and observed that the thermal decomposition of turpentine and derived monoterpenes yielded the basic C₅ “isoprene unit” (2-methyl-1,3-butadiene) [5]. Isoprenoids, also called terpenoids or terpenes, are synthesized by the condensation of C₅ isoprene units from head-to-tail, also referred as the “isoprene rule” defined by Leopold Ruzicka in 1953, in which terpenes diversify into hundreds of hydrocarbon structures (Figure 1) [6].

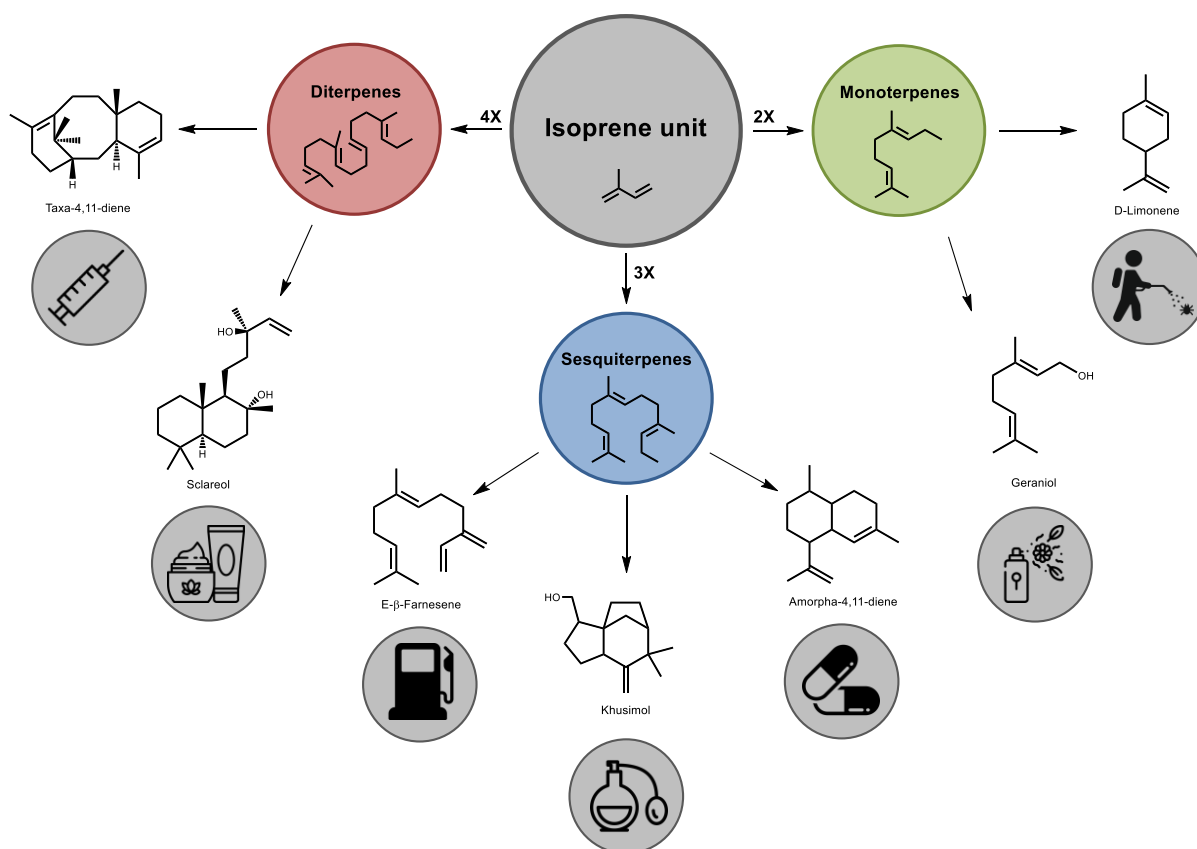


Figure 1. Terpene structures originating from C₅ isoprene unit blocks diversify into numerous variants with broad industrial applications.

There are few terpenes that display a linear head-to-tail structure as depicted in Figure 2, whereas triterpenes and tetraterpenes are condensed from two units of sesquiterpene and diterpenes respectively in a tail-to-tail fashion. In most of the cases, terpenes are structured as non-linear cyclic hydrocarbons to deliver an assortment of complex and stereo-specific arrangements [7].

3. Theoretical background

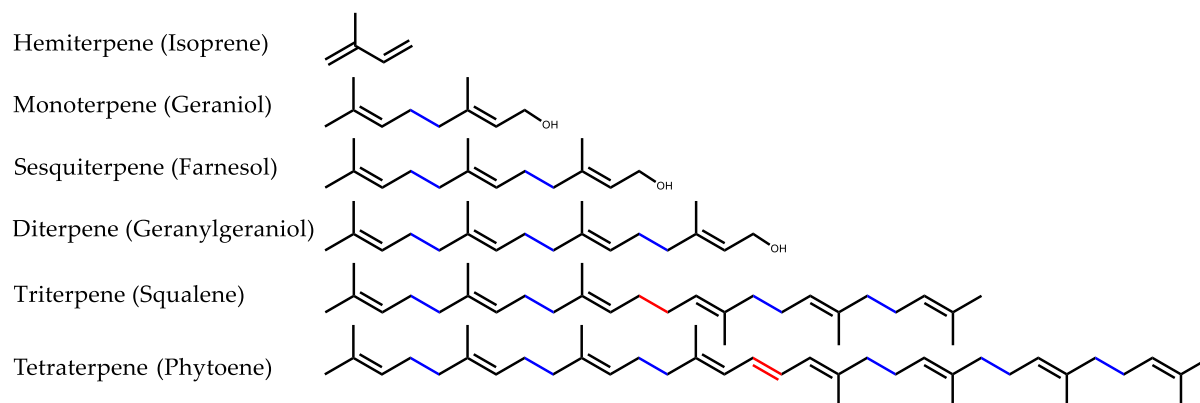


Figure 2. Building of terpenes by condensation of isoprene units according to their family. Blue bonds: Head-to-tail. Red bonds: Tail-to-tail [7].

Terpenes are classified into 6 families according to their number of isoprene units and carbon atoms, which in turn defines the specific terpene prefix, as shown in Table 1. The prenyl transferases are responsible for the specific number of isoprene units for each terpene family, by catalyzing with great specificity a particular prenyl diphosphate for each terpene family [8].

Table 1. Isoprenoid families according to their isoprene units and precursors.

Terpene Prefix	Carbon Atoms	Isoprene units	Terpene Precursor	Synthase Class
Hemi-	5	1	IPP/DMAPP	I
Mono-	10	2	GDP	I
Sesqui-	15	3	FDP	I
Di-	20	4	GGDP	I,II
Tri-	30	6	<u>FDP</u>	II
Tetra-	40	8	<u>GGDP</u>	II

Underlined terpene precursors are built by condensing 2 units of specific prenyl diphosphates.

3.2. Terpene biosynthesis

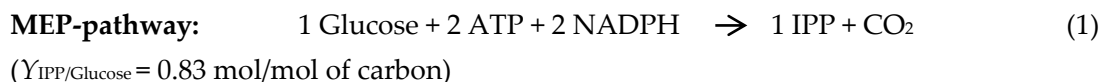
The biosynthesis of isoprenoids can be divided into four stages, starting from the glycolysis, which converts either C₅ or C₆ sugars, such as glucose, yielding the intermediates glyceraldehyde 3-phosphate (GAP), pyruvate and acetyl-CoA [4] (Figure 3). Eventually, these compounds are required for other metabolic routes such as the TCA-cycle for acetyl-CoA. However, these intermediates are crucial for terpene biosynthesis and are the starting point of the second biosynthetic stage by two independent pathways, the mevalonate (MEV) pathway and the methylerythritol phosphate (MEP) pathway [9].

3. Theoretical background

The MEV-pathway was the first characterized pathway for terpene biosynthesis and it is ubiquitous in the cytosol of eukaryotic cells [9]. The starting point is acetyl-CoA, which is catalyzed through an enzymatic cascade by acetoacetyl-CoA thiolase (*AACT*), hydroxymethylglutaryl-CoA synthase (*HMGS*) and hydroxymethylglutaryl-CoA reductase (*HMGR*) to yield mevalonate. Further processing by mevalonate kinase (*MK*), phosphomevalonate kinase (*PMK*), and mevalonate diphosphate decarboxylase (*MPDC*) leads to the isoprene unit precursors isopentenyl diphosphate (*IPP*), which is isomerized to dimethylallyl diphosphate (*DMAPP*) by the isopentenyl diphosphate (*Idi*) [10].

On the other hand, the MEP-pathway was characterized in the early 90s by Rohrer and co-workers [11], and is found in prokaryotes and plant plastids. The MEP-pathway requires two initial intermediates, GAP and pyruvate, which are condensed by the deoxyxylulose phosphate synthase (*Dxs*) to yield 1-Deoxy-D-xylulose 5-phosphate (*DXP*). Furthermore, *DXP* is catalyzed by the reductoisomerase (*Dxr*) to yield 2-C-Methyl-D-erythritol 4-phosphate and undergoes further into a multi-enzyme reaction (*MCT*, *CMK*, *MDS*, *HDS* and *HDR*) that leads to the formation of *IPP* and *DMAPP* [12].

In phototrophic organisms, both MEP and MEV-pathways converge for the exchange of *IPP/DMAPP* and other intermediates by a dynamic cross-regulation or crosstalk from plastids to cytoplasm and vice versa [10].



When comparing both pathways, the MEP-pathway is more efficient than the MEV-pathway for carbon utilization, disregarding metabolism energetics, whereas 1 mol of glucose yields 1 *IPP* and with a higher carbon theoretical yield of 0.83 c mol/c mol (Equations 1 and 2) [13]. On the contrary, MEV-pathway is more efficient than the MEP-pathway in terms of energetics by producing *NADPH* and *NADH*. Consequently, both pathways are relevant and plants commonly use both pathways to respond promptly to environmental changes [14].

The third stage for terpene biosynthesis is the catalyzation of the isoprene units *IPP/DMAPP* to yield the basic terpene substrates. For that, *DMAPP* is condensed by prenyl transferases with one or more units of *IPP*, which leads to prenyl diphosphates of distinct isoprene chain lengths [13].

3. Theoretical background

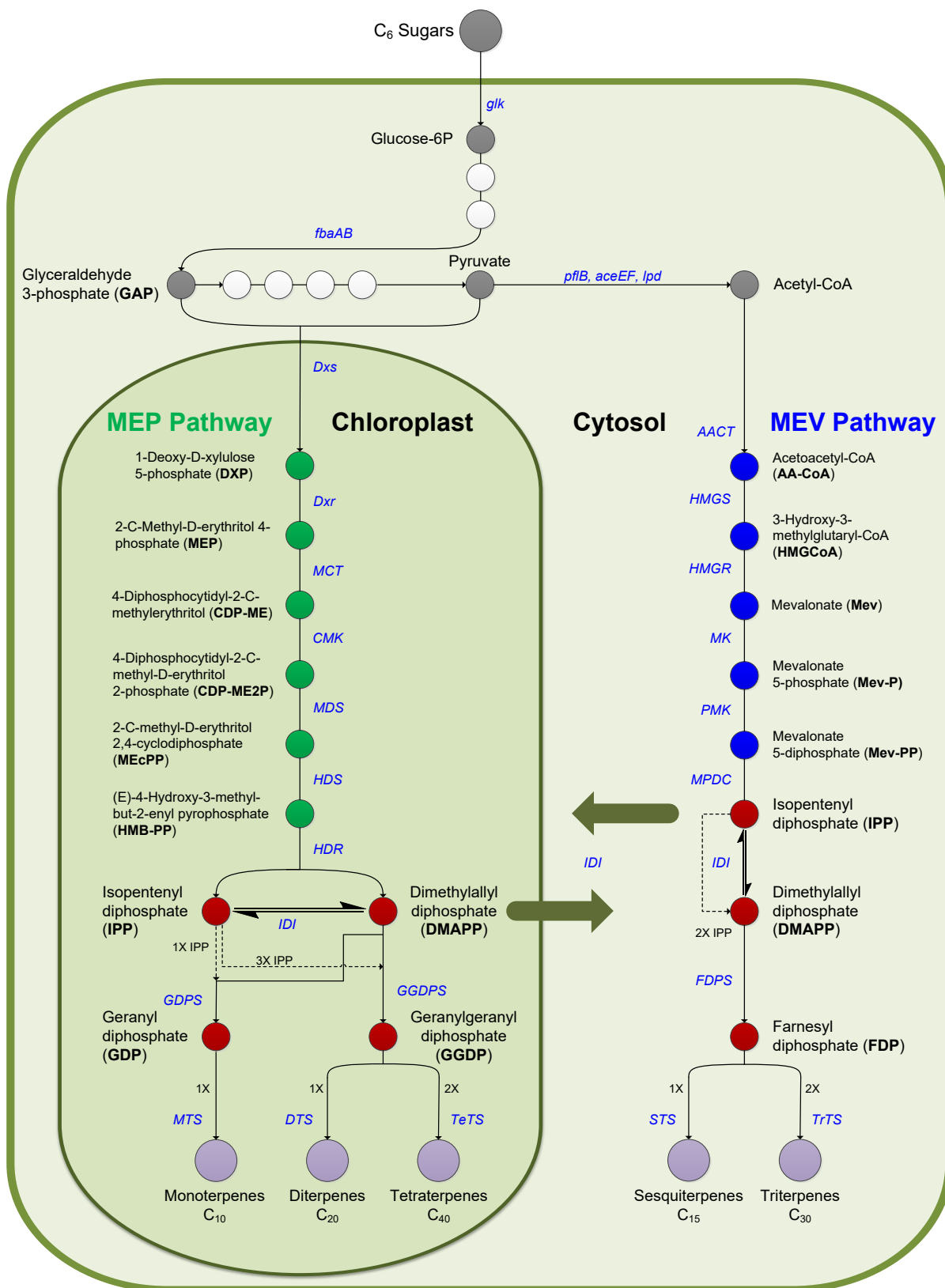


Figure 3. Biosynthetic pathway of terpenes in plant cells initiating from glucose to terpenes, divided into four stages: glycolysis (grey circles); MEP and MEV-pathway (green and blue circles); diphosphate prenylation for terpene substrates (red circles); terpene catalyzation by TPS (purple circles).

According to Figure 3, prenyl transferases catalyze the formation of terpene substrates: geranyl diphosphate (GDP)(1 DMAPP + 1 IPP), farnesyl diphosphate (FDP)(1 DMAPP + 2 IPP) and geranylgeranyl diphosphate (GGDP)(1 DMAPP + 3 IPP).

The last stage comprises the most variable and broad step, where terpene substrates are catalyzed by metal-dependent terpene synthases (TPS) for the formation of hundreds of acyclic and cyclic terpene variants. In detail, prenyl diphosphate substrates bind to metal ion cofactors, mostly Mg^{2+} , that are bound to aspartate rich motifs positioned in the docking site of the TPS [15]. The isoprenoid diphosphate substrate undergoes ionization and the prenyl tail is cleaved from the diphosphate moiety (PP_i) and is pulled into the active site cavity of the TPS. Hereafter, a series of carbocations takes place as the aromatic rings from the active site chaperone stereospecific rearrangements such as alkyl and methyl shifts until quenching occurs by deprotonation, resulting in a vast variety of terpene structures [16].

In addition, monoterpene and sesquiterpene synthases are characterized with the class I fold in the α -helix, whereas diterpenes synthases include the class I and/or class II folds in the α and β helices respectively [17]. In consequence, the condensation of 2 units of FDP yields the formation of C_{30} triterpenes and 2 units of GDP lead to C_{40} tetraterpenes [18].

Terpenes can undergo further modifications such as hydroxylations by cytochrome P450 monooxygenases. In plants, these membrane enzymes are anchored in the endoplasmic reticulum (ER) and operate together with cytochrome reductases and cofactors such as flavin adenine dinucleotide (FAD) and flavin mononucleotide (FMN) to provide a reducing regeneration system through a NADPH or NADH supply [19].

3.3. Biological roles of terpenes

Terpenes are found in all living organisms; however, they are found predominantly in the plant kingdom, functioning as primary and secondary metabolites. Primary metabolism terpenes are related to plant growth functions (cell division, elongation and inhibition), like plant hormones, which include gibberellins (C_{20}), brassinosteroids (C_{30}), abscisic acid and strigolactones [20].

Due to their structural variety, terpene elements, like isoprene C_5 units, form part of the structure of many natural products such as vitamins, phenolics and alkaloids [5]. Likewise, cytokinins are formed of an isoprene C_5 unit side chain; abscisic acid is synthesized originally from a sesquiterpene backbone and strigolactones are the product of the cleavage of diterpene carotenoids [20]. Moreover, terpene elements can decorate proteins with long linear farnesyl or geranylgeranyl chains that bind to cysteine residues, enhancing the molecules' hydrophobicity and serve as transport tags to anchor into cell membranes [6].

Despite the importance of primary metabolism terpenes as structural elements, secondary metabolism terpenes play a critical role for plant interaction with the environment and enable

3. Theoretical background

plants to respond properly to biotic and abiotic stresses [4]. A case for abiotic stress is isoprene, which protects leaves against high temperatures due to ozone-induced oxidative damage in tobacco plants [21]. Similarly, carotenoids (C₄₀), which are red, orange or yellow pigments, are involved in tissue protection against oxidation due to high light exposition by preventing the accumulation of damaging radical oxygen species (ROS) [22]. An additional function of carotenoids is to attract insects to flowers for further pollen dispersal [22]. Nevertheless, most terpenes are recognized for their role against biotic stresses such as phytopathogens due to their antimicrobial properties [23]. Thus, terpenes are produced in most of the plant organs as the first line of defense; consequently, there are many reports of terpenes as insecticides, bactericides, fungicides, and nematocides as described in Table 2. Due to their volatile properties, terpenes are well known natural products for flavors and fragrances, which in nature play an important function as signals for communication within plants, to repel dangerous insects, or to attract predatory insects against other harmful insects [23].

Table 2. Biological roles of selected terpenes from plant origin

Function	Plant organ	Terpene	Plant	Reference
Abiotic stress				
Light and thermal protection	Leaves	Isoprene	<i>Populus alba</i>	[21]
Light and thermal protection	Leaves	Zeaxanthin	<i>Hordeum vulgare</i>	[24]
Biotic stress				
Insecticide	Seeds	Azadiractin	<i>Azadirachta indica</i>	[20]
Insecticide	Foliar trichomes	Menthol and neomenthol	<i>Mentha x piperita</i> L.	[25]
Insecticide	Roots	Rhizathalene	<i>Arabidopsis thaliana</i>	[26]
Bactericide	Flowers	(E)- β -Caryophyllene	<i>Arabidopsis thaliana</i>	[27]
Fungicide	Leaves	Cineole and citronellol	<i>Eucalyptus globulus</i> and <i>E. citriodora</i>	[28]
Repellent	Foliar trichomes	E- β -farnesene	<i>Solanum berthaultii</i>	[29]
Repellent	Leaves	(S)-Linalool	<i>Fragaria x anannasa</i> cv. Elsanta	[30]
Flavoring	Leaves	Geraniol	<i>Ocimum basilicum</i> L. cv. Sweet Dani	[31]
Attract pollinators	Flowers	S-linalool and 8-hydroxylinalool	<i>Clarkia breweri</i>	[32]

3.4. Industrial application of terpenes

Terpenes are used currently in numerous applications in different industrial sectors. The pharmaceutical industry uses terpenes as active pharmaceutical ingredients (API) such as taxa-4, 11-diene, perillyl alcohol, zerumbone and geraniol for the formulation of pharmaceuticals. Likewise, the terpenes isoprene and α/β -pinene are used for rubber and resin precursors respectively for the chemical industry.

Due to their pesticide properties, many terpenes are used in agriculture for organic control, such as limonene (insecticide), geraniol (repellent), farnesene (aphid repellent), linalool (predator attractant), and E- β -caryophyllene (pathogen resistance) [27].

Terpenes such as β -farnesene, are used recently as renewable fuel for the airplane industry, which is produced by microbial platforms [33]. The most notorious application of terpenes is for flavors and fragrances by using essential oils or purified terpenes such as limonene, menthol, eucalyptol, nootkatone and applying them in house-cleaning and cosmetic formulations (Figure 1) [23].

3.5. Essential oils in the cosmetic industry

The cosmetic industry is a broad market consisting of diverse products such as color cosmetics (make-up), skincare, hair care, hygiene products, men's grooming, and fragrances, reaching a global market of USD 525.33 billion for 2018 and with an expected growth for cosmetic ingredients of USD 26.8 billion for 2020 [34].

Essential oils represent an important share for cosmetic ingredients in which 29% of the total essential oil production is directed for fragrances, aromatherapy and cosmetic ingredients; holding a global market of USD 6 billion for 2017, with an expected growth of USD 10 billion for 2020 [35]. The most economically relevant essential oils in the worldwide market are orange, corn mint, eucalyptus and peppermint [36].

An important share of the essential oils market is directed towards the formulation of perfumes due to their fragrant volatiles. Essential oils are constituted of lipophilic and non-polar molecules, mainly fragrant terpenes, and are used at low concentrations in perfume formulations [37]. Consequently, each essential oil grants a specific scent note to the formulation; whereas top notes are light scents lasting 5–10 min, middle notes grant prominent scents lasting several hours and base notes bring deeper fragrances and last the longest [38].

Table 3. Essential oils of plant origin used in perfumery according to their scent note [38].

Top note	Middle note	Base note
Basil	Black pepper	Amyris
Bergamot	Cassia	Lavender
Citronella	Chamomile	Balsam
Coriander	Cinnamon	Cedarwood
Eucalyptus	Clove	Jasmine
Ginger	Cypress	Myrrh
Lemon	Marjoram	Patchouli
Orange (Neroli)	Pine	Rosewood
Peppermint	Rose	Sandalwood
Spearmint	Rosemary	Vetiver
Tea tree	Thyme	Ylang ylang

The Table 3 summarizes the most important essential oils used for perfume formulations in the cosmetic industry. In addition, individual fragrances (purified terpenes) are applied also in perfume formulations, for example, bisabolol, carvone, farnesol, geranial, geraniol, linalool, limonene, and menthol [37].

3.6. Vetiver essential oil

The vetiver essential oil (VEO) is one of the oldest and most significant essential oils in fine perfumery, characterized as a dark, grapefruit, earthy, woody scent, and used as base note for more than 37% of Western perfumes and 20% of men's perfumes, including Chanel No. 5, Guerlain Vetiver, Berdoues 1902 Trèfle & Vétiver, Caleche, Opium, Parure, Dioressence and Vetiver extraordinaire [1]. In 2018, the global production of VEO was estimated at 300–350 ton per year [39] with prices oscillating between USD 380–500 per kg [40]. Due to the increase in the cosmetic demand, the world market of VEO is expected to grow to USD 169.5 million for 2022 [41]. The main producers worldwide are Haiti (100 t/year), Indonesia (80 t/year), China (20 t/year), India (20 t/year), Brazil (15 t/year) and Madagascar (0.5 t/year) [42].

VEO is obtained from the vetiver grass, *Chrysopogon zizanioides* (Poaceae), which is native to north India. *Ch. zizanioides* is a tufted perennial grass with 80 cm long bladed-elongated leaves branching basally from clumps, with a massive-deep root system (Figure 4) [43]. VEO is extracted from mature roots of 1–2 m of length and harvested after 12–18 months of growth. The most common extraction method is steam distillation that yields approximately 0.2–3% [42], and by super-critical fluid extraction, the extraction yield can be increased up to 4% [44]. Eventually, yields depend on the extraction method, but also from agronomical factors such as cultivars, weather, soil and fertilization.



Figure 4. Right: Foliage and roots of the vetiver grass *Ch. zizanioides*. Left: Traditional steam distillation facility for VEO production [45].

The chemical composition of VEO is a complex mixture of more than 300 molecules, mostly sesquiterpenes, and its oxygenated derivatives in which khusimol, α -vetivone, β -vetivone and isovalencenol are the main constituents (Figure 5) [42,46]. Although olfactory analyses are variable, the khusimol and zizaane derivatives grant the classical woody vetiver note, β -vetivone confers a grapefruit scent, α -vetivone provides a citrus rosy lime note and isovalencenol lends a strong sandalwood scent [47].

However, VEO composition differs from the origin of production, wherein “normal” VEO is produced by a sterile vetiver grass cultivar. Moreover, its composition includes additionally vetivane, zizaane, eremophilane and eudesmane derivatives, which are the main VEO on the market, produced by Haiti, Indonesia, China, Brazil and South India [42,48]. Normal VEO is characterized by a dextrorotatory character with woody, smoky-earthly notes with a long-lasting scent due to the low rate of volatility [42,46]. The Bourbon VEO produced from La Réunion contains roseate notes and is considered of high quality [1].

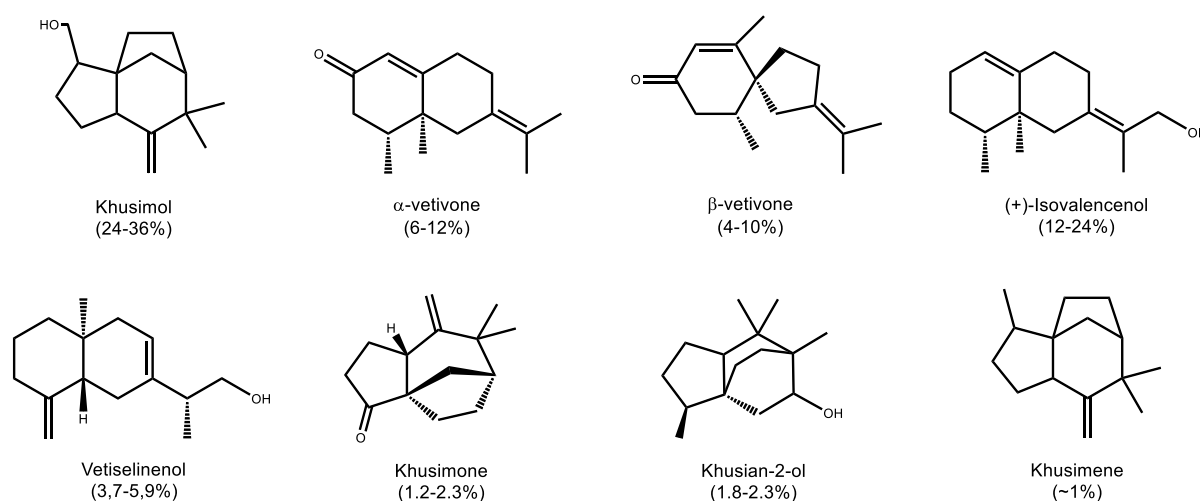


Figure 5. Main sesquiterpene structures contained in the “normal” VEO and their abundance.

The VEO produced by the fertile vetiver grass cultivar in northern India, called “khusoil”, is a highly regarded oil and lacks vetivones, containing high amounts of khusinol and khusilal (cadinanes derivatives) and is characterized by a balsamic woody notes with a levorotatory scent [1,42].

3.7. The fragrant sesquiterpene Khusimol

Recent interest has increased for the biotechnological production of fragrant sesquiterpenes from the VEO, to be used as individual fragrances and replace the VEO supply, which has lately suffered important shortages. This situation has increased from its main producer Haiti in the production area of Les Cayes, formerly due to natural disasters such as earthquakes and floods [40], and currently due to political unrest. This has resulted in shortages of the fuel supply required for the operation of VEO distilleries and transport of goods, resulting in the impossibility to extract VEO from fresh material and delaying the exports of the final product [45]. Of special importance is the fragrant sesquiterpene khusimol, the most abundant constituent of VEO, which grants a woody vetiver note [47].

Like most sesquiterpenes, the khusimol biosynthesis initiates from the sesquiterpene substrate FDP, which is catalyzed by a metal-dependent class-I fold TPS called zizaene synthase (ZS). This is the central enzyme for the khusimol biosynthesis, catalyzing FDP through distinct carbocation rearrangements and cyclizations to yield the tri-cyclic (+)-zizaene (syn. khusimene). Furthermore, (+)-zizaene is hydroxylated by a cytochrome P450 monooxygenase, accompanied by a cytochrome reductase and FMN/FAD cofactors, which leads to khusimol as main product. The hydroxylation reactions also yield zizaene oxygenated derivatives such as zizanal and zizanoic acid as side products (Figure 6) [49].

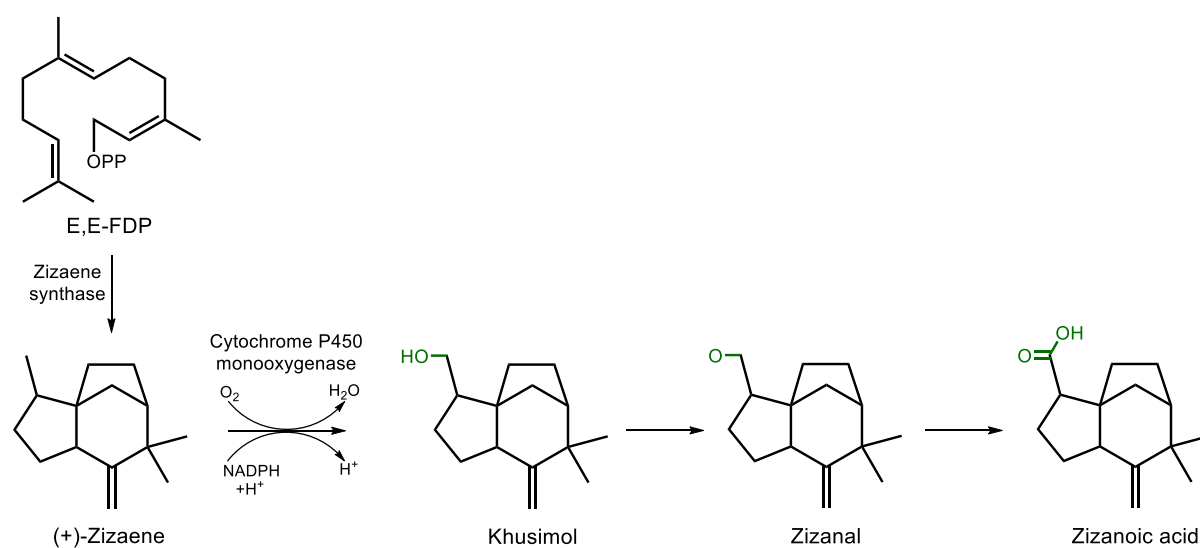


Figure 6. Biosynthesis of khusimol initiating from the sesquiterpene substrate E,E-FDP. Hydroxylation modifications are indicated in green color.

3.8. The direct-precursor of khusimol, (+)-zizaene

In an effort to produce khusimol as an individual fragrance, the production of the direct precursor (+)-zizaene has been the subject of study, comprising its chemical synthesis, enzymology and biotechnological production. The first stereocontrolled total synthesis of (+)-zizaene was described by Coates et al. [50], using as initial material norcamphor, which undergoes different arrangements, reductions and oxidations to yield a racemic mixture of (\pm)-zizaene. Piers et al. [51] developed a new formal total synthesis of (\pm)-zizaene starting from β -iodo enones, yielding a 2:1 epimeric mixture of the sesquiterpene. Another stereocontrolled total synthesis approach was developed by Chandra Pati et al. [52], initiating from indanone through a base induced pinacol type rearrangement as a key step, followed by a Wittig olefination.

However, the industrialization of the production of (\pm)-zizaene by chemical synthesis is challenging due to the costs associated with the multiple reactions and the toxicity of harmful chemicals. Hence, the production of (+)-zizaene by green chemistry methods such as enzymatical biotransformations or whole-cell based systems could solve the shortcomings from the chemical synthesis to yield a stereospecific (+)-zizaene at a lower production cost. An important milestone for the production of (+)-zizaene was achieved in 2014 by the cloning, overexpression and characterization of the native ZS gene, obtained from *Ch. zizanioides* [53]. In both in vitro and in vivo production systems, the terpene profile demonstrated 60-90% (+)-zizaene as main product, and pre-zizaene, α -funebrene and β -funebrene as side products [53].

Furthermore, a recombinant variant of the ZS gene was engineered with a small ubiquitin-related modifier (SUMO) as a fusion domain on the N-terminal end [54]. Such SUMO-fused ZS variant improved the solubility when compared to that of the native ZS version when heterologously overexpressed in *E. coli*. Furthermore, the in vitro biotransformation of E,E-FDP with the SUMO-fused ZS produced a different product profile than the native ZS version by lacking the funebrene side products [54].

3.9. Production of fragrant terpenes by metabolically engineered microorganisms

The production of fragrant terpenes by metabolically engineered microorganisms provides an alternative towards a cost-effective, reliable, environmentally friendly and sustainable production system from renewable sources, independent from environmental conditions [55,56].

Two important milestones have contributed to the engineering of isoprenoids into microbes: the elucidation and engineering of terpene biosynthetic pathways and the heterologous overexpression and characterization of plant TPS. Additionally, progress in synthetic biology tools has also contributed importantly to the development of terpene-producing strains, for example, genome sequencing technologies, bioinformatics tools, expanding omics databases,

tailoring of codon-optimized synthetic genes and improved PCR-based gene cloning methods [57,58].

The engineering of the MEV-pathway into microorganisms in the early 2000s by Keasling and co-workers [59] revolutionized the isoprenoid engineering by constructing a MEV-pathway into two operons (MevT and MBIS) with genes originating from *E. coli* and *Saccharomyces cerevisiae*, improving significantly the amorpha-4,11-diene titers. Since then, it has been applied for the engineering of numerous terpenes in combination with enhanced versions of the MEP-pathway, employing variants of the DXS and DXR genes, and heterologous prenyl transferases, as demonstrated for the production of valerenadiene and longifolene [60,61].

In addition to these developments, more than 100 monoterpene and sesquiterpene synthases genes of plant origin have been overexpressed in microbial hosts and characterized as reviewed elsewhere [62], which is a critical asset to the engineering of terpene biosynthetic pathways in microorganisms, commonly into *E. coli* or yeasts.

3.10. Downstreaming of terpenes

The recovery of terpenes from the fermentation of metabolically engineered microorganisms requires special considerations due to their non-polar and hydrophobic nature [63]. Thus, terpenes can be degraded by microbial strains or volatilized, which is increased in bioreactors by the gassing of air. Depending on their hydrophobicity, terpenes can be highly toxic to microbial cells, in which terpenes with low log P values usually partition to microbial cell membranes, altering the cell integrity and metabolic functions [64]. To overcome such drawbacks, in situ product recovery (ISPR) is applied commonly in terpene fermentation by removing products during cultivation [65].

ISPR techniques can be implemented whether by liquid or solid extractants that trap the terpenes due to hydrophobic interactions or adsorption, and avoid their volatilization. Thus, the liquid-liquid phase partitioning cultivation (LLPPC) utilizes organic solvents as extractants, resulting in an aqueous phase (media and cells) and organic phase (terpenes and solvents) in the fermentation [63]. The organic solvents are usually bio-compatible with cells and have high log P values [66]. The solid-liquid phase partitioning cultivation (SLPPC) uses zeolites, activated carbon, or polymeric adsorbers as solid extractants, in which terpenes are selectively adsorbed from fermentation [67]. Afterwards, desorption of terpenes is performed by eluting the solid extractants with a suitable organic solvent.

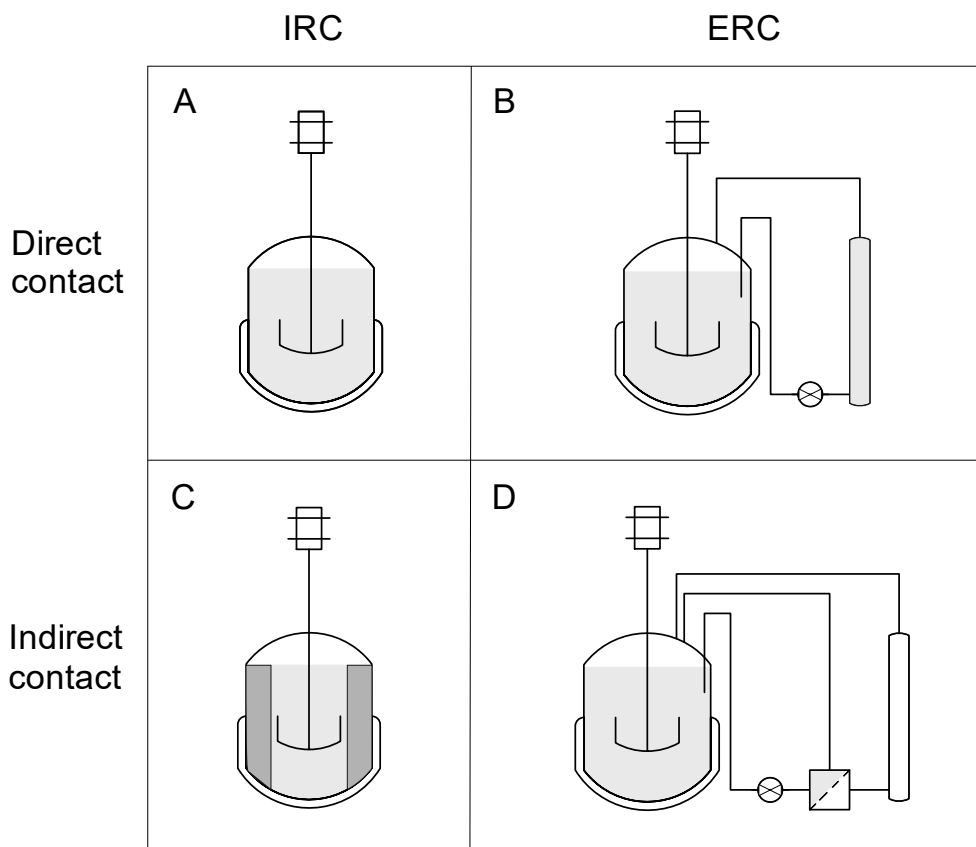


Figure 7. Configurations for in situ product recovery of terpenes in bioreactors. (A) Extractants in direct contact inside the vessel. (B) Extractants inside an EBA in direct contact by an external loop. (C) Extractants inside a gel matrix (dark grey) or separated from culture by a membrane without cell contact. (D) Extractants inside an EBA without cell contact by a perfusion external loop. Light grey color indicates cells and media. Modified from Buque-Taboada [68], Freeman [69] and Schewe [63].

The ISPR can be integrated to bioreactors using different basic configurations, classified into two variables: contact of extractant (direct or indirect) and localization of extractant (internal or external) as shown in Figure 7. In the direct contact, the extractant is in contact with the cells and media, whereas the indirect mode, the extractant is in contact with the cell-free broth through a perfusion unit. In the internal recovery configuration (IRC), the extractants remain inside the bioreactor vessel, either dispersed [70] or inside an internal basket [71]. In contrast, in the external recovery configuration (ERC), the culture broth is recirculated to an external loop with an expanded bed adsorption (EBA) unit, enabling a semi-continuous recovery of the product [65,72]. Consequently, the configuration of choice is dependent on the chemical properties of the terpene and the production costs [68].

As a result of the advances in both metabolic engineering and downstreaming of isoprenoids, many terpene bioprocesses have reached industrial levels and are currently marketed for the following applications: pharmaceutical: artemisinin; biofuel: β -farnesene; cosmetic ingredient: squalane; fragrance: nootkatone, patchouli oil, sclareol and valencene [13,33,73,74].

4. EXPERIMENTAL RESEARCH

4. Experimental research

This section includes the experimental investigation for the study of the sesquiterpene (+)-zizaene from basic to applied research by investigating the zizaene synthase enzymology, the microbial production and recovery of (+)-zizaene.

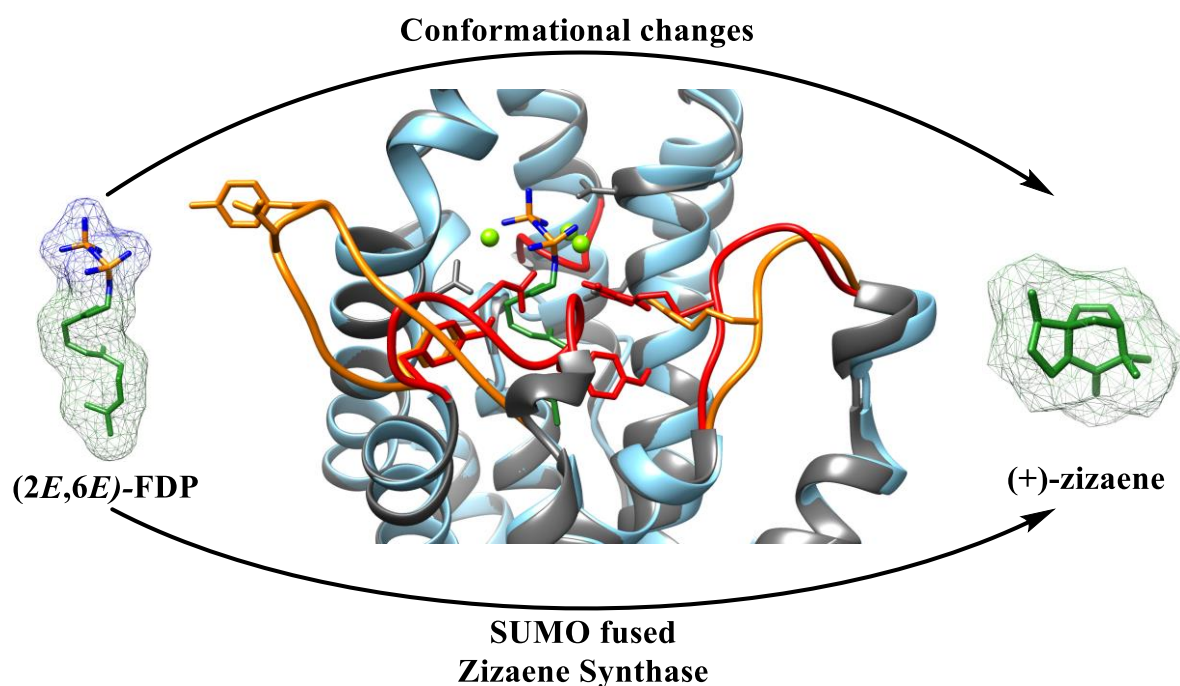
Consequently, the experimental research is divided into three research articles. The first chapter addresses the enzymology of the critical enzyme in the biosynthesis of (+)-zizaene, the zizaene synthase. This study comprises the product profile, enzyme kinetics, optimization of the reaction conditions, catalytical specificity, reaction mechanisms and conformational changes during catalysis.

The second chapter deals with the metabolic engineering for the production of (+)-zizaene in *E. coli*. Hence, distinct constructs were tested to modulate the supply of the precursor FDP and the zizaene synthase to enhance the (+)-zizaene levels. In addition, the optimization of the fermentation conditions was studied to further improve the (+)-zizaene amounts.

The third and last chapter applies the basic knowledge gathered from the initial chapters to scale-up the (+)-zizaene production at bioreactor scale and to further improve the (+)-zizaene titers. For that, the integration of fermentation and in situ product recovery was addressed by polymeric adsorbers and distinct bioreactor configurations were evaluated.

CHAPTER 1

Catalytical specificity, reaction mechanisms, and conformational changes during catalysis of the recombinant SUMO (+)-zizaene synthase from *Chrysopogon zizanioides*



Chapter published in: Aguilar, F.; Hartwig, S.; Scheper, T.; Beutel, S. Catalytical specificity, reaction mechanisms, and conformational changes during catalysis of the recombinant SUMO (+)-zizaene synthase from *Chrysopogon zizanioides*. *ACS Omega* 2019, 4, 6199–6209. DOI:[10.1021/acsomega.9b00242](https://doi.org/10.1021/acsomega.9b00242)

4.1. Catalytical specificity, reaction mechanisms, and conformational changes during catalysis of the recombinant SUMO (+)-zizaene synthase from *Chrysopogon zizanioides*

The VEO is an important fragrant ingredient for the cosmetic industry and used in nearly 20% of all men's perfumes. The main compound of this essential oil is the sesquiterpene khusimol, which grants the characteristic dark woody smell. The biotechnological production of khusimol has raised interest for its potential to replace the traditional supply of VEO, which had suffered shortages from its main producer, Haiti, due to natural disasters and political unrest.

For the development of a biotechnological process of khusimol, understanding the biosynthetic pathway is paramount. The critical enzyme for the biosynthesis of terpenes is the TPS which catalyzes the naturally occurring substrate E,E-FDP to yield products with high specificities. For the khusimol biosynthesis, the ZS is the TPS, where its characterization and optimal overexpression can provide the basis for the metabolic engineering towards khusimol.

In this chapter we address a further enzymatic characterization of the ZS by analyzing the enzyme kinetics, in vitro catalytical reactions, substrate specificities, reactions mechanisms and docking model.

Initially, we analyzed the terpene profile from in vitro biotransformation reactions with the substrate E,E-FDP and the recombinant SUMO-fused ZS variant, which was produced from *E. coli* and constructed from a previous report [54]. The in vitro reaction yielded over 90% (+)-zizaene and 8.5% β -acoradiene as side product. Furthermore, the reaction conditions of the biotransformation reaction were optimized, where pH 7.5 and temperature 36 °C were found as optimal. Additionally, enzyme kinetics was studied under optimal reaction conditions, where ZS catalysis followed a substrate inhibition kinetic model.

Catalytic specificity was also evaluated by monoterpenes substrates GPP and NPP that led to a variety of cyclic, acyclic and hydroxylated monoterpenes. Sesquiterpene substrate isomers E,Z-FDP and Z,E-FDP were additionally tested, yielding β -Z-farnesene by E,Z-FDP and β -E-farnesene and β -acoradiene. Consequently, the ZS demonstrated promiscuity for monoterpenes substrates but a high fidelity towards sesquiterpene substrates.

Furthermore, the reaction conditions with E,E-FDP were studied under a wide range of temperature and pH values, revealing minimal changes in the product profile that suggests a strong and stable closed conformation during catalysis. To understand such behavior, the conformational changes during catalysis were studied via an in silico docking model. Interestingly, the surrounding loops from the active site (J-K and A-C loop) were constituted of neutral and hydrophobic residues, which grant stability against pH changes from the reaction buffer.

Moreover, distinct residues from the J-K loop could be involved in the efficient sealing of the active site, stabilizing the closed conformation against dynamic fluctuations that occur at higher temperatures.

Accordingly, this study demonstrated new insights concerning the enzymology of the ZS and builds the foundations towards the metabolic engineering of the (+)-zizaene biosynthetic pathway.

Catalytic Specificity, Reaction Mechanisms, and Conformational Changes during Catalysis of the Recombinant SUMO (+)-Zizaene Synthase from *Chrysopogon zizanioides*

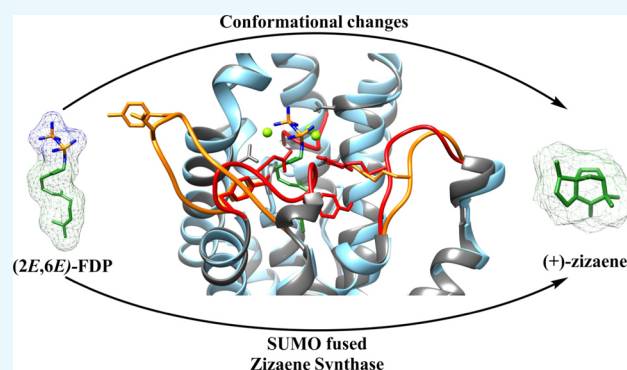
Francisco Aguilar,^{†,‡} Stephan Hartwig,[†] Thomas Scheper,[†] and Sascha Beutel^{*,†}

[†]Institute of Technical Chemistry, Leibniz University of Hannover, Callinstr. 5, 30167 Hannover, Germany

[‡]National Center for Biotechnological Innovations of Costa Rica—CENIBiot, 1174-1200 San José, Costa Rica

Supporting Information

ABSTRACT: Zizaene synthase (ZS) from *Chrysopogon zizanioides* (Poaceae) is the critical enzyme in the biosynthesis of the fragrant sesquiterpene khusimol, a major component of the vetiver essential oil used widely by the cosmetic industry. As reported previously, we heterologously and successfully expressed the active ZS with a small ubiquitin-related modifier (SUMO) fusion domain. In this study, we report the optimization of reaction conditions and determination of enzyme kinetics of ZS. Moreover, we investigate the catalytic specificity and reaction mechanisms with the ubiquitous (2*E*,6*E*)-farnesyl diphosphate (FDP) and with C₁₀ and C₁₅ prenyl diphosphate isomers. Catalytic promiscuity occurs with monoterpene substrates generating eight products that comprise acyclic, cyclic, and hydroxylated monoterpenes. In contrast, ZS is a high-fidelity terpene cyclase when used with C₁₅ isomer substrates, yielding as major products (*Z*)- β -farnesene (100%) for (2*E*,6*Z*)-FDP and (+)-zizaene (81.7%), β -acoradiene (12.8%), and (*E*)- β -farnesene (5.5%) for (2*Z*,6*E*)-FDP. Cyclization of the ubiquitous substrate (2*E*,6*E*)-FDP demonstrates a higher catalytic specificity, whereas the reaction proceeds via the acorenyl cation that generates (+)-zizaene (91.5%) and β -acoradiene (8.5%). Furthermore, catalytic specificity with (2*E*,6*E*)-FDP was stable in reactions tested at distinct pH and temperatures, suggesting a stable and efficient closed conformation of the active site during catalysis. To understand such stability, open and closed structural conformations of ZS were modeled in silico and revealed putative residues in the active site and in the A-C and J-K surrounding loops, which could explain the high fidelity of ZS.



1. INTRODUCTION

Sesquiterpene cyclases (STC) catalyze more than 300 distinct C₁₅ carbon skeletons, giving origin to a variety of sesquiterpene lactones, ketones, alcohols, and aldehydes, which are the main constituents of plant essential oils, many used for flavor and fragrant applications.^{1–3} STC are metal-dependent enzymes that catalyze the conversion of the universal sesquiterpene substrate (2*E*,6*E*)-FDP, which originates from isopentenyl diphosphate and dimethylallyl diphosphate from the mevalonic acid pathway that operates in the cellular cytosol.⁴ Their structure includes the active class I terpenoid synthase fold, which contains the conserved aspartate-rich motifs DDXXD and DTE/NSE located in the α -helices.⁵ Plant STC also contains an N-terminal domain resembling the class II terpenoid synthase fold with no specific catalytic activity.¹

The reaction mechanisms of plant STC initiate through the binding of divalent metal ions, mostly Mg²⁺, to the conserved aspartate-rich motifs, which in turn coordinate the binding of the phosphate moiety (PP_i) from FDP by hydrogen bonds.⁶ Thereafter, the enzyme undergoes a conformational change in which the surrounding loops seal the active site, creating a

hydrophobic environment that prevents solvent entry.^{7–9} Consequently, the substrate undergoes ionization; thus, PP_i is cleaved and a transoid-allylic carbocation (farnesyl cation) is generated. At this point, the reaction can be quenched to generate linear cisoid or transoid sesquiterpenes, such as (*E*)- β -farnesene,¹⁰ or can undergo cyclizations by two pathways: (1) farnesyl cation undergoes immediate 10,1-cyclization for (*E*,*E*)-germacradienyl cation or 11,1-cyclization for (*E*,*E*)-humulyl cation. (2) farnesyl cation undergoes isomerization, leading to the cisoid nerolidyl cation, followed by further cyclizations and generates distinct intermediates: bisabolyl cation (1,6-cyclization), cycloheptanyl cation (1,7-cyclization), (*Z*,*E*)-germacradienyl cation (1,10-cyclization), or (*Z*)-humulyl cation (1,11-cyclization).¹¹ Further reactions comprise carbocation rearrangements, hydride shifts, and cyclizations, which finalize by deprotonation quenching; thus, the

Received: January 26, 2019

Accepted: March 1, 2019

Published: April 3, 2019

possibilities for rearrangements are vast and lead to a particular product spectrum.¹²

The active site of each STC is characterized by a specific conformation of residues, especially aromatic residues, which guide the reactions of the prenyl tail and determines the product specificity.^{6,11} For this reason, some STC generate multiple products and are considered promiscuous, such as γ -humulene synthase, which produces more than 52 products.¹³ Nevertheless, most STC generate few products and therefore are considered high-fidelity enzymes, as shown by tobacco 5-epi-aristolochene synthase (TEAS) that generates epi-aristolochene, the precursor for the plant defense compound capsidiol.⁸ Most STC are promiscuous in catalyzing alternative substrates, accepting isoprene diphosphate substrates and isoprenoid isomers.⁶ Acceptance for monoterpene substrates, such as the ubiquitous geranyl diphosphate (GPP), has been reported elsewhere.^{14,15} Moreover, acceptance of both GPP and cisoid neryl diphosphate (NPP) has been demonstrated by the patchoulol synthase.¹⁶ STC are also prone to accept isomers from the sesquiterpene substrate (2*E*,6*E*)-FDP, whereas catalyzation of isomers (2*Z*,6*Z*)-FDP,¹⁷ (2*Z*,6*E*)-FDP,¹⁸ and (2*E*,6*Z*)-FDP¹⁶ has been reported.

Of particular interest is the sesquiterpene khusimol, contained in the vetiver essential oil from the tropical grass *Ch. zizanioides* and used in nearly 20% of men's perfumes due to its woody smell.¹⁹ Further research has focused on its medicinal properties and has reported antioxidant,²⁰ antimicrobial,²¹ and anti-inflammatory activity.²² Together with α - and β -vetivone, khusimol is one of its main constituents and its industrial extraction is performed by steam distillation from dried roots.²³

Despite its importance, there are few studies concerning the biosynthesis of khusimol, which is most relevant to the development of a biotechnological process. Previously, our group described the heterologous expression in *Escherichia coli* of ZS from *Ch. zizanioides*, which is the key enzyme in the biosynthesis of khusimol.²⁴ ZS was expressed fused with the SUMO domain in the N-terminal section to improve solubility, yielding a 64 kDa enzyme. ZS catalytical functionality was demonstrated by the cyclization of (2*E*,6*E*)-FDP, which generated the three-cyclic sesquiterpene (+)-zizaene (syn. khusimene), the precursor for khusimol. However, further knowledge is still required to understand the complex enzymatic mechanisms of ZS. Hereby, we report for the first time to our knowledge the product spectrum and reaction mechanisms involved in ZS with the ubiquitous substrate (2*E*,6*E*)-FDP and the alternative substrates NPP, GPP, (2*E*,6*Z*)-FDP, and (2*Z*,6*E*)-FDP. Furthermore, dependence on pH and temperature for product specificity was assessed by altering the reaction conditions. Moreover, we analyze the conformational changes during catalysis and the identification of putative key residues that take part in the catalytical process. The generated knowledge provides the basis for understanding the reaction mechanisms of ZS for further protein engineering studies.

2. RESULTS AND DISCUSSION

2.1. Biotransformation Assays and Product Identification of ZS with (2*E*,6*E*)-FDP. The product spectrum of the reaction of ZS with the naturally occurring substrate (2*E*,6*E*)-FDP was assessed by biotransformation assays based on the single-vial method reported by O'Maille et al.²⁵ Similar to our previous report,²⁴ the main product of the reaction was

sesquiterpene (+)-zizaene (91.46% abundance). Additionally, we identified β -acoradiene (8.54% abundance) as a side product (Figure 1), which is found in traces in the vetiver essential oil¹⁹ and is a deprotonated compound from the acorenyl cation, an intermediate in the biosynthesis of (+)-zizaene.²⁶

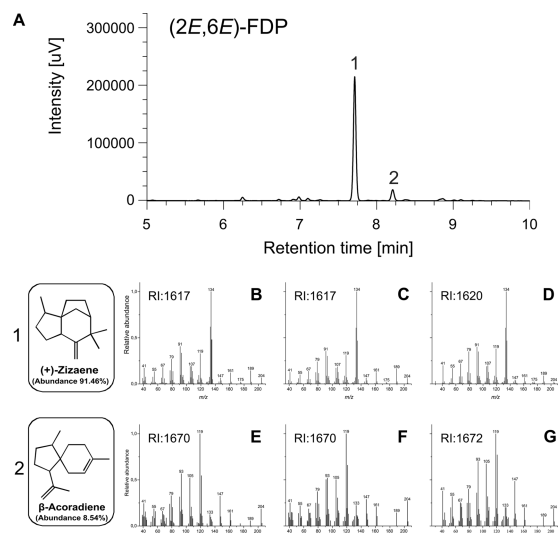


Figure 1. (A) Product spectrum of the biotransformation assay of (2*E*,6*E*)-FDP with ZS by gas chromatography-mass spectroscopy (GC-MS). (+)-Zizaene: (B) mass spectrum from peak 1. (C) Mass spectrum of authentic (+)-zizaene from vetiver oil. (D) Mass spectrum of authentic (+)-zizaene from ref 27. β -Acoradiene: (E) mass spectrum from peak 1. (F) mass spectrum of authentic β -acoradiene from vetiver oil. (G) Mass spectrum of authentic β -acoradiene from ref 28.

2.2. Optimization of Reaction Conditions. The optimal temperature and pH of the reaction of ZS with (2*E*,6*E*)-FDP was determined for the main product (+)-zizaene; thus, the optimal region for the reaction rate ($>1.6 \mu\text{M min}^{-1}$) was calculated between pH 7.33–7.65 and temperature 34.15–38.10 °C (Figure 2a). The medium reaction rate ($1.4\text{--}1.6 \mu\text{M min}^{-1}$) was determined between pH 7.0–7.8 and 32.5–42.0 °C of temperature. Consequently, optimal reaction conditions were defined at pH 7.5 and 36 °C for further tests. The activity of STC takes place in cytosol,²⁹ which is characterized by pH 7.5.³⁰ Therefore, optimal pH of ZS was found within the expected range and was similar to that for other reported STC.^{31–33} Activity of ZS was detected even between 21 and 42 °C at pH 7.0. Consequently, the broad temperature range for ZS activity allows the vetiver grass to produce (+)-zizaene under different climates.³⁴

2.3. Analysis of Kinetic Parameters. A study for the ZS kinetic parameters was carried out under the determined optimal reaction conditions (36 °C, pH 7.5) with 0.1 μM purified ZS and monitored in a range of 1–50 μM (2*E*,6*E*)-FDP. Respective velocities were calculated by the product formation only for the main product: (+)-zizaene. Figure 2b describes the kinetics of ZS, where velocities increased from 1 to 5 μM of (2*E*,6*E*)-FDP with V_{max} 0.35 $\mu\text{M min}^{-1}$, K_M 0.88 μM , and k_{cat}/K_M $6.71 \times 10^4 \text{ M}^{-1} \text{ s}^{-1}$. Consequently, the catalytic efficiency of ZS was higher under optimal conditions when compared with our previous report,²⁴ which achieved V_{max} 0.32 $\mu\text{M min}^{-1}$, K_M 1.11 μM , and k_{cat}/K_M $4.43 \times 10^4 \text{ M}^{-1}$

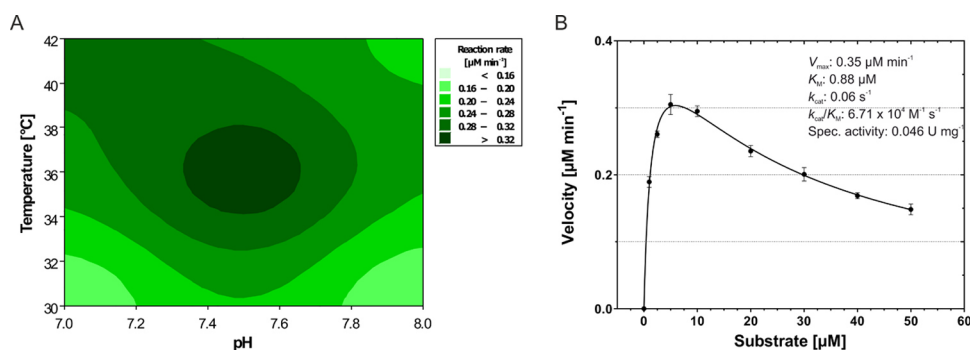


Figure 2. (A) Optimization of temperature and pH in the biotransformation of (2*E*,6*E*)-FDP with ZS. Variable of study corresponds to the reaction rate of zizaene. (B) Enzyme kinetics plot of ZS showing reaction velocities at increasing concentrations of (2*E*,6*E*)-FDP. Reaction velocities calculated from five measurements by a discontinuous assay method and performed in triplicates. Error bars represent standard deviation (SD) of three independent measurements.

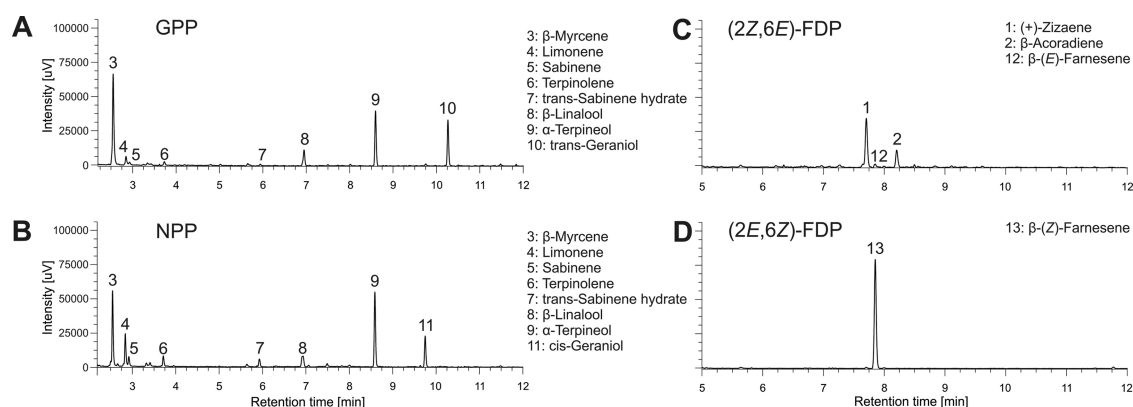


Figure 3. GC-MS analysis of the product spectrum of the reaction of ZS with alternative substrates. Monoterpene substrates: (A) GPP. (B) NPP. Sesquiterpene isomer substrates: (C) (2*Z*,6*E*)-FDP. (D) (2*E*,6*Z*)-FDP. Mass spectra for each product can be found in Tables S1 and S2.

Table 1. Identification of the Product Spectrum Obtained from the Biotransformation of Monoterpene Substrates (GPP and NPP) with ZS

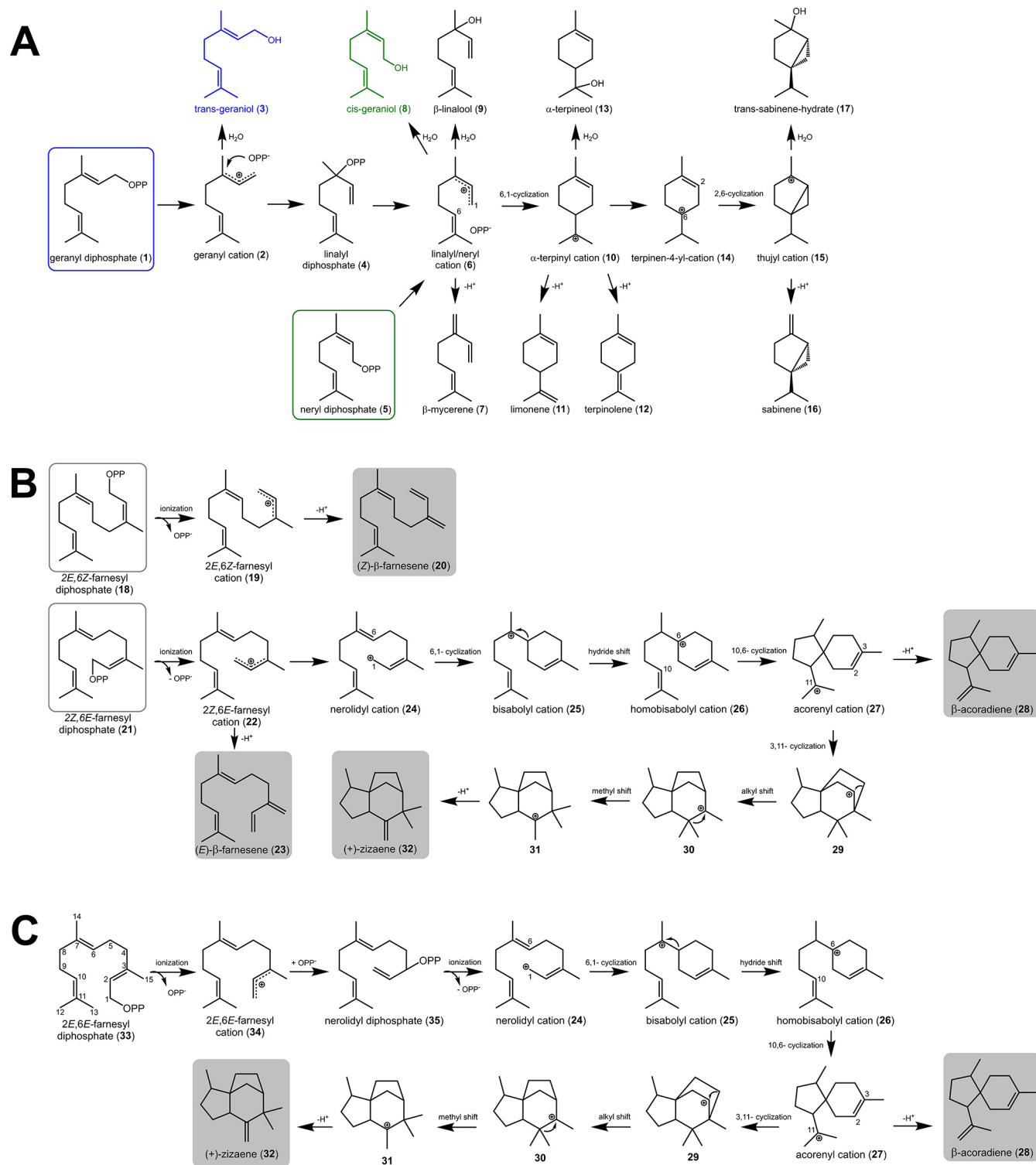
peak	compound	abundance (%)		RI samples		RI literature	identification ^a	references
		GPP	NPP	GPP	NPP			
3	<i>β</i> -myrcene	40.32	26.93	1151	1151	1155	(a)(b)	43
4	limonene	4.2	12.68	1182	1182	1180	(a)(b)	44
5	sabinene	1.45	3.72	1185	1185	1156	(a)(b)	45
6	terpinolene	1.71	3.73	1266	1266	1266	(a)(b)	46
7	trans-sabinene hydrate	1.12	3.28	1440	1440	1447	(a)(b)	47
8	<i>β</i> -linalool	8.21	7.28	1524	1524	1531	(a)(b)	48
9	<i>α</i> -terpineol	23.87	29.63	1669	1669	1669	(a)(b)(c)	49
10	trans-geraniol	19.12		1817		1822	(a)(b)	50
11	cis-geraniol		12.75		1772	1777	(a)(b)	50

^aIdentification of compounds: (a) Mass spectrum from the sample matches the library mass spectrum. (b) Retention index of sample matches the retention index in the literature. (c) Mass spectrum and the retention index of the sample matches the authentic standard; both run in the same GC-MS system. Mass spectrum of samples can be found in Supporting Information (SI), Table 1.

s^{-1} . The difference between both studies was the increase in temperature to 36 °C, which favored reaction rates and lowered K_M . The low values of the obtained kinetic parameters were expected for plant enzymes from the secondary metabolism, because their products are not required for essential metabolic functions.³⁰ Consequently, our results are in accordance with similar reported STC activities.^{35–38}

In our previous report, ZS followed an apparent Michaelis–Menten kinetics,²⁴ although a slight decrease in velocity was observed from 30 to 40 μM (2*E*,6*E*)-FDP. In optimal reaction conditions, ZS showed a decrease in velocities from 10 to 50

μM (2*E*,6*E*)-FDP (velocities of 0.29–0.15 $\mu M \text{ min}^{-1}$). Consequently, ZS kinetics follows a substrate inhibition model when the reaction is held at optimal conditions. Such kinetics were also reported for the recombinant patchouli synthase³⁹ and ent-Copalyl diphosphate synthase (diterpene cyclase). Apparently, an excess of substrate binds to two different sites in the enzyme: the substrate binding site (aspartate-rich motif) and the active site,⁴⁰ forming non-productive binding (ESS). Moreover, the above-mentioned study demonstrated that the cofactor (Mg^{2+}) served also as an inhibitor at levels higher than 0.1 μM $MgCl_2$. In the case of ZS,

Scheme 1. Proposed Reaction Mechanisms of ZS with Distinct C₁₀ and C₁₅ Substrates^a

^a(A) Reaction mechanism for monoterpene substrates GPP and NPP. Colors indicate unique products according to the substrate. The mechanism is modified from Alonso and Croteau.¹⁵ (B) Reaction mechanism from sesquiterpene substrate isomers (2E,6Z)-FDP and (2Z,6E)-FDP. (C) Reaction mechanism from the naturally occurring sesquiterpene substrate (2E,6E)-FDP. Final products are highlighted in gray. Mechanisms are modified from Mercke et al.³² and Aaron et al.⁷

amounts higher than 10 mM MgCl₂ proved also inhibition. Consequently, substrate inhibition plays a role in the regulation of terpene metabolism; hence, the levels of cofactors (divalent metal ions) are modulated by physical factors, such as light.⁴⁰ Further studies are required to clarify whether physical

factors or nutrient uptake regulate the levels of cofactors and khusimol biosynthesis in roots of *Ch. zizanioides*.

2.4. Reaction Mechanisms of ZS with C₁₀ Substrates.

To analyze the enzymatic versatility of ZS, the alternative substrates C₁₀, C₁₅, and C₂₀ prenyl diphosphates were

Table 2. Identification of the Product Spectrum Obtained from the Biotransformation of Sesquiterpene Substrates with ZS

alternative substrate	peak	compound	compound abundance (%)	retention index		identification ^a	references
				sample	literature		
(2 <i>E</i> ,6 <i>Z</i>)-FDP	13	β -(<i>Z</i>)-farnesene	100	1621	1630	(a)(b)	51
(2 <i>Z</i> ,6 <i>E</i>)-FDP	1	(+)-zizaene	81.7	1617	1620	(a)(b)(c)	27
	12	β -(<i>E</i>)-farnesene	5.51	1651	1659	(a)(b)	52
	2	β -acoradiene	12.79	1670	1672	(a)(b)(c)	28

^aIdentification of compounds: (a) Mass spectrum from the sample matches the library mass spectrum. (b) Retention index of sample matches the retention index in the literature. (c) Mass spectrum and the retention index of the sample match those of terpene from the vetiver oil; both run in the same GC-MS system. The mass spectrum of samples can be found in SI, Table 2.

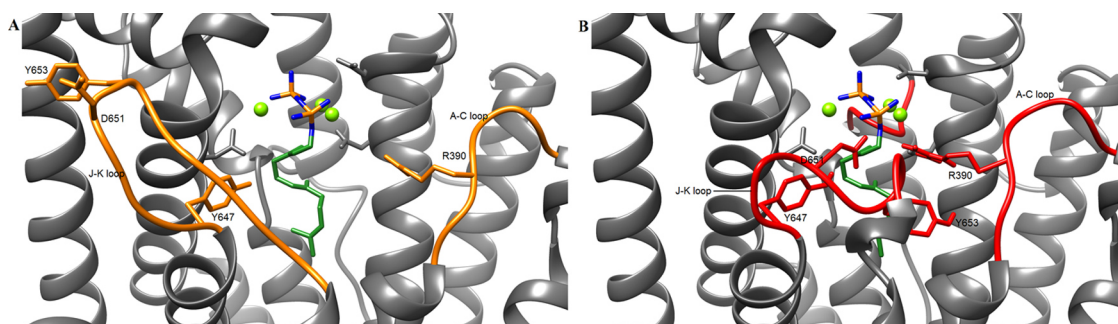


Figure 4. Structural homology models of the open and closed conformations of the ZS active site docked with (2*E*,6*E*)-FDP. (A) Open conformation of ZS shows the J-K and A-C loops in orange and Mg²⁺ divalent ions in green. (B) Closed conformation of ZS shows folding of the J-K and A-C loops in red. Putative relevant residues for capping the active site are labeled.

evaluated (Figure 3). ZS accepted both monoterpene precursors (NPP and GPP) and produced a mixture of cyclic and acyclic monoterpenes (Table 1). Product formation was catalyzed due to the activity of ZS; hence, no products were observed in negative controls (reactions with alternative substrates without ZS). Accordingly, ZS was able to accept monoterpene substrates due to the large active cavity compared to that of the short C₁₀ prenyl tail, as demonstrated by other STCs.^{32,41,42}

As shown in the proposed reaction mechanisms for monoterpene substrates (Scheme 1a), GPP undergoes ionization to geranyl cation (2). On one side, it hydroxylates to trans-geraniol (3) and on the other, isomerizes to linalyl diphosphate (4) for further ionization to form linalyl/neryl cation (6). In contrast, NPP leads directly to neryl cation (6) after ionization and leads further to cis-geraniol (syn. Nerol) (8). As a result, both substrates converge into linalyl/neryl cation, leading to three paths: (1) deprotonation to the acyclic β -mycerene (7), (2) hydroxylation to β -linalool (9), and (3) 6,1-cyclization to α -terpinyl cation (10), the precursor of cyclic monoterpenes. Further, both follow quenching by deprotonation to yield limonene (11) and terpinolene (12), water addition for α -terpineol (13), and 2,6-ring closure to thujyl cation (15). Finally, sabinene (16) and trans-sabinene-hydrate (17) are formed.

As a consequence, product specificity of both substrates was low, generating eight monoterpenoids. GPP and NPP yielded as major products β -mycerene (40.3%, 26.9%) and α -terpineol (23.8%, 29.6%), respectively, and geraniol isomers (GPP: trans-geraniol 19.1% NPP: cis-geraniol 12.7%). Interestingly, both substrates converted more than 50% to hydroxylated monoterpenes (α -terpineol, β -linalool, trans-sabinene hydrate, trans-geraniol, and cis-geraniol). Possibly, water molecules surrounding the active site of ZS are activated and assist the hydroxylation process. Such hydroxylation was demonstrated

before, wherein a water molecule found in the active site of salvia monoterpene synthase participated in the water addition of α -terpinyl cation to generate α -terpineol.⁵³

2.5. Reaction Mechanisms of ZS with C₁₅ and C₂₀ Substrates. Assays with FDP isomers converted only to nonhydroxylated sesquiterpenes (Table 2), whereas geranyl-geranyl diphosphate did not produce any products. It is known that STC do not accept C₂₀ prenyl diphosphates substrates because the prenyl tail is too large to fit in the cavity of STC.^{17,54}

The proposed reaction mechanism for isomer (2*E*,6*Z*)-FDP leads to (2*E*,6*Z*)-farnesyl cation (19) after ionization and further premature quenching to form (*Z*)- β -farnesene (20) (Scheme 1b). Therefore, isomerization to nerolidyl diphosphate is not possible due to the (2*E*,6*Z*) stereochemistry of the prenyl tail. Possibly, the prenyl tail does not position correctly into the inner cavity of the active site and cannot undergo further rearrangements. Consequently, (2*E*,6*Z*)-FDP reaction resembles the functioning of farnesene synthases^{55,56} and showed the highest product specificity with 100% abundance of the main product in relation to all substrates tested.

Regarding (2*Z*,6*E*)-FDP, the proposed mechanism leads directly to (2*Z*,6*E*)-farnesyl cation (22), after ionization of PP_i (Scheme 1b). One path leads to (*E*)- β -farnesene (23) (5.51% abundance) and most of the flux leads to nerolidyl cation (24) and further 6,1 ring closure to bisaboyl cation (25). After a hydride shift, a 10,6-cyclization leads to acorenyl cation (27). From here, two paths occur: one leads to β -acoradiene (26) (12.79% abundance) by deprotonation and the other leads to 3,11-cyclization to form a three ring carbocationic intermediate (29). The latter passes through a carbocation cascade with final deprotonation to the main product (+)-zizaene (32). Consequently, (2*Z*,6*E*)-FDP shows a high product specificity for (+)-zizaene with an abundance of 81.7%. Additionally, the low abundance of (*E*)- β -farnesene suggests a premature exit of

the (2*Z*,6*E*)-farnesyl cation from the active site for further carbocation deprotonation.

2.6. Conformational Changes During Catalysis.

Analysis of docking models in open and closed conformations shows the structural changes occurring during substrate binding. Most relevant is the closing of the J-K and A-C loops, wherein in the open conformation, they remain unfolded, allowing the entrance of molecules (Figure 4a). In the closed conformation, they fold to the active site (Figure 4b), acting as a lock to create a hydrophobic environment suitable for carbocation cascades. Residue D651 from the J-K loop is directed toward the binding site and possibly participates in the coordination of divalent Mg^{2+} ions. Additionally, Y653 folds toward the prenyl tail and is involved in its stabilization. Contrary to Y653, Y647 does not suffer major positioning because it is already near to the active site. Subsequently, the R390 from the A-C loop folds toward the PP_i , completing the capping of the active site.

According to the docking model in the closed conformation, Mg_A^{2+} and Mg_C^{2+} ions bind to the $D^{427}DIYD^{431}$ motif, and Mg_B^{2+} ion, to the $ND^{572}IASHE^{577}$ motif (Figure 5). Divalent

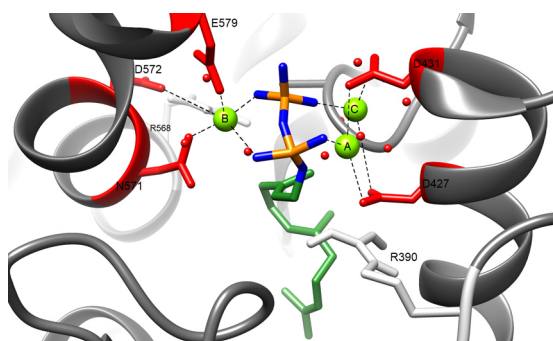


Figure 5. Docking model showing the interactions that occur during binding of (2*E*,6*E*)-FDP in the active site of ZS. Metal coordination interactions are shown between D572, E579, D427, and D431 residues (red) from the aspartate-rich motifs with the Mg^{2+} divalent ions (light green) and water molecules (red spheres). Putative hydrogen bond interactions shown between R390 and R568 (light gray) with the phosphate moiety of FDP (blue/orange).

ions coordinate the metal binding of PP_i from (2*E*,6*E*)-FDP accompanied by hydrogen bond interactions, and water

molecules occupy the surrounding area, binding to the Mg^{2+} ions. Furthermore, the prenyl tail is located in the interior of the active site (Figure 6a), surrounded by V423 and D651 residues and the aromatic residues Y647, Y653, W399, and F420, which in turn, stabilize the complex in the closed active site conformation.

2.7. Reaction Mechanism of ZS with (2*E*,6*E*)-FDP. The proposed reaction mechanism undergoes ionization of (2*E*,6*E*)-FDP, whereas the PP_i group is cleaved and the (2*E*,6*E*)-farnesyl cation is formed (Figure 6b). The D651 assists the FDP isomerization by sequestering the farnesyl cation (34) at C_1 , which in turn captures further the PP_i moiety, leading to nerolidyl diphosphate (35) (Scheme 1c). Likewise, the positively charged residues R390 and R568 sequester the PP_i anion and pull it apart from the prenyl tail, as reported by Bohlmann et al.⁶ After ionization of the diphosphate isomer, nerolidyl cation (4) is formed and V423 together with Y653 assists the positioning of the carbocation inside the inner cavity.

Furthermore, C_1 bends toward C_6 , promoting the 6,1-cyclization, leading to the bisabolyl cation (25). The C_6 positive charge could be stabilized either by Y653 or W399 through π -cation interactions, and after an alkyl shift, the homobisabolyl cation (26) is formed. Further cyclizations and rearrangements could be concerted by aromatic residues positioned in the interior of the cavity (F639, W399, and F420), as shown in Figure 6b. Thereafter, electrophilic attack of C_{10} of homobisabolyl cation leads to the 10,6-cyclization to form the double-ring acorenyl cation (27), which branches into two paths: deprotonation to form β -acoradiene (28) and 3,11 ring closure that leads to a triple ring intermediate (29). Further carbocation rearrangements include an alkyl shift (30), methyl shift (31), and deprotonation to form the main product (+)-zizaene (32). Eventually, W399 functions as a proton acceptor in the final deprotonation reaction.⁸

The latter reaction mechanism follows a related biogenic origin for sesquiterpenes derived from the bisabolyl cation, a primary intermediate for diverse sesquiterpene families: bisabolene, curcumene, β -acoradiene, zizaene, cedrene, duprezianene, and sesquithuriferol.²⁶ ZS is able to undergo successfully the 10,6-ring closure that leads to acorenyl cation. Nevertheless, the complex 3,11-cyclization is not fully processed; thus, the side product β -acoradiene is formed. Although the 2,11-cyclization could be another favorable path,

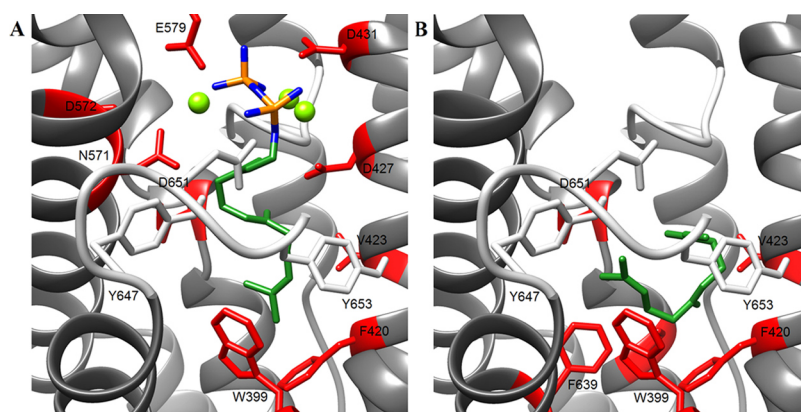


Figure 6. Proposed interacting residues of ZS with (2*E*,6*E*)-FDP (A) and (2*E*,6*E*)-farnesyl cation (B) during binding and isomerization of FDP based on docking modeling. Putative interacting residues from helices are marked in red, and residues from J-K loop are marked in light gray. Phosphate moiety of FDP is shown in blue/orange, prenyl tail/farnesyl cation in dark green, and Mg^{2+} divalent ions in light green.

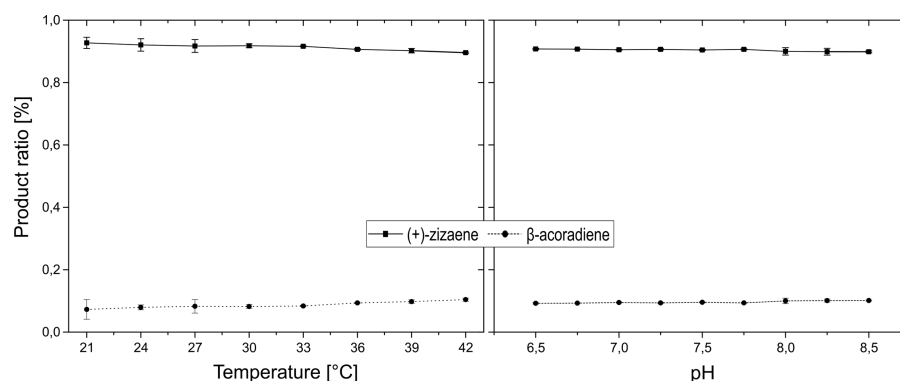


Figure 7. Study of the dependency of temperature and pH to the product ratio of (+)-zizaene (■) and β -acoradiene (●) in cyclization assays of (2*E*,6*E*)-FDP with ZS. Error bars represent the SD of three independent measurements.

it seems at this point that ZS is prone to early quenching and deprotonation occurs. However, most of the flux successfully undergoes 3,11-cyclization and, after different rearrangements, (+)-zizaene is formed with a 91.46% abundance, resulting in high product specificity.

It is known that aromatic residues in the active site are able to stabilize the partial positive charges of carbocation intermediates either by charge–quadrupole or cation– π interactions.¹ Accordingly, plant STC comprise conserved aromatic residues in the active cavity,⁸ such as Y647, Y653, and W399, found in both ZS and TEAS. Interestingly, ZS includes two additional aromatic residues (F420 and F639), which are crucial for the stabilization of the complex carbocations and cyclizations in the biosynthesis of (+)-zizaene. Additionally, the active cavity volume of ZS was calculated in 367.7 Å³, which could be considered tight when compared with other STC cavity volumes that are over 415 Å³.^{57,58} This suggests that the ZS cavity does not have enough space to allow alternative conformations of the prenyl tail, which results in an almost unique reaction pathway and high product specificity.

2.8. Effect of Temperature and pH on Product Specificity. The complex mechanisms of STC are affected by reaction conditions, such as pH and temperature, which regulate the product ratio (proportion of generated terpenoids), as demonstrated by others.^{12,18} To evaluate the pH and temperature effect on product specificity, an analysis was conducted on the product spectrum of ZS with the substrate (2*E*,6*E*)-FDP by the single-vial method assay.²⁵ Accordingly, the temperature was evaluated from 21 to 42 °C at pH 7.5 and pH was tested from pH 6.5 to 8.5 at 36 °C. In the case of temperature, a minor decrease in the product ratio for the main product (+)-zizaene was observed at increasing temperatures (Figure 7); hence, it shifted from 92.73 to 89.6% in temperatures from 21 to 42 °C. On the contrary, the side product β -acoradiene showed an increase from 7.27 to 10.4% at increasing temperatures (21–42 °C).

It has been demonstrated previously that temperature has an effect on product specificity for other STCs;^{16,18} thus, 5-epiaristolochene synthase (TEAS) showed a trend in which higher temperatures decreased the production of the main product from 87.6 to 66.2% (21.4% shift). It was proposed that higher temperatures increased the protein motion and destabilized the J-K loop, allowing the exit of intermediates from the active site prior to cyclization.¹⁸ On the contrary, the slight shift observed in the product ratio of ZS (3.13%) suggests a strong global conformation of the enzyme to endure energetic fluctuations. Moreover, it suggests an efficient

binding of the J-K and A-C loops to the binding site, which seals the active site from external solvents, creating a hydrophobic environment. According to our model (Figure 4), distinct residues from the surrounding loops could be responsible for the binding efficiency, as they change their position drastically from an open to a closed conformation. The D651 residue from the J-K loop points to be critical in binding efficiency, as it is positioned strategically in the closed conformation and possibly participates in Mg²⁺ coordination and farnesyl cation capture during FDP isomerization. In addition, aromatic residues Y647 and Y653 seem also relevant because they are able to bind and stabilize the prenyl tail.

Concerning pH experiments, it could be shown that pH had less effect than temperature on the product ratio (Figure 7), since (+)-zizaene levels decreased slightly from 90.75 to 89.88% in the studied pH range (6.5–8.5). Similar to temperature, the alternative product β -acoradiene tends to increase its product ratio from 9.25 to 10.12% at higher pH values. Distinct STCs have shown product ratio dependence on pH^{12,16,59} because it affects the reaction solvent and, in turn, distinct reactions such as hydride shifts, deprotonations, and hydroxylations. A relevant mechanism for pH dependence was proposed for the fungal STC Cop4 from *Coprinus cinereus*, where basic residues (histidines) in the H-1 α loop showed susceptibility to pH changes due to net charge shifts.⁶⁰ As a result, this decreased the binding efficiency of the H-1 α loop to the binding pocket, allowing early quenching. In the case of ZS, the H-1 α loop (L⁴⁹⁴IDAAKCY⁵⁰¹), J-K loop (Y⁶⁴⁷NGVDLYTI⁶⁵⁵), and A-C loop (L³⁸⁶TFARDR³⁹²) are composed mostly of hydrophobic and neutral residues. Because of their polarity, they remain unaffected at the tested pH and are able to seal efficiently the binding pocket, creating a hermetic hydrophobic cavity.

3. CONCLUDING REMARKS

The described work leads to new insights into the characteristics, product spectrum, and reaction mechanisms of the recombinant ZS. A deeper study of the enzyme kinetics reveals that ZS follows a substrate inhibition model that has been observed in other terpene cyclases as a putative regulation mechanism for the biosynthesis of terpenoids.

Furthermore, analysis with alternative substrates shows low product specificity of ZS when assayed with C₁₀ substrates but high product specificity when converting C₁₅ isoprenoid diphosphate substrates. The proposed reaction mechanisms reveal critical carbocations and cyclizations through the

biosynthesis of the generated terpenoids. Moreover, the conformational changes during catalysis were analyzed and putative residues were identified involved in the efficient capping of the active site. Our results provide new insights into the complex reaction mechanisms of ZS, pointing to further studies that require an interdisciplinary approach concerning molecular biology, enzymology, and protein engineering.

4. MATERIALS AND METHODS

4.1. Chemicals. Monoterpene substrates GPP, NPP, sesquiterpene substrate (2*E*,6*E*)-FDP, terpene standards, and additional chemicals were purchased from Sigma-Aldrich. FDP isomers (2*E*,6*Z*)-FDP and (2*Z*,6*E*)-FDP were chemically synthesized according to Frister.³⁹ Vetiver oil from Haiti was kindly provided by Symrise.

4.2. Strain and Cultivation. Expression vector harboring the recombinant fused SUMO zizaene synthase gene used for enzyme production corresponds to the pETSUMO::ZIZ(co) (GenBank: KP231534) and was transformed into *E. coli* strain Bl21 (DE3) from Novagen, as described in Hartwig.³⁹ Cultivation was carried out in a 2 L stirred-tank bioreactor (Biostat-B Sartorius, Germany) with 2 L of defined medium⁶¹ supplemented with 20% glucose as the sole carbon source and 50 $\mu\text{g mL}^{-1}$ kanamycin. Inoculation was performed to obtain an initial OD₆₀₀ of 0.1 rel. AU and the bioreactor controller was set to 37 °C, pH 7.5 and controlled with 1 M NaOH, initial stirring at 300 rpm, and air gassing at 0.5 vvm. The dissolved oxygen (pO₂) was monitored by a polygraphic pO₂ sensor, set above 30% saturation, and controlled in cascade mode with the following settings: (1) stirring and (2) pure oxygen gassing. Induction of ZS was initiated when the culture reached OD₆₀₀ 0.7 rel. AU. Thereafter, the temperature was lowered to 20 °C and 0.5 mM isopropyl- β -D-thiogalactoside was added. The induction stage was carried out for 24 h, thereafter the culture broth was centrifuged for 20 min (10000 \times g at 4 °C) and the pellet was stored at -20 °C until further use.

4.3. Enzyme Purification. Cells were resuspended at a concentration of 50 mg of fresh weight per mL with binding buffer (50 mM 3-(*N*-morpholino) propane sulphonic acid (MOPS), pH 7.5, 150 mM NaCl, 10 mM MgCl₂, 10 mM imidazole) and then cell disrupted by ultrasonication (Sartorius Labsonic, Germany) using the following parameters: 0.6 s cycle, 100% amplitude. After centrifugation, soluble protein fractions were filtered through 0.2 μm polyethersulfone syringe filters. Enzyme purification was carried out by immobilized metal affinity chromatography (IMAC) through an ÄKTA Pure FPLC system (GE Healthcare), whereas clarified soluble fractions were applied to a HiPrep IMAC FF 16/10 20 mL column (GE Healthcare) decorated with Ni²⁺ ions. After a proper column wash, the enzyme was eluted with elution buffer (50 mM MOPS, pH 7.5, 150 mM NaCl, 10 mM MgCl₂, 500 mM imidazole). Purified fractions were pooled into a vivaspin 20 10-kDa cut ultrafiltration tubes and the buffer was exchanged to STC storage buffer (50 mM MOPS, pH 7.5, 1 mM dithiothreitol (DTT), 10 mM MgCl₂, 10% (v/v) glycerol) and stored at -20 °C.

4.4. Biotransformation Assay. The catalytic reaction was performed following a modified single-vial assay method from O'Maille et al.²⁵ consisting of reactions of 1 mL with activity buffer (50 mM MOPS, 1 mM DTT, 10 mM MgCl₂, 10% (v/v) glycerol) at pH 7.5, 5 μM (2*E*,6*E*)-FDP, and 0.1 μM purified ZS. Reaction components were gently mixed in 8

mL glass vials and incubated at 30 °C in a water bath for 10 min. Reactions were stopped and products extracted by adding 250 μL of pentane and vigorously vortexed for 60 s. Vials were centrifuged for 10 min (4400 \times g, room temperature), and the organic phase was transferred to 1.5 mL GC vials for further measurements.

4.5. Gas Chromatography Analytics. Quantitative measurements of terpene products were performed by gas chromatography-flame ionization detector (GC-FID) with a GC-2010 plus GC system (Shimadzu, Japan) coupled to a flame ionization detector. Organic phase samples of 2 μL were injected via an autosampler under a splitless mode (injector temperature of 240 °C), and separation was carried out on a Zebron ZB-Wax Plus column (30 m length, 0.25 mm i.d., 0.25 μm film thickness) (Phenomenex). The oven temperature program was set to 40 °C for 20 s, then raised to 200 °C (10 °C min⁻¹) and 0.5 min hold, and then raised to 230 °C (30 °C min⁻¹) and 2 min hold. The FID was heated to 300 °C. Due to the lack of (+)-zizaene and β -acordiadiene standards, quantification was calculated with a calibration curve of α -cedrene standard, which has an equivalent mass (204 *m/z*), as demonstrated previously.²⁴

Reaction products were identified by GC-MS with a 7890B GC system (Agilent) coupled to an Agilent 5977A mass selective detector and equipped with a VF-WAXms capillary column (30 m \times 0.25 mm i.d. \times 0.25 μm) (J&W Scientific). The transfer line and ion source temperature were set at 230 °C and the quadrupole at 150 °C. The ionization energy was set at 70.0 eV, and the scan range, from 33 to 300 *m/z*. Samples of 0.5 μL were injected into the device by the on-column mode, using helium 5.0 as the carrier gas with a constant gas flow of 1 mL min⁻¹. The oven temperature program was set to 40 °C for 3 min and then raised to 230 °C (10 °C min⁻¹) and a 10 min hold. Mass spectra data were analyzed with MassHunter Qualitative Analysis 7.0 (Agilent) and retention indices (RI) calculated according to van Den Dool and Kratz⁶² by an alkane standard solution (C₈-C₃₀). For product identification, mass spectra and RI of samples were compared to those of others available in the mass spectral database NIST 14, literature references, terpenes from the vetiver oil of *Ch. zizanioides*, and/or authentic standards.

4.6. Optimization of the Reaction Conditions. The reaction conditions of the biotransformation assay of (2*E*,6*E*)-FDP with ZS were analyzed using a two-level factorial experimental design with the reaction rate of (+)-zizaene as the study variable. Analyzed factors included temperature and pH, each at two levels (30 °C/pH 7, 42 °C/pH 7, 30 °C/pH 8, and 42 °C/pH 8) and one central point (36 °C/pH 7.5). Reactions for each treatment were carried out in 6 mL of master reaction solutions of activity buffer (Section 2.4) with 5 μM (2*E*,6*E*)-FDP and 0.1 μM purified ZS in 8 mL glass vials. Master solutions were aliquoted rapidly into five 1 mL fractions in 8 mL glass vials and incubated in a water bath with the corresponding temperature for 2, 4, 6, 8, and 10 min. Immediately after incubation, 250 μL of iso-octane was promptly added and the reaction was quenched and products extracted by vigorous shaking. The organic phase was transferred to GC vials after centrifugation, and products were quantified by GC-FID. Each reaction condition was held in triplicates, and the reaction rate ($\mu\text{M min}^{-1}$) of (+)-zizaene was calculated from the average slope, obtained by linear regression.

4.7. Enzyme Kinetics Parameters. Kinetic parameters of ZS were determined using the optimal reaction conditions (36 °C, pH 7.5) with increasing concentrations of the ubiquitous substrate (2*E*,6*E*)-FDP (1–50 μM) and 0.1 μM purified ZS. Reactions proceeded as shown in Section 2.6, with the corresponding concentration of (2*E*,6*E*)-FDP and (+)-zizaene quantified by GC-FID. Kinetic parameters were calculated from the velocities, which corresponded to the reaction rate (μM min⁻¹) of the main product (+)-zizaene. Data was fitted to the substrate inhibition model (eq 1),⁶³ using the enzyme kinetics substrate inhibition module from GraphPad Prism 7 software (GraphPad).

$$v = \frac{V_{\max}[S]}{K_M + [S] \left(1 + \frac{[S]}{K_i}\right)} \quad (1)$$

4.8. Alternative Substrates. Product profiles of monoterpenes substrates GPP/NPP and sesquiterpene substrate isomers (2*E*,6*Z*)-FDP and (2*Z*,6*E*)-FDP were determined by biotransformation assays with ZS. Reactions were performed at 36 °C and pH 7.5 with 5 μM alternative substrate and 0.1 μM purified ZS. Negative controls were carried out by reactions with alternative substrates without ZS. Furthermore, reactions were carried out according to the method described in Section 2.5. Identification of the generated products was performed by GC-FID and GC-MS, as described in Section 2.6.

4.9. Temperature and pH Dependency in Product Specificity. The product ratio of (+)-zizaene and β-acoradiene was assessed through varying temperatures and pH by the biotransformation assay with 5 μM (2*E*,6*E*)-FDP and 0.1 μM purified ZS. Temperature dependence was studied between 21 and 42 °C at pH 7.5, and pH dependency, in the range of 6.5–8.5 pH at 36 °C. The biotransformation assay was performed as explained in Section 2.6, and sesquiterpenes were quantified by GC-FID. The product ratio was calculated as the amount of (+)-zizaene or β-acoradiene divided by the total amount of both.

4.10. Homology and Docking Modeling. Tridimensional structures of ZS were modeled using as templates the crystal structures of 5-epi-aristolochene synthase (TEAS) from *Nicotiana tabacum*, reported by Starks et al.⁸ The ZS open conformation model was built with the unliganded TEAS structure (PDB 5EAS, chain A, 32.4% identity) and the closed conformation with the TEAS structure liganded with 3 Mg²⁺ and FHP (PDB 5EAT, chain A, 31.9% identity). For constructing the homology models, the SWISS-MODEL homology-modeling tool⁶⁴ was used together with the ZS sequence (GenBank: KP231534) and the aforementioned templates.

Furthermore, molecular dockings of (2*E*,6*E*)-FDP and (2*E*,6*E*)-farnesyl cation with the ZS model in closed conformation were carried out using the AutoDockTools suite 1.5.6. (The Scripps Research Institute).⁶⁵ For this, preparation of the ZS receptor file involved the elimination of water molecules, adding and merging of hydrogen atoms, and adding Gasteiger charges. The grid was programmed as follows: grid box (60 × 60 × 100) with default grid spacing (0.375 Å) that covered the active site, map types set directly including Mg²⁺ to the list, and a grid parameter file computed by AutoGrid 4.0. Docking settings included 25 GA runs, Lamarckian genetic algorithm for output, and AutoDock 4.0⁶⁵ used for the generation of the docking parameter file. Docking conformations of both substrates presenting low binding

energy were selected, and metal interactions occurring in the binding site were analyzed by the metal geometry tool from UCSF Chimera 1.11.2 (University of California).⁶⁶ The active-site cavity volume of ZS was measured by the computer atlas of surface topology of proteins (CASTp) version 3.0.⁶⁷ Structural model images were rendered by the program UCSF Chimera.⁶⁶

■ ASSOCIATED CONTENT

Supporting Information

The Supporting Information is available free of charge on the ACS Publications website at DOI: 10.1021/acsomega.9b00242.

Mass spectra of the identified terpene products from the alternative substrates (Tables S1 and S2) (PDF)

■ AUTHOR INFORMATION

Corresponding Author

*E-mail: beutel@iftc.uni-hannover.de. Phone: +49 511 762 2867. Fax: +49 511 762 3004.

ORCID

Sascha Beutel: 0000-0002-0983-9748

Funding

This work was supported by the PINN program from the Ministry of Science, Technology and Telecommunications of Costa Rica (MICITT). The publication of this article was funded by the Open Access Fund of the Leibniz Universität Hannover.

Notes

The authors declare no competing financial interest.

■ ACKNOWLEDGMENTS

We are grateful for the assistance provided for the product identification by Dipl. Daniel Sandner and Dr Ulrich Krings from the Institute of Food Chemistry at the Leibniz Hannover University.

■ REFERENCES

- (1) Christianson, D. W. Structural Biology and Chemistry of the Terpenoid Cyclases. *Chem. Rev.* **2006**, *106*, 3412–3442.
- (2) Merfort, I. Review of the analytical techniques for sesquiterpenes and sesquiterpene lactones. *J. Chromatogr. A* **2002**, *967*, 115–130.
- (3) Cane, D. E. Isoprenoid Biosynthesis. Stereochemistry of the Cyclization of Allylic Pyrophosphates. *Acc. Chem. Res.* **1985**, *18*, 220–226.
- (4) Chen, F.; Tholl, D.; Bohlmann, J.; Pichersky, E. The family of terpene synthases in plants: a mid-size family of genes for specialized metabolism that is highly diversified throughout the kingdom. *Plant J.* **2011**, *66*, 212–229.
- (5) Wendt, K. U.; Schulz, G. E. Isoprenoid biosynthesis: manifold chemistry catalyzed by similar enzymes. *Structure* **1998**, *6*, 127–133.
- (6) Bohlmann, J.; Meyer-Gauen, G.; Croteau, R. Plant terpenoid synthases: Molecular biology and phylogenetic analysis. *Proc. Natl. Acad. Sci. U.S.A.* **1998**, *95*, 4126–4133.
- (7) Aaron, J. A.; Lin, X.; Cane, D. E.; Christianson, D. W. Structure of epi-isozizaene synthase from *Streptomyces coelicolor* A3(2), a platform for new terpenoid cyclization templates. *Biochemistry* **2010**, *49*, 1787–1797.
- (8) Starks, C. M.; Back, K.; Chappell, J.; Noel, J. P. Structural Basis for Cyclic Terpene Biosynthesis by Tobacco 5-Epi-Aristolochene Synthase. *Science* **1997**, *277*, 1815–1820.

- (9) Tarshis, L. C.; Yan, M.; Poulter, C. D.; Sacchetti, J. C. Crystal Structure of Recombinant Farnesyl Diphosphate Synthase at 2.6-Å Resolution. *Biochemistry* **1994**, *33*, 10871–10877.
- (10) Salmon, M.; Laurendon, C.; Vardakou, M.; Cheema, J.; Defernez, M.; Green, S.; Faraldos, J. A.; O'Maille, P. E. Emergence of terpene cyclization in *Artemisia annua*. *Nat. Commun.* **2015**, *6*, No. 6143.
- (11) Degenhardt, J.; Köllner, T. G.; Gershenzon, J. Monoterpene and sesquiterpene synthases and the origin of terpene skeletal diversity in plants. *Phytochemistry* **2009**, *70*, 1621–1637.
- (12) Miller, D. J.; Allemann, R. K. Sesquiterpene synthases: Passive catalysts or active players? *Nat. Prod. Rep.* **2012**, *29*, 60–71.
- (13) Steele, C. L.; Crock, J.; Bohlmann, J.; Croteau, R. Sesquiterpene Synthases from Grand Fir (*Abies grandis*). *J. Biol. Chem.* **1998**, *273*, 2078–2089.
- (14) Sugiura, M.; Ito, S.; Saito, Y.; Niwa, Y.; Koltunow, A. M.; Sugimoto, O.; Sakai, H. Molecular Cloning and Characterization of a Linalool Synthase from Lemon Myrtle. *Biosci. Biotechnol. Biochem.* **2011**, *75*, 1245–1248.
- (15) Alonso, W. R.; Croteau, R. Purification and characterization of the monoterpene cyclase γ -terpinene synthase from *Thymus vulgaris*. *Arch. Biochem. Biophys.* **1991**, *286*, 511–517.
- (16) Frister, T.; Hartwig, S.; Alemdar, S.; Schnatz, K.; Thöns, L.; Scheper, T.; Beutel, S. Characterisation of a Recombinant Patchoulol Synthase Variant for Biocatalytic Production of Terpenes. *Appl. Biochem. Biotechnol.* **2015**, *176*, 2185–2201.
- (17) Jones, C. G.; Moniodis, J.; Zulak, K. G.; Scaffidi, A.; Plummer, J. A.; Ghisalberti, E. L.; Barbour, E. L.; Bohlmann, J. Sandalwood Fragrance Biosynthesis Involves Sesquiterpene Synthases of Both the Terpene Synthase (TPS)-a and TPS-b Subfamilies, including Santalene Synthases. *J. Biol. Chem.* **2011**, *286*, 17445–17454.
- (18) O'Maille, P. E.; Chappell, J.; Noel, J. P. Biosynthetic potential of sesquiterpene synthases: Alternative products of tobacco 5-epi-aristolochene synthase. *Arch. Biochem. Biophys.* **2006**, *448*, 73–82.
- (19) Pripdeevech, P.; Wongpornchai, S.; Marriott, P. J. Comprehensive two-dimensional gas chromatography-mass spectrometry analysis of volatile constituents in Thai vetiver root oils obtained by using different extraction methods. *Phytochem. Anal.* **2010**, *21*, 163–173.
- (20) Anthony, K. P.; Deolu-Sobogun, S. A.; Saleh, M. A. Comprehensive Assessment of Antioxidant Activity of Essential Oils. *J. Food Sci.* **2012**, *77*, C839–C843.
- (21) Alifano, P.; Giudice, L. Del; Talà, A.; Stefano, M. De; Maff, M. E. Microbes at work in perfumery: the microbial community of vetiver root and its involvement in essential oil biogenesis. *Flavour Fragrance J.* **2010**, *25*, 121–122.
- (22) Chou, S.; Lai, C.; Lin, C.; Shih, Y. Study of the chemical composition, antioxidant activity and anti-inflammatory activity of essential oil from *Vetiveria zizanioides*. *Food Chem.* **2012**, *134*, 262–268.
- (23) Belhassen, E.; Filippi, J. J.; Brévard, H.; Joulain, D.; Baldovini, N. Volatile constituents of vetiver: A review. *Flavour Fragrance J.* **2015**, *30*, 26–82.
- (24) Hartwig, S.; Frister, T.; Alemdar, S.; Li, Z.; Scheper, T.; Beutel, S. SUMO-fusion, purification, and characterization of a (+)-zizaene synthase from *Chrysopogon zizanioides*. *Biochem. Biophys. Res. Commun.* **2015**, *458*, 883–889.
- (25) O'Maille, P. E.; Chappell, J.; Noel, J. P. A single-vial analytical and quantitative gas chromatography-mass spectrometry assay for terpene synthases. *Anal. Biochem.* **2004**, *335*, 210–217.
- (26) Hong, Y. J.; Tantillo, D. J. Consequences of conformational preorganization in sesquiterpene biosynthesis: Theoretical studies on the formation of the bisabolene, curcumene, acoradiene, zizaene, cedrene, duprezianene, and sesquithuriferol sesquiterpenes. *J. Am. Chem. Soc.* **2009**, *131*, 7999–8015.
- (27) Martinez, J.; Rosa, P. T. V.; Menut, C.; Leydet, A.; Brat, P.; Pallet, D.; Meireles, M. A. A. Valorization of brazilian vetiver (*Vetiveria zizanioides* (L.) Nash ex Small) oil. *J. Agric. Food Chem.* **2004**, *52*, 6578–6584.
- (28) Zellner, B. D.; Amorim, A. C. L.; de Miranda, A. L. P.; Alves, R. J. V.; Barbosa, J. P.; da Costa, G. L.; Rezende, C. M. Screening of the odour-activity and bioactivity of the essential oils of leaves and flowers of *Hyptis passerina* Mart. from the Brazilian Cerrado. *J. Braz. Chem. Soc.* **2009**, *20*, 322–332.
- (29) Tholl, D. Terpene synthases and the regulation, diversity and biological roles of terpene metabolism. *Curr. Opin. Plant Biol.* **2006**, *9*, 297–304.
- (30) Buchanan, B. B.; Gruissem, W.; Jones, R. L. *Biochemistry and Molecular Biology of Plants*, 2nd ed.; Wiley Blackwell, 2015; pp 1–1280.
- (31) Munk, S. L.; Croteau, R. Purification and Characterization of the Sesquiterpene Cyclase Patchoulol Synthase from *Pogostemon cablin*. *Arch. Biochem. Biophys.* **1990**, *282*, 58–64.
- (32) Mercke, P.; Crock, J.; Croteau, R.; Brodelius, P. E. Cloning, Expression, and Characterization of epi-Cedrol Synthase, a Sesquiterpene Cyclase from *Artemisia annua* L. *Arch. Biochem. Biophys.* **1999**, *369*, 213–222.
- (33) Hartwig, S.; Frister, T.; Alemdar, S.; Li, Z.; Krings, U.; Berger, R. G.; Scheper, T.; Beutel, S. Expression, purification and activity assay of a patchoulol synthase cDNA variant fused to thioredoxin in *Escherichia coli*. *Protein Expression Purif.* **2014**, *97*, 61–71.
- (34) Chahal, K. K.; Bhardwaj, U.; Kaushal, S.; Sandhu, A. K. Chemical composition and biological properties of *Chrysopogon zizanioides* (L.) Roberty syn. *Vetiveria zizanioides* (L.) Nash—A Review. *Indian J. Nat. Prod. Resour.* **2015**, *6*, 251–260.
- (35) Köllner, T. G.; Schnee, C.; Li, S.; Svatoš, A.; Schneider, B.; Gershenzon, J.; Degenhardt, J. Protonation of a neutral (S)- β -bisabolene intermediate is involved in (S)- β -macrocarypene formation by the maize sesquiterpene synthases TPS6 and TPS11. *J. Biol. Chem.* **2008**, *283*, 20779–20788.
- (36) Picaud, S.; Olsson, M. E.; Brodelius, M.; Brodelius, P. E. Cloning, expression, purification and characterization of recombinant (+)-germacrene D synthase from *Zingiber officinale*. *Arch. Biochem. Biophys.* **2006**, *452*, 17–28.
- (37) Rising, K. A.; Starks, C. M.; Noel, J. P.; Chappell, J. Demonstration of germacrene A as an intermediate in 5-Epi-aristolochene synthase catalysis. *J. Am. Chem. Soc.* **2000**, *122*, 1861–1866.
- (38) Mathis, J. R.; Back, K.; Starks, C.; Noel, J.; Poulter, C. D.; Chappell, J. Pre-steady-state study of recombinant sesquiterpene cyclases. *Biochemistry* **1997**, *36*, 8340–8348.
- (39) Frister, T. H. W. Herstellung, Charakterisierung und Anwendung einer rekombinanten Patchoulolsynthase zur biokatalytischen Herstellung von Sesquiterpenen. Thesis, Leibniz Hannover Universität, 2015.
- (40) Priscic, S.; Peters, R. J. Synergistic Substrate Inhibition of ent-Copalyl Diphosphate Synthase: A Potential Feed-Forward Inhibition Mechanism Limiting Gibberellin Metabolism. *Plant Physiol.* **2007**, *144*, 445–454.
- (41) Crock, J.; Wildung, M.; Croteau, R. Isolation and bacterial expression of a sesquiterpene synthase cDNA clone from peppermint (*Mentha x piperita*, L.) that produces the aphid alarm pheromone (E)- β -farnesene. *Proc. Natl. Acad. Sci. U.S.A.* **1997**, *94*, 12833–12838.
- (42) Landmann, C.; Fink, B.; Festner, M.; Dregus, M.; Engel, K.-H.; Schwab, W. Cloning and functional characterization of three terpene synthases from lavender (*Lavandula angustifolia*). *Arch. Biochem. Biophys.* **2007**, *465*, 417–429.
- (43) Mahattanatawee, K.; Perez-Cacho, P. R.; Davenport, T.; Rouseff, R. Comparison of three lychee cultivar odor profiles using gas chromatography - Olfactometry and gas chromatography - Sulfur detection. *J. Agric. Food Chem.* **2007**, *55*, 1939–1944.
- (44) Politeo, O.; Jukic, M.; Milos, M. Chemical composition and antioxidant capacity of free volatile aglycones from basil (*Ocimum basilicum* L.) compared with its essential oil. *Food Chem.* **2007**, *101*, 379–385.
- (45) Stashenko, E. E.; Cervantes, M.; Combariza, Y.; Fuentes, H.; Martinez, J. R. HRGC FID and HRGC MSD analysis of the secondary metabolites obtained by different extraction methods from

Lepechinia schiedeana, and *in vitro* evaluation of its antioxidant activity. *J. High Resolut. Chromatogr.* **1999**, *22*, 343–349.

(46) Varming, C.; Andersen, M. L.; Poll, L. Volatile monoterpenes in black currant (*Ribes nigrum* L.) juice: Effects of heating and enzymatic treatment by β -glucosidase. *J. Agric. Food Chem.* **2006**, *54*, 2298–2302.

(47) Verzera, A.; Trozzi, A.; Zappalá, M.; Concurso, C.; Cotroneo, A. Essential oil composition of *Citrus meyerii* Y. Tan. and *Citrus medica* L. cv. Diamante and their lemon hybrids. *J. Agric. Food Chem.* **2005**, *53*, 4890–4894.

(48) Aubert, C.; Chanforan, C. Postharvest changes in physicochemical properties and volatile constituents of apricot (*Prunus armeniaca* L.). Characterization of 28 cultivars. *J. Agric. Food Chem.* **2007**, *55*, 3074–3082.

(49) Peña, R. M.; Barciela, J.; Herrero, C.; García-Martín, S. Optimization of solid-phase microextraction methods for GC-MS determination of terpenes in wine. *J. Sci. Food Agric.* **2005**, *85*, 1227–1234.

(50) Brat, P.; Rega, B.; Alter, P.; Reynes, M.; Brillouet, J. M. Distribution of volatile compounds in the pulp, cloud, and serum of freshly squeezed orange juice. *J. Agric. Food Chem.* **2003**, *51*, 3442–3447.

(51) Bartley, J. P.; Jacobs, A. L. Effects of drying on flavour compounds in Australian-grown ginger (*Zingiber officinale*). *J. Sci. Food Agric.* **2000**, *80*, 209–215.

(52) Seo, W. H.; Baek, H. H. Identification of characteristic aroma-active compounds from water dropwort (*Oenanthe javanica* DC.). *J. Agric. Food Chem.* **2005**, *53*, 6766–6770.

(53) Kampranis, S.; Ioannidis, D.; Purvis, A.; Mahrez, W.; Ninga, E.; Katerelos, N. A.; Anssour, S.; Dunwell, J. M.; Degenhardt, J.; Makris, A. M.; Goodenough, P. W.; Johnson, C. B. Rational Conversion of Substrate and Product Specificity in a *Salvia* Monoterpene Synthase: Structural Insights into the Evolution of Terpene Synthase Function. *Plant Cell* **2007**, *19*, 1–13.

(54) Schnee, C.; Köllner, T. G.; Gershenzon, J.; Degenhardt, J. The Maize Gene terpene synthase 1 Encodes a Sesquiterpene Synthase Catalyzing the Formation of (E)- β -Farnesene, (E)-Nerolidol, and (E,E)-Farnesol after Herbivore Damage. *Plant Physiol.* **2002**, *130*, 2049–2060.

(55) Rupasinghe, H. P. V.; Paliyath, G.; Murr, D. P. Sesquiterpene α -Farnesene Synthase: Partial Purification, Characterization, and Activity in Relation to Superficial Scald Development in Apples. *J. Am. Soc. Hortic. Sci.* **1998**, *123*, 882–886.

(56) Picaud, S.; Brodelius, M.; Brodelius, P. E. Expression, purification, and characterization of recombinant amorpho-4,11-diene synthase from *Artemisia annua* L. *Phytochemistry* **2005**, *66*, 961–967.

(57) Vedula, L. S.; Rynkiewicz, M. J.; Pyun, H.; Coates, R. M.; Cane, D. E.; Christianson, D. W. Molecular Recognition of the Substrate Diphosphate Group Governs Product Diversity in Trichodiene Synthase Mutants. *Biochemistry* **2005**, *44*, 6153–6163.

(58) Vedula, L. S.; Cane, D. E.; Christianson, D. W. Role of Arginine-304 in the Diphosphate-Triggered Active Site Closure Mechanism of Trichodiene Synthase. *Biochemistry* **2005**, *44*, 12719–12727.

(59) López-Gallego, F.; Wawrzyn, G. T.; Schmidt-Dannert, C. Selectivity of Fungal Sesquiterpene Synthases: Role of the Active Site's H-1 α Loop in Catalysis. *Appl. Environ. Microbiol.* **2010**, *76*, 7723–7733.

(60) Lopez-Gallego, F.; Agger, S. A.; Pella, D. A.; Distefano, M. D.; Schmidt-Dannert, C. Sesquiterpene synthases Cop4 and Cop6 from *Coprinus cinereus*: Catalytic promiscuity and cyclization of farnesyl pyrophosphate geometrical isomers. *Chembiochem* **2010**, *11*, 1093–1106.

(61) Rodríguez-Aparicio, L. B.; Reglero, A.; Ortiz, A. I.; Luengo, J. M. Effect of physical and chemical conditions on the production of colominic acid by *E. coli* in defined medium. *Appl. Microbiol. Biotechnol.* **1988**, *27*, 474–483.

(62) van Den Dool, H.; Kratz, P. A generalization of the retention index system including linear temperature programmed gas-liquid partition chromatography. *J. Chromatogr. A* **1963**, *11*, 463–471.

(63) Copeland, R. A. *Enzymes: A Practical Introduction to Structure, Mechanism, and Data Analysis*, 2nd ed.; Wiley-VCH, 2000; pp 1–416.

(64) Biasini, M.; Bienert, S.; Waterhouse, A.; Arnold, K.; Studer, G.; Schmidt, T.; Kiefer, F.; Cassarino, T. G.; Bertoni, M.; Bordoli, L.; Schwede, T. SWISS-MODEL: modelling protein tertiary and quaternary structure using evolutionary information. *Nucleic Acids Res.* **2014**, *42*, W252–W258.

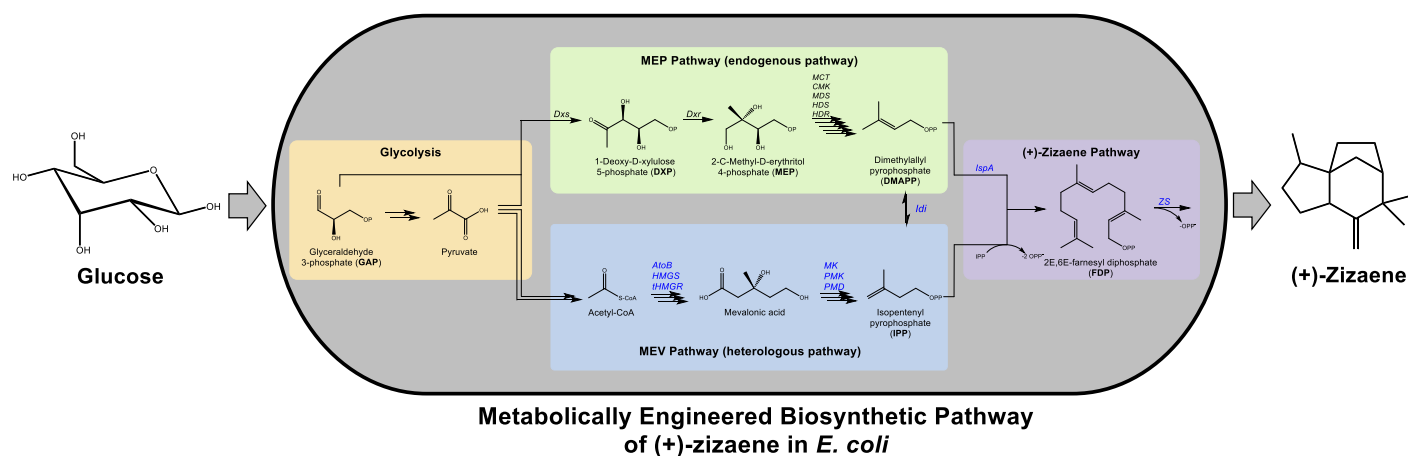
(65) Morris, G. M.; Huey, R.; Lindstrom, W.; Sanner, M. F.; Belew, R. K.; Goodsell, D. S.; Olson, A. J. AutoDock4 and AutoDockTools4: Automated docking with selective receptor flexibility. *J. Comput. Chem.* **2009**, *30*, 2785–2791.

(66) Pettersen, E. F.; Goddard, T. D.; Huang, C. C.; Couch, G. S.; Greenblatt, D. M.; Meng, E. C.; Ferrin, T. E. UCSF Chimera - A visualization system for exploratory research and analysis. *J. Comput. Chem.* **2004**, *25*, 1605–1612.

(67) Dundas, J.; Ouyang, Z.; Tseng, J.; Binkowski, A.; Turpaz, Y.; Liang, J. CASTp: computed atlas of surface topography of proteins with structural and topographical mapping of functionally annotated residues. *Nucleic Acids Res.* **2006**, *34*, W116–W118.

CHAPTER 2

Modulating the precursor and terpene synthase supply for the whole-cell biocatalytic production of the sesquiterpene (+)-zizaene in a pathway engineered *E. coli*



Chapter published in: Aguilar, F.; Scheper, T.; Beutel, S. Modulating the precursor and terpene synthase supply for the whole-cell biocatalytic production of the sesquiterpene (+)-zizaene in a pathway engineered *E. coli*. *Genes* 2019, 10, 478. DOI:10.3390/genes10060478

4.2. Modulating the precursor and terpene synthase supply for the whole-cell biocatalytic production of the sesquiterpene (+)-zizaene in a pathway engineered *E. coli*

Advances in synthetic biology have enabled the metabolic engineering of biosynthetic pathways from plant-based terpenes into microorganisms, usually engineered into *E. coli* or yeast as host systems. Specifically, the engineering of the MEV-pathway and the TPS, the critical enzyme for terpene biosynthesis, have contributed to the microbial production of fragrant terpenes. However, the efficient production of terpenes requires a balance in the supply of FDP and TPS. Therefore, chapter 2 tackles the optimization of the metabolic flux towards (+)-zizaene by optimizing the supply of FDP and the ZS, engineered in *E. coli* strains.

As a first attempt for (+)-zizaene bio-production, the ZS gene was overexpressed in *E. coli*, using the FDP from the endogenous MEP-pathway from *E. coli*. Although the titers were low, the overexpression of soluble ZS protein amounts was high, suggesting a low supply of endogenous FDP.

To improve the substrate supply, the exogenous MEV-pathway was engineered with the ZS gene cloned downstream from the operon in a poly-cistronic pMevZS vector, which augmented the (+)-zizaene titer by 2.7-fold when compared to the first attempt. Paradoxically, the soluble ZS protein amounts declined, suggesting that the limiting supply shifted to the ZS.

As a solution, the cloning strategy changed towards multiple mono-cistronic plasmid strains and two promoters (T7 and P_{BAD}) were tested. As expected, the multi-plasmid TZS+Mev strain with the strong T7 promoter improved the zizaene titer 7.2-fold more than the poly-cistronic MevZS strain. Moreover, SDS-PAGE gels confirmed a dramatic improvement in the overexpression of the soluble ZS protein amounts from the TZS+Mev strain.

In an effort to further improve the (+)-zizaene titer, the ZS supply was increased by applying a technique used mostly for plant transformation, the overexpression of multi-gene copies. Therefore, the TZS+MevZS strain was constructed by cloning two copies of the ZS gene into two different plasmids, under the control of two different promoters (T7 and *lacUV5*). As a result, this strain improved the (+)-zizaene titer 1.3-fold more when compared to that of the one gene copy strain (TZS+Mev). These observations confirmed that the bottleneck with the one gene copy strain was still the ZS supply and that the metabolic flux between the substrate FDP and ZS achieved its maximum optimization level by overexpressing the ZS gene with two gene copies.

After demonstrating the biotechnological production of (+)-zizaene, the optimization of the fermentation conditions was studied. For that, the culture media, pH, temperature and *E. coli* B strains were evaluated and the (+)-zizaene titers improved 2.2-fold, achieving a (+)-zizaene production of 25.09 mg L⁻¹. These results offer the basis for the development of the (+)-zizaene bioprocess and provide an alternative method for the metabolic engineering of terpenes.

Article

Modulating the Precursor and Terpene Synthase Supply for the Whole-Cell Biocatalytic Production of the Sesquiterpene (+)-Zizaene in a Pathway Engineered *E. coli*

Francisco Aguilar , Thomas Scheper and Sascha Beutel *

Institute of Technical Chemistry, Leibniz University of Hannover, Callinstr. 5, 30167 Hannover, Germany; aguilar@iftc.uni-hannover.de (F.A.); scheper@iftc.uni-hannover.de (T.S.)

* Correspondence: beutel@iftc.uni-hannover.de; Tel.: +49-511-762-2867; Fax: +49-511-762-3004

Received: 19 May 2019; Accepted: 20 June 2019; Published: 24 June 2019



Abstract: The vetiver essential oil from *Chrysopogon zizanioides* contains fragrant sesquiterpenes used widely in the formulation of nearly 20% of men's cosmetics. The growing demand and issues in the supply have raised interest in the microbial production of the sesquiterpene khusimol, the main compound of the vetiver essential oil due to its woody smell. In this study, we engineered the biosynthetic pathway for the production of (+)-zizaene, the immediate precursor of khusimol. A systematic approach of metabolic engineering in *Escherichia coli* was applied to modulate the critical bottlenecks of the metabolic flux towards (+)-zizaene. Initially, production of (+)-zizaene was possible with the endogenous methylerythritol phosphate pathway and the codon-optimized zizaene synthase (ZS). Raising the precursor E,E-farnesyl diphosphate supply through the mevalonate pathway improved the (+)-zizaene titers 2.7-fold, although a limitation of the ZS supply was observed. To increase the ZS supply, distinct promoters were tested for the expression of the ZS gene, which augmented 7.2-fold in the (+)-zizaene titers. Final metabolic enhancement for the ZS supply by using a multi-plasmid strain harboring multiple copies of the ZS gene improved the (+)-zizaene titers 1.3-fold. The optimization of the fermentation conditions increased the (+)-zizaene titers 2.2-fold, achieving the highest (+)-zizaene titer of 25.09 mg L⁻¹. This study provides an alternative strategy to enhance the terpene synthase supply for the engineering of isoprenoids. Moreover, it demonstrates the development of a novel microbial platform for the sustainable production of fragrant molecules for the cosmetic industry.

Keywords: khusimene; (+)-zizaene; vetiver essential oil; khusimol; sesquiterpenes; microbial production; metabolic engineering

1. Introduction

The cosmetic industry has extensively used essential oils for the formulation of perfumes due to their complex mixture of fragrant hydrocarbons such as ketones, ethers, esters, alcohols, aldehydes, and terpenoids [1]. From these natural products, terpenes such as volatile monoterpenes, sesquiterpenes, and diterpenes are the main constituents, which confer the specific odor to each essential oil [2].

Among the distinct essential oils, the vetiver essential oil (VEO) from the *Ch. zizanioides* grass has drawn growing attention, because it is used in nearly 20% of men's luxury perfumes [3]. Characterized by its dark woody smell, VEO holds a world production of 300–350 tons per year [4] with prices ranging from \$380–\$500 per kg in 2018 [5] and expected growth in the market of \$169.5 million for 2022 [6]. Industrial production of VEO is performed traditionally by steam distillation from vetiver roots, harvested after 12–18 months of growth and at 1–2 m length; usually, this process attains

an extraction yield of 0.2–3% and can be improved to 4% through supercritical fluid extraction [3,7]. The recurrent shortages in the supply of VEO from the main producer, Haiti due to rainfalls and earthquakes [3,5], and the increasing market demand has raised the interest towards a reliable biotechnological production of the main constituent of VEO, the sesquiterpene khusimol, which grants the distinctive woody smell.

Similar to most plant sesquiterpenes, the biosynthesis of khusimol initiates from the glycolysis cycle, which generates the precursors' glyceraldehyde 3-phosphate (GAP) and pyruvate for the plastidial methylerythritol phosphate (MEP) pathway, and acetyl coenzyme A (Acetyl-CoA) for the cytoplasmic mevalonate (MEV) pathway [8]. Both pathways converge and catalyze the formation of the terpene precursors isopentenyl pyrophosphate (IPP) and isomer dimethylallyl pyrophosphate (DMAPP), which are further assembled by the farnesyl diphosphate synthase (*IspA*) to form the universal sesquiterpene substrate E,E-farnesyl diphosphate (FDP) [9]. In the (+)-zizaene (syn. khusimene) pathway, FDP is cyclized by the zizaene synthase (ZS) to yield (+)-zizaene and further hydroxylated to khusimol by a specific P450 cytochrome monooxygenase [10].

The biosynthetic pathway of khusimol should be possible in *E. coli* because of the positive results for the in vivo production of many sesquiterpenes [11]. Contrary to plants, *E. coli* produces endogenous FDP exclusively by the MEP pathway and is vital for the biosynthesis of the intermediates undecaprenyl diphosphate (UDP) and octaprenyl diphosphate (ODP) [12]. Accordingly, UDP is the direct precursor of peptidoglycans, used for cell wall formation [13], and ODP is involved in the respiratory chain for the biosynthesis of distinct quinones [14]. Consequently, amounts of FDP in *E. coli* are limited; thus, efforts have been made to engineer the MEP pathway to enhance the supply of FDP. As an example, the overexpression of the MEP pathway genes 1-Deoxy-D-xylulose 5-phosphate synthase (DXS) and 1-deoxy-D-xylulose 5-phosphate reductoisomerase (DXR) increased the FDP levels and improved the amounts of lycopene up to 22 mg L⁻¹ [15]. Similarly, overexpression of the DXS synthase and additionally, the isoprenyl diphosphate isomerase (Idi) with the farnesyl pyrophosphate synthase (FPS) reached valerenadiene titers of 2.09 mg L⁻¹ [12]. Although overexpression of the MEP pathway improved the precursor supply, the terpene titers did not reach industrial levels, possibly due to control mechanisms of *E. coli* or the formation of intermediates that limited the precursor supply [16,17].

As an alternative to raise the FDP supply, the heterologous MEV pathway was engineered in *E. coli* by Keasling and co-workers for the in vivo production of amorpho-4,11-diene [17]. The heterologous pathway involved the cloning of eight genes from *E. coli* and *Saccharomyces cerevisiae* into two operons: MevT operon converted acetyl-CoA to mevalonate and MBIS operon catalyzed mevalonate to IPP and DMAPP that led to FDP, yielding 112.2 mg L⁻¹ as the highest amorpho-4,11-diene titer. The microbial platform was further enhanced for the production of bisabolene by optimizing the codon usage to *E. coli* for the *S. cerevisiae* genes and assembling the eight genes into one single operon under the control of the *lacUV5* (MevT genes) and *trc* promoter (MBIS genes) [18]. As a result, the upgraded platform boosted the FDP supply and achieved titers of 900 mg L⁻¹ of bisabolene.

The previously mentioned studies augmented the supply of the substrate FDP, which is further catalyzed in the terpene pathway by a terpene synthase (TPS), performing complex reactions that yield sesquiterpenes with precise structure and stereochemistry [19]. In the biosynthesis of khusimol, the TPS is the ZS that catalyzes the cyclization of FDP to the tricyclic (+)-zizaene. Its enzymatic characterization has been described by a recombinant codon-optimized variant fused to the small ubiquitin-related modifier (SUMO), which increased the solubility of ZS and expressed heterologously in *E. coli* [10]. Moreover, the catalytical specificity and enzymatic kinetics of the ZS enzyme have been further characterized [20].

In this study, we report the metabolic engineering of (+)-zizaene biosynthesis in *E. coli* strains. The engineering of the biosynthetic pathway involved the overexpression of the MEV pathway to enhance the FDP supply, the evaluation of promoters to efficiently express the ZS, and the engineering of multi-plasmid strains with multiple copies of ZS to boost the ZS supply. Moreover, optimization of

the fermentation conditions and evaluation of *E. coli* strains were analyzed to improve the production of (+)-zizaene.

2. Materials and Methods

2.1. Engineering of Vectors and Strains

The description of vectors and strains is summarized in Table 2. The pETSUMO::ZIZ(co) vector was obtained from our previous study [10], and the sequence of the codon-optimized SUMO-fused ZS gene was described in GenBank accession KP231534. The vector pBbA5c-MevT(CO)-MBIS (CO, ispA), encoding the MEV pathway, was a gift from Jay Keasling & Taek Soon Lee (Addgene plasmid #35151). The pJbei-6411 vector for the expression with the arabinose operon was a gift from Taek Soon Lee (Addgene plasmid #47050).

The cloning procedures were carried out by the NEBuilder HiFi DNA Assembly method, and PCR reactions were performed with the Q5 HiFi DNA polymerase, both following the provider protocols (New England BioLabs, USA). Synthesis of oligonucleotides and sanger sequencing for clone confirmation were performed by Microsynth Seqlab (Germany), and primer sequences are described in Table 1.

Table 1. Primers used in this investigation.

Primers	Description	Reference
ZS-F-Mev	catccagcgtaataaataagGATCTAGGAGGTAATGGGCAGCAGCCATCATC	This study
ZS-R-Mev	gagatccttactcgagttgTCACACCGGAATCAGATTACATAC	This study
pJ6411-F-ZS	cccaagattacgtacattg	This study
pJ6411-R-ZS	tctttatcctctagatctttgaattcccaaaaaaacg	This study
ZS-F-pJ6411	ccgttttttgggaattcaaaagatctaggagataaagaaATGGGCAGCAGCCATCATC	This study
ZS-R-pJ6411	tcaatgtacgtaactctgggTCACACCGGAATCAGATTACATAC	This study

Upper case sequences: Inserts. Lower case sequences: backbone vector. Upper case underlined sequences: IRES

For the production of (+)-zizaene by a single polycistronic vector, the ZS gene was cloned into the pMev vector, directly after the *IspA* gene to yield the pMevZS vector. In brief, the ZS gene was amplified from the pETZS vector by respective primers with complementary overhangs to the BamHI site of the pMev vector. Additionally, an internal ribosome entry site (IRES) (GATCTAGGAGGTA) from the MEV operon was cloned upstream from the ZS gene. Thereafter, the pMev vector was digested with BamHI, assembled with the ZS gene and *E. coli* NEB 10-beta competent cloning strain (New England BioLabs), which is specific for large vectors, was transformed with the pMev vector. For the testing of the P_{BAD} promoter through the pJbeiZS plasmid, the cytochrome P450 operon from pJbei-6411 vector was removed, and the ZS gene from the pETZS vector was inserted instead. For that, both the insert and backbone were amplified with complementary overhangs by PCR methods, seamlessly assembled, and *E. coli* TOP10 competent cloning strains (IBA, Germany) were transformed for respective screening.

For the production of (+)-zizaene, *E. coli* expression strains were transformed or co-transformed with the respective plasmids by common methods [21]. An exception was the BZS+Mev strain, where the *E. coli* TOP10 competent cloning strain was used because expression with the arabinose operon requires a non-metabolizing arabinose strain [22].

Table 2. Strains and plasmids used in this investigation.

Plasmid Reference	Plasmid Name	Description (Origin of Replication, Promoter, Antibiotic Resistance and Genes)	Reference
pETZS	pETSUMO::ZIZ(co)	pBR322, PT7, Kan, harboring the codon-optimized SUMO-fused ZS gene from <i>Ch. zizanioides</i>	[10]
pMev	pBbA5c-MevT(CO)-MBIS (CO, ispA)	p15A, PlacUV5, Cam, harboring the mevalonate pathway genes: <i>AtoB</i> , <i>HMGs</i> , <i>tHMGs</i> , <i>MK</i> , <i>PMK</i> , <i>PMD</i> , <i>Idi</i> and <i>IspA</i> *	[18]
pJbei-6411	pJbei-6411	pBBR1, P _{BAD} , Kan, harboring the arabinose operon with the cytochrome P450 (CYP153A6) from <i>Sphingomonas</i> sp.	[23]
pMevZS	pBbA5c-MevT(CO)-MBIS (CO, ispA)-SUMO::ZIZ(co)	p15A, PlacUV5, Cam, harboring the mevalonate pathway genes* and the codon-optimized SUMO-fused ZS gene from <i>Ch. zizanioides</i>	This study
pJbeiZS	pJbei-6411-SUMO::ZIZ(co)	pBBR1, P _{BAD} , Kan, harboring the arabinose operon and the codon-optimized SUMO-fused ZS gene from <i>Ch. zizanioides</i>	This study
Strains	Genotype/Description		Reference
<i>E. coli</i> TOP10	F ⁺ <i>mcrA</i> (<i>mrr-hsdRMS-mcrBC</i>) ϕ 80 <i>lacZ</i> Δ M15 Δ <i>lacX74</i> <i>recA1</i> <i>ara</i> Δ 139 (<i>ara-leu</i>)7697 <i>galU galK rpsL</i> (Str ^R) <i>endA1 nupG</i>		IBA
<i>E. coli</i> BL21(DE3)	F ⁺ <i>ompT hsdS_B</i> (<i>r_B⁻ m_B⁻</i>) <i>gal dcm</i> (DE3)		Novagen
<i>E. coli</i> Tuner(DE3)	F ⁺ <i>ompT hsdS_B</i> (<i>r_B⁻ m_B⁻</i>) <i>gal dcm lacY1</i> (DE3)		Novagen
<i>E. coli</i> NEB 10-beta	Δ (<i>ara-leu</i>) 7697 <i>ara</i> Δ 139 <i>fhuA</i> Δ <i>lacX74 galK16 galE15 e14-ϕ80dlacZ</i> Δ M15 <i>recA1 relA1 endA1 nupG rpsL</i> (Str ^R) <i>rph spoT1</i> Δ (<i>mrr-hsdRMS-mcrBC</i>)		NEB
<i>E. coli</i> SHuffle T7	<i>fhuA2 lacZ::T7 gene1</i> (lon) <i>ompT ahpC gal</i> <i>latt::pNEB3-r1-cDsbC</i> (Spec ^R , lacI ^{fl}) Δ <i>trxB sulA11 R</i> (<i>mcr-73::miniTn10-Tet^S</i>) Δ 2 (<i>dcm</i>) <i>R</i> (<i>zgb-210::Tn10-Tet^S</i>) <i>endA1</i> Δ <i>gor</i> Δ (<i>mcrC-mrr</i>)114::IS10		NEB
<i>E. coli</i> SHuffle T7 <i>lysY</i>	MiniF <i>lysY</i> (Cam ^R)/ <i>fhuA2 lacZ::T7 gene1</i> (lon) <i>ompT ahpC gal</i> <i>latt::pNEB3-r1-cDsbC</i> (Spec ^R , lacI ^{fl}) Δ <i>trxB sulA11 R</i> (<i>mcr-73::miniTn10-Tet^S</i>) Δ 2 (<i>dcm</i>) <i>R</i> (<i>zgb-210::Tn10-Tet^S</i>) <i>endA1</i> Δ <i>gor</i> Δ (<i>mcrC-mrr</i>)114::IS10		NEB
Mev	<i>E. coli</i> BL21(DE3) harboring pMev		This study
ZS	<i>E. coli</i> BL21(DE3) harboring pETZS		This study
MevZS	<i>E. coli</i> BL21(DE3) harboring pMevZS		This study
BZS+Mev	<i>E. coli</i> TOP10 harboring pMev and pJbeiZS		This study
TZS+Mev	<i>E. coli</i> BL21(DE3) harboring pMev and pETZS		This study
TZS+MevZS	<i>E. coli</i> BL21(DE3) harboring pMevZS and pETZS		This study
T-TZS+MevZS	<i>E. coli</i> Tuner(DE3) harboring pMevZS and pETZS		This study
SH-TZS+MevZS	<i>E. coli</i> SHuffle T7 harboring pMevZS and pETZS		This study
SHL-TZS+MevZS	<i>E. coli</i> SHuffle T7 <i>lysY</i> harboring pMevZS and pETZS		This study

Kan, kanamycin and Cam, chloramphenicol.

2.2. Evaluation of the Engineered Strains for the Production (+)-zizaene

Cultivations of *E. coli* were performed by inoculating 100 μ L of respective strains from glycerol stocks to 10 mL Lysogeny Broth (LB) pre-culture broths at 37 °C with respective antibiotics (kanamycin at 30 μ g L⁻¹ and, or chloramphenicol at 34 μ g L⁻¹) until the stationary phase. Furthermore, production cultures in sealed baffled shake-flasks with 35 mL of defined non-inducing broth (DNB) [24] were inoculated with 2% (v/v) of seed culture and grown at 37 °C on a rotatory shaker (150 rpm). After cultures reached a cell density of OD₆₀₀ 0.6, (+)-zizaene production was induced by adding varying levels (0.1, 0.5, and 1.0 mM) of isopropyl- β -D-1-thiogalactopyranoside (IPTG) and an overlay of 4 mL iso-octane at 20 °C, (150 rpm) as a two-phase partitioning culture. After 24 h of induction, samples were taken promptly for analytical measurements that included dried cell weight (DCW), cell density, soluble ZS protein, and (+)-zizaene concentrations.

2.3. Optimization of the Fermentation Conditions for the Production (+)-zizaene

Cultivation and analytical procedures for media evaluation, optimization of growth temperature and media pH, and testing of *E. coli* strains were carried out as described before with the best performing strain. The evaluation of media comprised the defined media: defined non-inducing broth (DNB), M9 minimal medium (M9) [25], and a modified Aparicio defined medium (ADM) with the following composition (g L⁻¹): (NH₄)₂SO₄ 10.0, NaCl 1.2, K₂SO₄ 1.1, MgSO₄·7H₂O 0.15, K₂HPO₄ 9.3, KH₂PO₄ 2.03, CaCl₂ 0.01, FeSO₄·7H₂O 0.001, and CuSO₄·5H₂O 0.001 [26]. Defined media were

set to pH 7.2 and 5 g L⁻¹ of glucose respectively. Additionally, the complex terrific broth (TB) [21] was used as a control. The factorial design for the pH and temperature optimization consisted of two factors with the following levels: pH (6.5, 7, and 7.5) and temperature (16, 20, 24, and 28 °C), for a total of 12 combinations with three replicates. Data were analyzed and plotted using the Minitab 16 software (USA).

2.4. Analytical Measurements

2.4.1. ZS Protein Gel Electrophoresis Analysis

Production culture samples were normalized to an OD₆₀₀ 2, centrifuged for 10 min (10,000× g at 4 °C) and free-media pellet was resuspended in 300 µL extraction buffer (50 mM MOPS, 150 mM NaCl, 5 mM DTT, 10% (v/v) glycerol, pH 7.5). Cells were disrupted through an ultrasonicator (Sartorius Labsonic, Goettingen, Germany) and soluble and insoluble protein fractions were separated after 30 min centrifugation (10,000× g at 4 °C). Protein fraction samples were mixed with 2X loading buffer, heated at 95 °C for 5 min and analyzed through a 10% sodium dodecyl sulfate polyacrylamide gel electrophoresis (SDS-PAGE).

2.4.2. Identification and Measurement of (+)-zizaene by Gas Chromatography Analysis

Samples of 150 µL from the iso-octane overlay from production cultures were transferred to GC-vials for gas chromatography analysis and product identification was carried out through GC-MS using an Agilent 7890B system (Agilent, Santa Clara, CA, USA) with the following settings: sample injections of 0.5 µL on-column mode through a 30 m VF-WAXms capillary column (0.25 mm internal diameter I.D. × 0.25 µm, Agilent, USA); oven program of 40 °C for 3 min, increasing to 230 °C (10 °C min⁻¹) and final hold of 10 min; helium 5.0 carrier gas at a constant gas flow of 1 mL min⁻¹; temperature of 230 °C for ion source, and 150 °C for quadrupole; mass scan range of 33–300 *m/z* and ionization energy to 70 eV. Terpene products were identified by comparison of retention indices [27] and mass spectra of samples with authentic standards from the VEO and references from the mass spectral NIST 14 database.

Quantification of (+)-zizaene was performed by GC-FID with a GC-2010 plus GC system coupled to a flame ionization detector (Shimadzu, Japan) equipped with a 30 m Zebron ZB-Wax Plus column (0.25 mm I.D. × 0.25 µm, Phenomenex, USA). Samples of 1 µL were injected under a splitless mode with an injector temperature of 240 °C. The initial oven temperature was set to 40 °C for 20 s, ramped at 10 °C min⁻¹ to 200 °C, held for 0.5 min, increased at a rate of 30 °C min⁻¹ to 230 °C, and held finally for 2 min. Because the (+)-zizaene standard is not commercially available, an α-cedrene standard was used as an equivalent standard due to the relative abundance of the main peaks from the mass spectra as described in our previous report [20].

3. Results

3.1. Engineering the Production of (+)-zizaene by the MEP Pathway

In this study, we engineered the biosynthetic pathway in *E. coli* for the production of (+)-zizaene, using glucose as the sole carbon source (Figure 1). The key enzyme of the biosynthesis of (+)-zizaene is the ZS, which catalyzes the cyclization of the substrate FDP to (+)-zizaene. Due to the plant origin of TPS, most are expressed poorly in *E. coli*, leading to the formation of insoluble proteins (inclusion bodies) [28,29]. To improve TPS solubility, a recombinant ZS variant was used, which was codon-optimized for *E. coli* and fused with the SUMO moiety from our previous work [30].

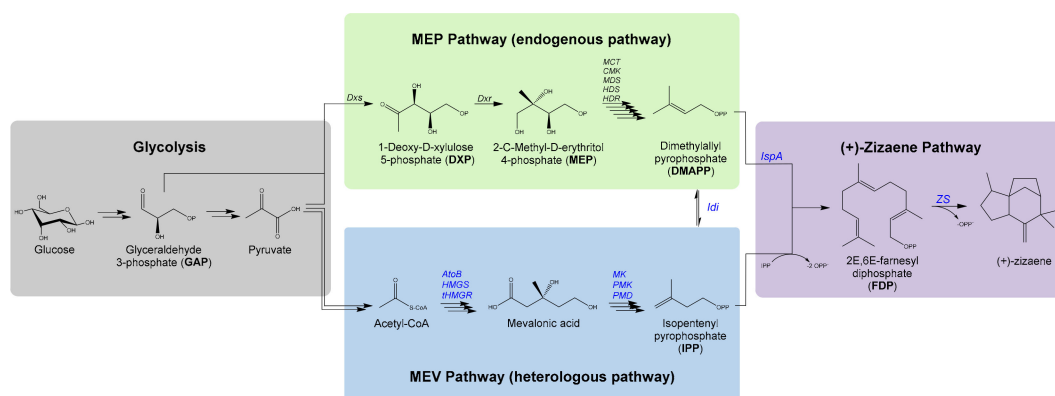


Figure 1. Biosynthetic pathway engineered for the production of (+)-zizaene in *E. coli* by the expression of the native methylerythritol phosphate (MEP) pathway, the heterologous MEV pathway and the (+)-zizaene pathway. Heterologous expressed enzymes highlighted in blue. The MEP pathway comprise the following enzymes: 1-Deoxy-D-xylulose 5-phosphate synthase (*Dxs*), 1-deoxy-D-xylulose 5-phosphate reductoisomerase (*Dxr*), MEP cytidyl transferase (*MCT*), cytidyl MEP kinase (*CMK*), MEP-2,4-cyclodiphosphate synthase (*MDS*), (E)-4-hydroxy-3-methylbut-2-enyl diphosphate synthase (*HDS*), and (E)-4-hydroxy-3-methylbut-2-enyl diphosphate reductase (*HDR*). The MEV heterologous pathway consisted of the following enzymes: acetyl-CoA acetyltransferase (*AtoB*), HMG-CoA synthase (*HMGs*), truncated HMG-CoA reductase (*tHMGR*), mevalonate kinase (*MK*), phosphomevalonate kinase (*PMK*), mevalonate diphosphate decarboxylase (*PMD*), and isoprenyl diphosphate isomerase (*Idi*). The (+)-zizaene pathway comprises the farnesyl diphosphate synthase (*IspA*) and the zizaene synthase (*ZS*).

For the overexpression of (+)-zizaene, the production cultures were performed by the two-phase partitioning method [31] with a DNB medium and an overlay of iso-octane, which reduces the loss of (+)-zizaene due to its volatility. After 24 h of culture, organic phases from production cultures were obtained and analyzed through GC-MS for the identification of terpenes. All tested strains produced (+)-zizaene as the main product (90%) and β -acoradiene as a side product (10%) (Figure 2), except for the *Mev* strain (negative control) because it lacks the *ZS* gene and harbors the MEV pathway (Figure 3a). Additionally, the *Mev* strain produced farnesol, which is a product from the hydroxylation of FDP by endogenous phosphatases from *E. coli* [32].

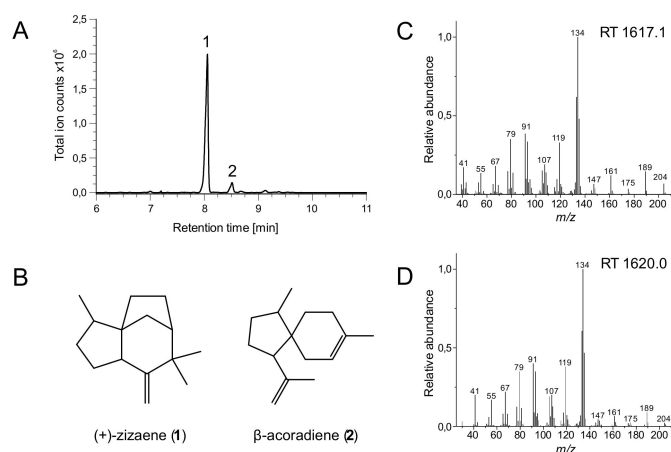


Figure 2. Identification of terpene products by GC-MS. (A) Total ion chromatogram. (B) Chemical structures of the identified products. (C) Mass spectra of (+)-zizaene from the sample of the *ZS+MevZS* strain. (D) Mass spectra of (+)-zizaene authentic standard from the vetiver essential oil. Comparison of mass spectra for β -acoradiene is shown in the Supplementary Table S1.

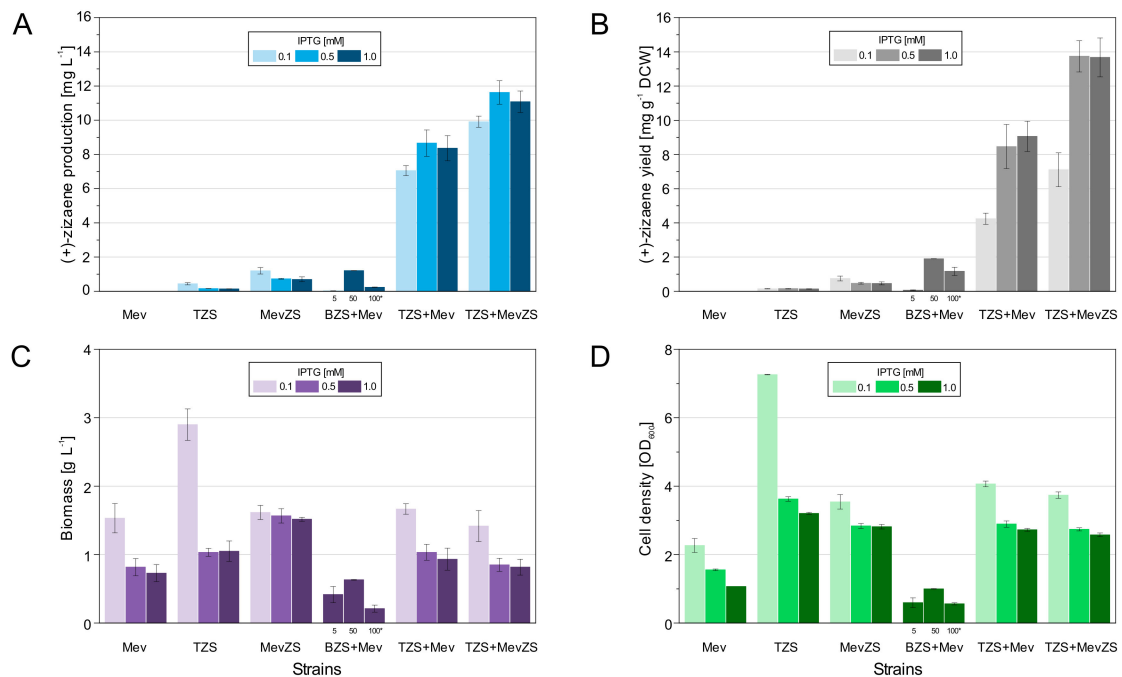


Figure 3. Comparison of the performance of the engineered *E. coli* BL21(DE3) strains induced at different IPTG levels. (A) (+)-zizaene titers. (B) (+)-zizaene yields. (C) biomass from cell dry weight (D) cell density. Data are the mean of four independent replicates from production cultures after 24 h of induction with DNB medium, and the error bars represent the standard deviation. * BZS+Mev *E. coli* Top10 strain induced with 1 mM IPTG and different levels of arabinose (Ara).

As a first attempt to produce (+)-zizaene, the TZS strain was constructed with the ZS gene under the control of the T7 promoter and the FDP supply originated from the endogenous MEP pathway from *E. coli* BL21(DE3) strain. As shown in Figure 3a, the (+)-zizaene titer of the TZS strain was the lowest when compared to all the tested strains; however, it achieved the highest cell growth (biomass 2.9 g L^{-1} and cell density of $\text{OD}_{600} 7.2$, Figure 3c,d) and amounts of soluble ZS protein (Figure 4b) for the TZS strain induced at 0.1 mM IPTG. These observations suggest a low metabolic burden due to the overexpression of a single recombinant protein (ZS). Moreover, it evidences the limited supply of the endogenous FDP from *E. coli*, which is required for the biosynthesis of isoprenoid quinones and peptidoglycans [13,14].

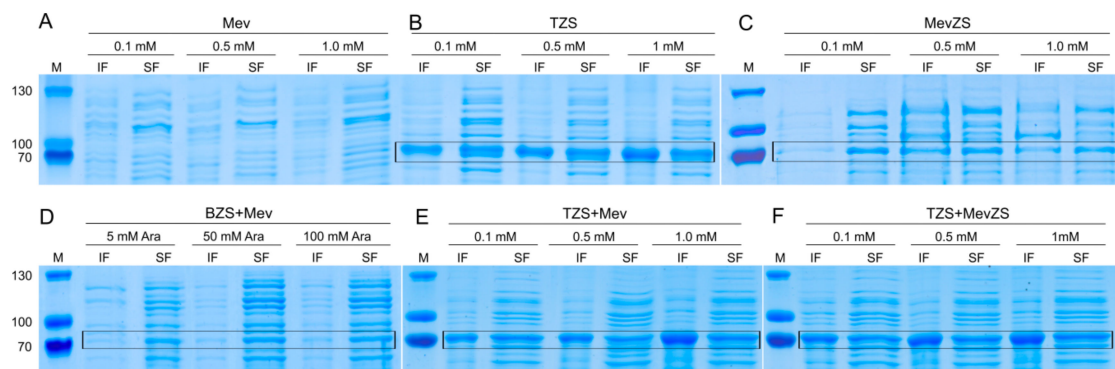


Figure 4. Evaluation of the overexpression of the soluble (SF) and insoluble (IF) ZS protein fractions from the engineered *E. coli* BL21(DE3) strains, induced at different IPTG levels by 10% SDS-PAGE. (M) molecular marker. * BZS+Mev induced with 1 mM IPTG and different levels of arabinose (Ara).

3.2. Improving the Titers of (+)-zizaene through the Mevalonate Pathway

To raise the supply of the precursor FDP, the polycistronic pMevZS vector was constructed with the ZS gene and the exogenous MEV pathway (Figure S1), which was obtained from the pMEV vector that harbors the following genes: *AtoB*, *HMGS**, *tHMGR**, *MK**, *PMK**, *PMD*, *IDI*, and *IspA* (*genes from *S. cerevisiae* that were codon-optimized to *E. coli*) [18]. Consequently, a single mRNA transcript was expressed under the control of the *lacUV5* promoter. As a result, overexpression of the heterologous MEV pathway with the ZS gene (MevZS strain) induced with 0.1 mM IPTG augmented the (+)-zizaene production and yield by 2.7 and 5-fold respectively when compared to the TZS strain (Figure 3a,b). Thus, a relation was observed in both TZS and MevZS strains, where higher amounts of IPTG increased the overexpression of insoluble ZS protein (Figure 4a,c). Moreover, overexpression of the MEV pathway generated a strong metabolic burden, where cell growth diminished by 1.8-fold biomass and 2.1-fold cell density when compared to that of the strain lacking the MEV pathway (TZS strain) (Figure 3c,d). Although the overexpression of the MEV pathway raised the FDP supply, the production of soluble ZS protein declined dramatically when compared to the TZS strain (Figure 4c), suggesting that the ZS supply became the limiting factor.

3.3. Effect of Promoters on the Overexpression of the ZS Gene

The low ZS supply demonstrated by the MevZS strain could result from either expression mechanisms of polycistronic vectors and, or by the promoter strength. To prove these hypotheses, multi-vector strains were constructed harboring the following plasmids: polycistronic pMev vector (MEV pathway) and monocistronic ZS vector ((+)-zizaene pathway). Two versions of the ZS vectors were constructed in order to test the effect of promoters on the ZS supply. The designed ZS vectors comprised the pETZS vector with the strong T7 promoter and the pJbeiZS vector harboring the weak P_{BAD} promoter (Figure S2). The overexpression of the ZS gene under the control of the P_{BAD} promoter (BZS+Mev strain) did not enhance the (+)-zizaene titers when compared to the MevZS strain, but it did increase the (+)-zizaene yield by 2.5-fold when induced with 50 mM arabinose (Figure 3b). Nevertheless, the BZS+Mev strain showed the lowest cell growth of all the tested strains (biomass 0.63 g L⁻¹ and cell density of OD₆₀₀ 1.0, Figure 3c,d). Furthermore, overexpression of the ZS gene controlled by the T7 promoter (TZS+Mev strain) raised the amounts of soluble ZS protein when compared to that of the induced with the P_{BAD} promoter (Figure 4d,e). As a consequence, the (+)-zizaene production and yield augmented 7.2 and 4.4-fold, respectively when compared to the BZS+Mev strain, and 7.2 and 11.3-fold correspondingly when compared to the MevZS strain (Figure 3a,b). Such strategy improved the ZS supply and consequently restored the flux balance of the (+)-zizaene biosynthesis.

3.4. Enhancing the ZS Supply by Engineering Multiple Copies of the ZS Gene

Overexpression of the ZS gene with the T7 promoter seemed to overcome the ZS supply limitations of the MevZS and BZS+Mev strains. Nevertheless, the optimal amount of ZS to catalyze the FDP supply still remains unknown. To increase the ZS supply even further, a multi-vector strain that harbored two copies of the ZS gene was engineered. For that, the TZS+MevZS strain was developed, harboring the pETZS and pMevZS vectors, and controlling the expression of the ZS genes by the T7 and *lacUV5* promoters. As a result, the multi-copy ZS gene strain achieved the best results of all the constructed strains (titer: 13.7 mg L⁻¹ and yield 11.6 mg g⁻¹ DCW) and raised 1.3-fold the (+)-zizaene titers and 1.6-fold the yields in comparison to the TZS+Mev strain (one ZS gene copy) (Figure 3a,b). Moreover, it augmented the (+)-zizaene production and titer by 9.7 and 18.4-fold correspondingly when compared to the single-vector MevZS strain. These results suggest that the bottleneck of the metabolic flux was still the ZS supply, which could be improved by the combination of the T7 promoter with multiple copies of the ZS gene, harbored on a multi-vector strain.

3.5. Optimization of Fermentation Conditions and Evaluation of *E. coli* Strains

To raise further the production of (+)-zizaene, fermentation tests were carried out at shake flask scale, comprising the evaluation of culture media, optimization of growth temperature and media pH, and testing of *E. coli* strains. Accordingly, the mineral-salt defined media DNB, ADM, and M9 were tested due to their previous use in metabolic engineering studies and suitability to control carbon-limited growth required for fed-batch or continuous cultivations to reach high-cell density cultures [33]. To compare the performance of defined media against complex media, the TB broth was used. As a result, substantial differences were observed between the defined media, where the highest (+)-zizaene levels and yields were obtained by ADM media, followed by DNB and M9 media (Figure 5a). Consequently, the ADM medium was 1.8-fold higher than the DNB medium for the (+)-zizaene titers and 1.2-fold higher for the (+)-zizaene yields. Both tested media were of similar formulation with the exception of the trace elements and nitrogen composition, whereas the concentration of nitrogen of the ADM medium was 2.5-fold higher than the DNB medium. Likewise, cell growth followed a similar behavior to that of the (+)-zizaene production among the tested media, where the complex TB broth had the highest cell growth when compared to the defined media tests (Figure 5b). However, the ADM medium obtained the highest (+)-zizaene yields ($16.2 \text{ mg g DCW}^{-1}$) when compared to all the tests and was consequently selected for further tests.

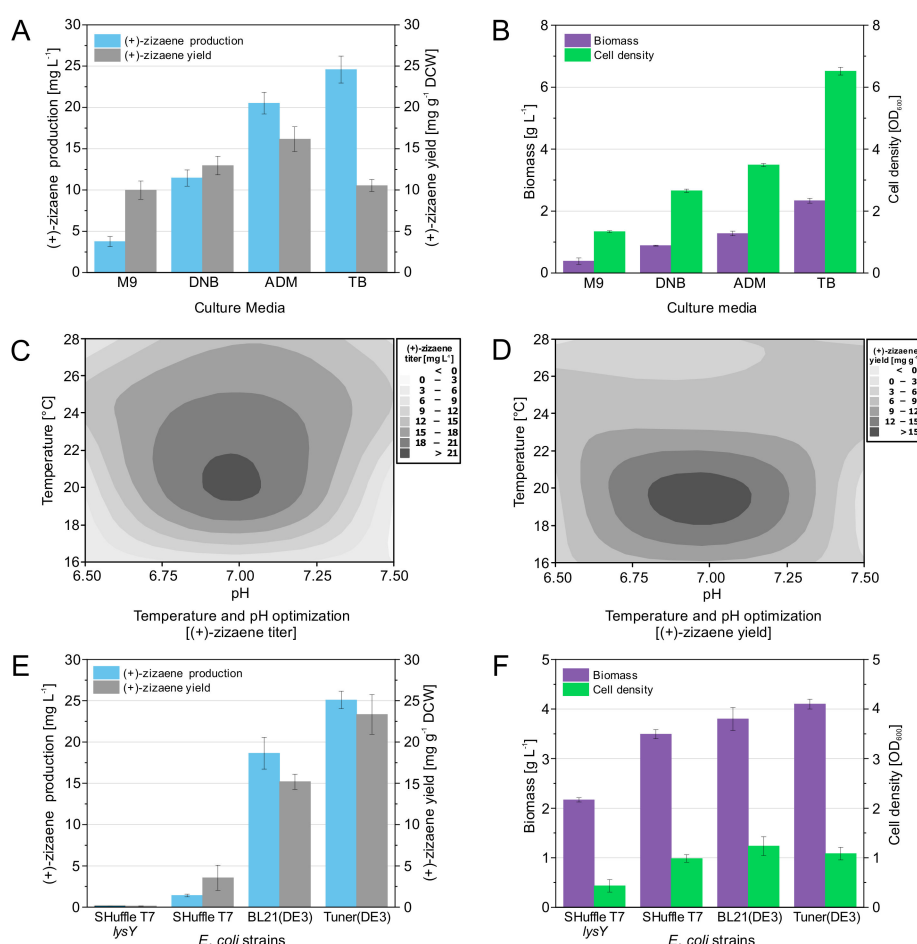


Figure 5. Optimization of the fermentation conditions and testing of *E. coli* strains for the improvement of the terpene performance. Evaluation of production media: (A) (+)-zizaene titers and yields, (B) biomass and cell density. Optimization of growth temperature and media pH: (C) (+)-zizaene titers, (D) (+)-zizaene yields. Evaluation of *E. coli* strains: (E) (+)-zizaene titers and yields, (F) biomass and cell density. Data are the mean of four independent replicates from production cultures after 24 h of induction, and the error bars represent the standard deviation.

To further improve the fermentation conditions, factorial designs of two levels were implemented for the optimization of growth temperature and pH of the ADM medium. Accordingly, optimal (+)-zizaene levels were found between 19.5–21.8 °C and pH 6.8–7.08 (Figure 5c) and for (+)-zizaene yields between 18–20.8 °C and pH 6.8–7.1 (Figure 5d). Temperature affected (+)-zizaene levels differently than yields, whereas moderate (+)-zizaene levels (15–21 mg L⁻¹) were shown at a broad range of temperature (17.5–27.7 °C). On the contrary, pH had nearly the same effect on both variables. Additionally, the highest levels of soluble ZS protein were found at lower pH and temperatures (Figure 6b). Tests at pH 6.5 also produced the highest amounts of insoluble ZS protein, resulting in the lowest (+)-zizaene levels. Similarly, tests carried out at 16 °C dropped the (+)-zizaene levels despite the high amounts of soluble ZS protein, possibly due to enzymatic mechanisms. As a result, the optimal fermentation conditions were determined as 20 °C and pH 7.0, which improved the (+)-zizaene levels to 21.5 mg L⁻¹ and yields to 16.2 mg g⁻¹ DCW.

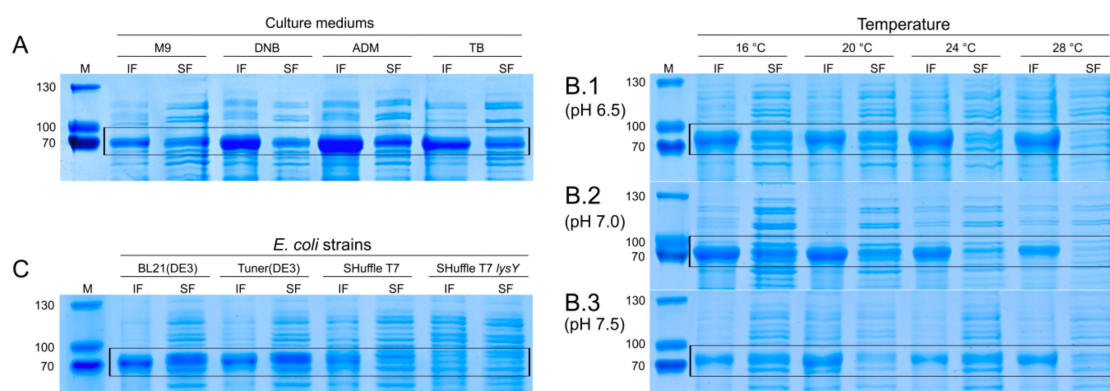


Figure 6. Analysis of the over-expression of soluble (SF) and insoluble (IF) ZS protein fractions from the optimization of fermentation conditions and testing of *E. coli* strains by 10% SDS-PAGE. (A) Culture media test. (B) Temperature and pH optimization. (C) *E. coli* strains test. (M) molecular marker.

Strain tests were carried out under optimal fermentation conditions (ADM medium, 20 °C and pH 7) to assess the features of the *E. coli* B strains SHuffle T7, SHuffle T7 *lysY*, Tuner(DE3) and BL21(DE3), and measure their impact on the production of (+)-zizaene. The SHuffle-based strains were selected to test if there could be an enhancement in the folding of ZS due to the effect of a disulfide bond chaperone DsbC. Additionally, the SHuffle T7 *lysY* variant reduces the basal expression for toxic genes through the expression of lysozyme, coded by the *lysY* gene. Similarly, the BL21(DE3) variant, the Tuner(DE3) strain lacks the *lacY* gene that codes for the β -galactosidase permease, which allows fine-tuning for induction and reduces basal expression. As a control, the BL21(DE3) strain was used. As presented in Figure 5e, the differences between the BL21-based and SHuffle-based strains were remarkable; unexpectedly, the best results were shown by the Tuner(DE3) strain, followed by the BL21(DE3), SHuffle T7, and SHuffle T7 *lysY* strains. These observations demonstrate that the strains expressing the lowest number of recombinant proteins produced the highest cell growth (Figure 5f), and soluble ZS protein amounts (Figure 6c), and consequently, the highest (+)-zizaene titers and yields (shown by increasing number of recombinant proteins: Tuner(DE3): ZS; BL21(DE3): ZS, *lacY*; SHuffle T7: ZS, *lacY*, *DsbC*; SHuffle T7 *lysY*: ZS, *lacY*, *DsbC*, *lysY*). Overexpression of the chaperones by the SHuffle-based strains did not have the expected results; instead, it showed deleterious effects as observed from the low amounts of ZS protein. As a result, the strain that expressed the minimum number of recombinant proteins, the Tuner(DE3) strain, enhanced 1.2-fold the (+)-zizaene levels and 1.4-fold the yields in comparison with the control BL21(DE3) strain.

Finally, the applied approach for the optimization of the fermentation conditions improved the (+)-zizaene titers 2.2-fold and yields 1.7-fold when compared to the strains without optimization

(Section 3.4), achieving the highest (+)-zizaene production of 25.09 mg L⁻¹ and yield 23.33 mg g⁻¹ DCW for this study.

4. Discussion

The production of (+)-zizaene was metabolically engineered in *E. coli* by a recombinant codon-optimized SUMO-fused ZS that enhanced the amounts of soluble ZS protein [10]. Moreover, the optimization of the metabolic flux to (+)-zizaene was the greatest challenge, where the FDP and ZS supply were identified as the limiting factors. Consequently, a strategy was applied to gradually increase the supply of both and augment the metabolic rate driving force towards (+)-zizaene.

Initially, production of (+)-zizaene was possible by using the endogenous MEP pathway from *E. coli* (TZS strain) but at a lower extent. The high amounts of soluble ZS protein and low titers of (+)-zizaene suggest a limitation on the FDP supply. For that reason, the exogenous MEV pathway was applied, which is the ubiquitous pathway in plants for the biosynthesis of the sesquiterpene substrate FDP [34]. Hence, the pMevZS vector was constructed as a polycistronic vector, including all the required genes for terpene production into one vector. Such a strategy has been used for the engineering of many terpenes [23,28,35] because the maintenance of a single vector by the host cells is more efficient than for multi-vectors [36]. As a result, the overexpression of the MevZS strain did not increase the levels of (+)-zizaene as expected; possibly due to the lower amounts of soluble ZS protein than the TZS strain. This could be explained by the moderate strength of the *lacUV5* promoter [37], the improved variant of the *lac* promoter from *E. coli* [38]. Additionally, the ZS gene was placed eight genes downstream from the promoter in the polycistronic pMevZS vector and eventually, this gene order could affect the overexpression of ZS, as demonstrated by other studies [39–41]. Moreover, the overexpression of the nine genes produced a large mRNA transcript, which is usually more unstable as short transcripts [42]. Thus, the increase in the FDP supply and the decline in the soluble ZS protein amounts suggest that the limiting factor shifted to the ZS supply. This scenario was deleterious for an optimal metabolic rate, because ZS suffers substrate inhibition from FDP at higher levels of 5 μM, as shown in our previous report [20].

To raise the ZS supply, the monocistronic vectors pJbeiZS and pETZS were designed by cloning the ZS gene directly after the promoter and further co-transformed into the strain with the pMev vector. The use of the BZS+Mev strain was initially promising because it is capable of tuning the metabolic flux, using unique inducers for FDP (IPTG) and ZS (Arabinose). However, results with the P_{BAD} promoter were similar to those obtained by the MevZS strain, possibly due to the similarity in the strength of the P_{BAD} promoter versus the *lacUV5* promoter [37]. Similar outcomes were demonstrated by others, where the *lacUV5* and P_{BAD} promoters produced low or even undetectable levels of sesquiterpenes [11,12]. Additionally, accumulation of toxic intermediates due to a higher metabolic burden could occur because the BZS+Mev strain harbors the high-copy pJbeiZS plasmid with the pBBR1 origin of replication [43]. On the other hand, overexpression of soluble ZS protein with the T7-promoter (TZS+Mev strain) was drastically higher than with the P_{BAD} promoter (BZS+Mev strain) and subsequently, the production of (+)-zizaene increased considerably.

We ventured to raise further the ZS supply by adding a second copy of the ZS gene through the TZS+MevZS strain. As a result, the production of (+)-zizaene was the greatest of all the engineered strains and suggests that the limiting factor was still the ZS supply. The improvement in (+)-zizaene levels could be due to the effect of overexpressing the ZS genes by two different promoters on two different vectors (T7 in pETZS and *lacUV5* in pMevZS). Such strategy could have been a contributive factor, possibly by overexpressing the ZS gene by different promoters, by RBS strength differences from the used vectors, and by the vector copy numbers, which are unequal on multi-plasmid strains due to differences between replication origins, antibiotic markers, and plasmid sizes [16,42]. However, more tests are required to draw such conclusions. Additionally, it seems that the *in vivo* production of (+)-zizaene requires higher amounts of the TPS when compared to other sesquiterpenes such as vetispiradiene ($K_M = 0.7 \mu\text{M}$ for the vetispiradiene synthase) [44], due to the low enzyme activity

of ZS ($K_M = 0.88 \mu\text{M}$) [20]. Therefore, increasing the copy number of the TPS gene in a multi-vector strain was a plausible strategy to improve the flux to (+)-zizaene.

Optimal fermentation conditions are crucial for efficient microbial growth and metabolization of glucose flux towards terpenes, as demonstrated by many reports [11,45,46]. Regarding the media evaluation, the ADM medium achieved the highest production of (+)-zizaene when compared to the other defined media tests. The main difference in media formulation between tests was the higher amount of nitrogen from the ADM medium, suggesting that nitrogen concentration was the most relevant factor; particularly, because nitrogen is required for the biosynthesis of amino acids that regulates the production of cellular and recombinant proteins [47]. This could explain the higher cell growth and soluble ZS protein levels from the ADM medium tests when compared to the other tests, which in turn improved the (+)-zizaene levels.

Optimization of the temperature and media pH can enhance the production of sesquiterpene as observed with the microbial production of vetispiradiene, 5-*epi*-aristolechene and (+)- δ -cadinene [11]. For the production of (+)-zizaene, the optimal fermentation conditions were found at 20 °C and pH 7.0, which differ from the optimal reaction conditions from the ZS in in vitro biotransformations with FDP (36 °C, pH 7.5) [20]. Thus, the greatest difference between the experimental conditions was the temperature, due to its relevant effect over protein synthesis rate, cell growth, and enzyme activity [11,48]. Accordingly, tests cultivated at 16 °C and pH 6.5-7, overexpressed high amounts of soluble ZS protein but the (+)-zizaene levels and cell growth were low. These results suggest that the activity of the ZS was drastically reduced at 16 °C, due to its preference for higher temperatures (optimal at 36 °C). On the other hand, temperatures higher than 20 °C resulted in higher amounts of insoluble ZS protein than the soluble form. These observations confirm that an optimal temperature of 20 °C was required to achieve a balance between cell growth and active ZS protein. Regarding the effect of the media pH on (+)-zizaene production, the optimal pH was found to be neutral pH and values different than that lowered the (+)-zizaene titers. Additionally, lower pH values promoted the formation of insoluble ZS protein. Such behavior was observed before in uncontrolled-pH *E. coli* cultures grown in shake flasks, whereas overexpression of fused SpA- β gal protein at pH < 5.5 augmented the inclusion body formation, possibly due to regulatory mechanisms for pH homeostasis [49]. Therefore, tests grown at pH 7 at 20 °C achieved the balance between insoluble and soluble ZS protein fractions that led to the highest production of (+)-zizaene.

The evaluation of *E. coli* B strains revealed considerable differences in terpene production due to the particular feature of each strain. The terpene performance increased with the strains that expressed the lower number of recombinant proteins such as the BL21(DE3)-based strains. These results suggest that the expression of the ZS protein is not affected by basal expression (*lysY* gene), neither the β -galactoside permease is required (*lacY* gene), nor the chaperon DsbC enhanced the protein folding and disulfide bond formation, although the ZS protein contains cysteines. On the contrary, overexpression of DsbC drastically dropped the amounts of soluble ZS protein and the (+)-zizaene titers. Consequently, the Tuner(DE3) strain achieved the best performance for terpene production by overexpressing the minimum number of recombinant proteins, thus avoiding the production of unnecessary proteins (β -galactoside permease, DsbC, and lysozyme). This strategy diminished the metabolic burden, defined as the resources consumed for cell maintenance and recombinant protein synthesis that is inversely proportional to cell growth [48]. This was confirmed by the higher biomass amount from the Tuner(DE3) strain when compared to the other tested strains. As a result, the lower metabolic burden from the Tuner(DE3) strain improved the efficiency of the carbon flux towards (+)-zizaene.

5. Conclusions

In this work, we demonstrated the metabolic engineering of *E. coli* strains for the in vivo production of (+)-zizaene. Moreover, we optimized the limiting factors of the metabolic flux to (+)-zizaene by the overexpression of the MEV pathway, and by boosting the ZS supply by increasing the number of copies

of the *ZS* gene with T7 promoters on a multi-plasmid strain. Final improvement was achieved by optimizing the fermentation conditions and testing of *E. coli* B strains to a final (+)-zizaene production of 25.09 mg L⁻¹ at the shake flask scale. This work offers new insights into the optimization of the metabolic pathway and fermentation conditions for the in vivo production of sesquiterpenes and the development of a novel microbial platform towards the industrialization of fragrant molecules.

Supplementary Materials: The following are available online at <http://www.mdpi.com/2073-4425/10/6/478/s1>, Figure S1: Confirmation of seamless cloning for pMevZS; Figure S2: Confirmation of seamless cloning for pJbeiZS; Table S1: Mass spectra of the identified products.

Author Contributions: Funding acquisition and conceptualization—T.S. and S.B.; Methodology—S.B. and F.A.; Experimentation, data analysis, and manuscript draft preparation—F.A.; Manuscript revision—S.B. All authors agreed to the final version.

Funding: This research was funded by the PINN program from the Ministry of Science, Technology and Telecommunications of Costa Rica (MICITT), grant PED-058-2015-1 and by the Open Access Fund of the Leibniz Universität Hannover.

Acknowledgments: We are grateful for the assistance provided for the product identification by Daniel Sandner and Ulrich Krings from the Institute of Food Chemistry at the Leibniz University of Hannover. We thank Lukas Koch for the technical support for the cultivations.

Conflicts of Interest: The authors declare no conflict of interest. The funders had no role in the design of the study; in the collection, analyses, or interpretation of data; in the writing of the manuscript, or in the decision to publish the results.

References

- Carvalho, I.T.; Estevinho, B.N.; Santos, L. Application of microencapsulated essential oils in cosmetic and personal healthcare products—A review. *Int. J. Cosmet. Sci.* **2016**, *38*, 109–119. [[CrossRef](#)] [[PubMed](#)]
- Hüsni, K.; Başer, C.; Demirci, F. Chemistry of essential oils. In *Flavours and Fragrances*; Berger, R.G., Ed.; Springer-Verlag: Berlin, Germany, 2007; pp. 43–86.
- Belhassen, E.; Filippi, J.J.; Brévard, H.; Joulain, D.; Baldovini, N. Volatile constituents of vetiver: A review. *Flavour Fragr. J.* **2015**, *30*, 26–82. [[CrossRef](#)]
- Gnansounou, E.; Alves, C.M.; Raman, J.K. Multiple applications of vetiver grass—A review. *Int. J. Environ. Sci.* **2017**, *2*, 125–141.
- Sanganeria, P. *Essential Oils Market Report Summer 2018*; Report summer 2018; Ultra International B.V: Spijkensisse, The Netherlands, 2018; pp. 36–39.
- Vetiver oil market expected to reach \$169 Million By 2022. Available online: <https://www.grandviewresearch.com/press-release/global-vetiver-oil-market> (accessed on 22 April 2019).
- Talansier, E.; Braga, M.E.M.; Rosa, P.T.V.; Paolucci-Jeanjean, D.; Meireles, M.A.A. Supercritical fluid extraction of vetiver roots: A study of SFE kinetics. *J. Supercrit. Fluids* **2008**, *47*, 200–208. [[CrossRef](#)]
- Akhila, A.; Rani, M. Chemical constituents and essential oil biogenesis in *Vetiveria zizanioides*. In *Vetiveria: The Genus Vetiveria*; Maffei, M., Ed.; Taylor & Francis: London, UK, 2002; pp. 80–117. ISBN 0-415-27586-5.
- Tholl, D. Terpene synthases and the regulation, diversity and biological roles of terpene metabolism. *Curr. Opin. Plant Biol.* **2006**, *9*, 297–304. [[CrossRef](#)] [[PubMed](#)]
- Hartwig, S.; Frister, T.; Alemdar, S.; Li, Z.; Scheper, T.; Beutel, S. SUMO-fusion, purification, and characterization of a (+)-zizaene synthase from *Chrysopogon zizanioides*. *Biochem. Biophys. Res. Commun.* **2015**, *458*, 883–889. [[CrossRef](#)]
- Martin, V.J.J.; Yoshikuni, Y.; Keasling, J.D. The in vivo synthesis of plant sesquiterpenes by *Escherichia coli*. *Biotechnol. Bioeng.* **2001**, *75*, 497–503. [[CrossRef](#)]
- Nybo, S.E.; Saunder, J.; McCormick, S. Metabolic engineering of *Escherichia coli* for production of valeradiene. *J. Biotechnol.* **2017**, *262*, 60–66. [[CrossRef](#)]
- Guan, Z.; Breazeale, S.D.; Raetz, C.R.H. Extraction and identification by mass spectrometry of undecaprenyl diphosphate-MurNAc-pentapeptide-GlcNAc from *Escherichia coli*. *Anal. Biochem.* **2005**, *345*, 336–339. [[CrossRef](#)]
- Okada, K.; Minehira, M.; Zhu, X.; Suzuki, K.; Nakagawa, T.; Matsuda, H.; Kawamukai, M. The *ispB* gene encoding octaprenyl diphosphate synthase is essential for growth of *Escherichia coli*. *J. Bacteriol.* **1997**, *179*, 3058–3060. [[CrossRef](#)]

15. Kim, S.; Keasling, J.D. Nonmevalonate isopentenyl diphosphate synthesis pathway in *Escherichia coli* enhances lycopene production. *Biotechnol. Bioeng.* **2001**, *72*, 408–415. [[CrossRef](#)]
16. Sørensen, H.P.; Mortensen, K.K. Advanced genetic strategies for recombinant protein expression in *Escherichia coli*. *J. Biotechnol.* **2005**, *115*, 113–128. [[CrossRef](#)] [[PubMed](#)]
17. Martin, V.; Pitera, D.; Withers, S.; Newman, J.; Keasling, J. Engineering a mevalonate pathway in *Escherichia coli* for production of terpenoids. *Nat. Biotechnol.* **2003**, *21*, 796–802. [[CrossRef](#)] [[PubMed](#)]
18. Peralta-Yahya, P.P.; Ouellet, M.; Chan, R.; Mukhopadhyay, A.; Keasling, J.D.; Lee, T.S. Identification and microbial production of a terpene-based advanced biofuel. *Nat. Commun.* **2011**, *2*, 483–488. [[CrossRef](#)] [[PubMed](#)]
19. Christianson, D.W. Structural biology and chemistry of the terpenoid cyclases. *Chem. Rev.* **2006**, *106*, 3412–3442. [[CrossRef](#)] [[PubMed](#)]
20. Aguilar, F.; Hartwig, S.; Scheper, T.; Beutel, S. Catalytic specificity, reaction mechanisms, and conformational changes during catalysis of the recombinant SUMO (+)-zizaene synthase from *Chrysopogon zizanioides*. *ACS Omega* **2019**, *4*, 6199–6209. [[CrossRef](#)]
21. Green, M.R.; Sambrook, J. *Molecular Cloning: A Laboratory Manual*, 4th ed.; Cold Spring Harbor Laboratory Press: New York, NY, USA, 2012; ISBN 978-1-936113-42-2.
22. Guzman, L.M.; Belin, D.; Carson, M.J.; Beckwith, J. Tight regulation, modulation, and high-level expression by vectors containing the arabinose PBAD promoter. *J. Bacteriol.* **1995**, *177*, 4121–4130. [[CrossRef](#)]
23. Alonso-Gutierrez, J.; Chan, R.; Batt, T.S.; Adams, P.D.; Keasling, J.D.; Petzold, C.J.; Lee, T.S.; Adams, P.D. Metabolic engineering of *Escherichia coli* for limonene and perillyl alcohol production. *Metab. Eng.* **2013**, *19*, 33–41. [[CrossRef](#)]
24. Li, Z.; Carstensen, B.; Rinas, U. Smart sustainable bottle (SSB) system for *E. coli* based recombinant protein production. *Microb. Cell Fact.* **2014**, *13*, 2–9. [[CrossRef](#)]
25. Song, J.M.; Wei, D.Z. Production and characterization of cellulases and xylanases of *Cellulosimicrobium cellulans* grown in pretreated and extracted bagasse and minimal nutrient medium M9. *Biomass Bioenergy* **2010**, *34*, 1930–1934. [[CrossRef](#)]
26. Rodríguez-Aparicio, L.B.; Reglero, A.; Ortiz, A.I.; Luengo, J.M. Effect of physical and chemical conditions on the production of colominic acid by *E. coli* in defined medium. *Appl. Microbiol. Biotechnol.* **1988**, *27*, 474–483. [[CrossRef](#)]
27. Van Del Dool, H.; Kratz, P. A generalization of the retention index system including linear temperature programmed gas-liquid partition chromatography. *J. Chromatogr. A* **1963**, *11*, 463–471. [[CrossRef](#)]
28. Wang, C.; Yoon, S.H.; Jang, H.J.; Chung, Y.R.; Kim, J.Y.; Choi, E.S.; Kim, S.W. Metabolic engineering of *Escherichia coli* for α -farnesene production. *Metab. Eng.* **2011**, *13*, 648–655. [[CrossRef](#)] [[PubMed](#)]
29. Hartwig, S.; Frister, T.; Alemdar, S.; Li, Z.; Krings, U.; Berger, R.G.; Scheper, T.; Beutel, S. Expression, purification and activity assay of a patchoulol synthase cDNA variant fused to thioredoxin in *Escherichia coli*. *Protein Expr. Purif.* **2014**, *97*, 61–71. [[CrossRef](#)]
30. Alemdar, S.; Hartwig, S.; Frister, T.; König, J.C.; Scheper, T.; Beutel, S. Heterologous expression, purification, and biochemical characterization of α -humulene synthase from *Zingiber zerumbet* Smith. *Appl. Biochem. Biotechnol.* **2016**, *178*, 474–489. [[CrossRef](#)] [[PubMed](#)]
31. Newman, J.D.; Marshall, J.; Chang, M.; Nowroozi, F.; Paradise, E.; Pitera, D.; Newman, K.L.; Keasling, J.D. High-level production of amorpho-4,11-diene in a two-phase partitioning bioreactor of metabolically engineered *Escherichia coli*. *Biotechnol. Bioeng.* **2006**, *95*, 684–691. [[CrossRef](#)]
32. Wang, C.; Yoon, S.H.; Shah, A.A.; Chung, Y.R.; Kim, J.Y.; Choi, E.S.; Keasling, J.D.; Kim, S.W. Farnesol production from *Escherichia coli* by harnessing the exogenous mevalonate pathway. *Biotechnol. Bioeng.* **2010**, *107*, 421–429. [[CrossRef](#)]
33. Korz, D.; Rinas, U.; Hellmuth, K.; Sanders, E.; Deckwer, W. Simple fed-batch technique for high cell density cultivation of *Escherichia coli*. *J. Biotechnol.* **1995**, *39*, 59–65. [[CrossRef](#)]
34. Tholl, D. Biosynthesis and biological functions of terpenoids in plants. In *Advances in Biochemical Engineering/Biotechnology*; Schrader, J., Bohlmann, J., Eds.; Springer International: Basel, Switzerland, 2015; pp. 63–106.
35. Cao, Y.; Zhang, R.; Liu, W.; Zhao, G.; Niu, W.; Guo, J.; Xian, M.; Liu, H. Manipulation of the precursor supply for high-level production of longifolene by metabolically engineered *Escherichia coli*. *Sci. Rep.* **2019**, *9*, 1–10. [[CrossRef](#)]

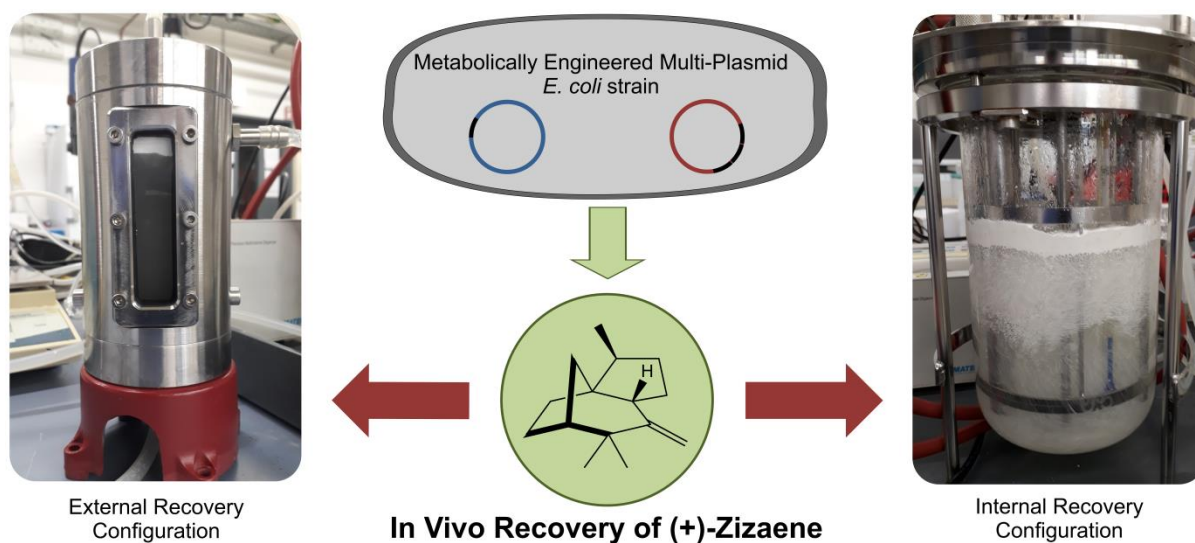
36. Kumar, S.; Jain, K.K.; Bhardwaj, K.N.; Chakraborty, S.; Kuhad, R.C. Multiple genes in a single host: Cost-effective production of bacterial laccase (cotA), pectate lyase (pel), and endoxyylanase (xyl) by simultaneous expression and cloning in single vector in *E. coli*. *PLoS ONE* **2015**, *10*, 1–15. [[CrossRef](#)]
37. Samuelson, J. Bacterial Systems. In *Production of Membrane Proteins: Strategies for Expression and Isolation*; Robinson, A.S., Ed.; Wiley-VCH Verlag GmbH & Co: Weinheim, Germany, 2011; pp. 11–35. ISBN 9780470871942.
38. Tegel, H.; Ottosson, J.; Hober, S. Enhancing the protein production levels in *Escherichia coli* with a strong promoter. *FEBS J.* **2011**, *278*, 729–739. [[CrossRef](#)] [[PubMed](#)]
39. Lv, X.; Xu, H.; Yu, H. Significantly enhanced production of isoprene by ordered coexpression of genes *dxs*, *dxr*, and *idi* in *Escherichia coli*. *Appl. Microbiol. Biotechnol.* **2013**, *97*, 2357–2365. [[CrossRef](#)] [[PubMed](#)]
40. Du, F.L.; Yu, H.L.; Xu, J.H.; Li, C.X. Enhanced limonene production by optimizing the expression of limonene biosynthesis and MEP pathway genes in *E. coli*. *Bioresour. Bioprocess.* **2014**, *1*, 1–10. [[CrossRef](#)]
41. Tan, S. A modular polycistronic expression system for overexpressing protein complexes in *Escherichia coli*. *Protein Expr. Purif.* **2001**, *21*, 224–234. [[CrossRef](#)] [[PubMed](#)]
42. Perrakis, A.; Romier, C. Assembly of protein complexes by coexpression in prokaryotic and eukaryotic hosts: An overview. In *Structural Proteomics High-Throughput Methods*; Kobe, B., Guss, M., Huber, T., Eds.; Humana Press: New York, NY, USA, 2008; ISBN 9781588298096.
43. Jones, K.L.; Kim, S.W.; Keasling, J.D. Low-copy plasmids can perform as well as or better than high-copy plasmids for metabolic engineering of bacteria. *Metab. Eng.* **2000**, *2*, 328–338. [[CrossRef](#)]
44. Mathis, J.R.; Back, K.; Starks, C.; Noel, J.; Poulter, C.D.; Chappel, J. Pre-steady-state study of recombinant sesquiterpene cyclases. *Biochemistry* **1997**, *36*, 8340–8348. [[CrossRef](#)]
45. Wu, W.; Liu, F.; Davis, R.W. Engineering *Escherichia coli* for the production of terpene mixture enriched in caryophyllene and caryophyllene alcohol as potential aviation fuel compounds. *Metab. Eng. Commun.* **2018**, *6*, 13–21. [[CrossRef](#)]
46. Huang, X.; Xiao, Y.; Köllner, T.G.; Zhang, W.; Wu, J.; Wu, J.; Guo, Y.; Zhang, Y. Identification and characterization of (E)- β -caryophyllene synthase and α/β -pinene synthase potentially involved in constitutive and herbivore-induced terpene formation in cotton. *Plant Physiol. Biochem.* **2013**, *73*, 302–308. [[CrossRef](#)]
47. Chubukov, V.; Desmarais, J.J.; Wang, G.; Chan, L.J.G.; Baidoo, E.E.K.; Petzold, C.J.; Keasling, J.D.; Mukhopadhyay, A. Engineering glucose metabolism of *Escherichia coli* under nitrogen starvation. *npj Syst. Biol. Appl.* **2017**, *3*, 1–7. [[CrossRef](#)]
48. Sørensen, H.P.; Mortensen, K.K. Soluble expression of recombinant proteins in the cytoplasm of *Escherichia coli*. *Microb. Cell Fact.* **2005**, *8*, 1–8. [[CrossRef](#)]
49. Strandberg, L.; Enfors, S.O. Factors influencing inclusion body formation in the production of a fused protein in *Escherichia coli*. *Appl. Environ. Microbiol.* **1991**, *57*, 1669–1674. [[PubMed](#)]



© 2019 by the authors. Licensee MDPI, Basel, Switzerland. This article is an open access article distributed under the terms and conditions of the Creative Commons Attribution (CC BY) license (<http://creativecommons.org/licenses/by/4.0/>).

CHAPTER 3

Improved production and in situ recovery of sesquiterpene (+)-zizaene from metabolically-engineered *E. coli*



Chapter published in: **Aguilar, F.**; Scheper, T.; Beutel, S. Improved Production and In Situ Recovery of Sesquiterpene (+)-Zizaene from Metabolically-Engineered *E. coli*. *Molecules* 2019, 24, 3356. DOI: [10.3390/molecules24183356](https://doi.org/10.3390/molecules24183356)

4.3. External and internal in situ product recovery of sesquiterpene (+)-zizaene produced from metabolically engineered *E. coli*

Recent progress in metabolic and bioprocess engineering has made possible the biotechnological production of terpenes at industrial levels. After a high investment in R&D, several chemical companies have deployed distinct terpenes to the market, produced from microbial platforms such as artemisinin, β -farnesene, nookatene, patchouli oil, valencene, sclareol and squalane. Among the challenges involved in the microbial production of terpenes is the product recovery from fermentation. The ubiquitous physical-chemical properties of terpenes such as hydrophobicity and volatility are the main constraints for the downstream process. As a result, the biotechnological production of the khusimol precursor, (+)-zizaene, suffers from such constraints during fermentation. In the previous chapter, the application of metabolic engineering methods made possible the production of (+)-zizaene by a multi-plasmid *E. coli* strain. Thus, this chapter addresses the development of a suitable method for the (+)-zizaene recovery in fed-batch fermentations at bioreactor scale.

Initially, the questions were, whether a loss of (+)-zizaene due to volatilization could exist, and eventually, how much could be lost. Experiments with cell-free media containing (+)-zizaene amounts were carried out at shake flask scale. After 60 min of incubation at 20 °C, more than half of the (+)-zizaene amounts were volatilized, ruling out the microbial degradation as main mechanism for (+)-zizaene loss. Furthermore, product loss by volatilization was measured as 27 mg L⁻¹ by comparing cultivations without extractants and with liquid-liquid phase partitioning cultivation (LLPPC) with a solvent as overlay after 48 h of growth.

The solid-liquid phase partitioning cultivation (SLPPC) by polymeric adsorbers was analyzed due to the advantages against LLPPC such as ease of adsorber removal, non-emulsion formation and reusability. As a result, the Diaion HP20 adsorber obtained the highest recovery ratio of all the tested adsorbers with results similar to that by LLPPC. Additionally, an evaluation of organic solvents was tested for the desorption of (+)-zizaene from the Diaion HP20 adsorbers. The isooctane, decane and ethyl acetate demonstrated the highest (+)-zizaene elution when compared to the rest of the tested solvents, whereas isooctane was chosen for further tests due to its low cost.

The bioprocess of (+)-zizaene was scaled up to 2 L stirred-tank bioreactors with fed-batch cultivations by integrating the in situ (+)-zizaene recovery to the fermentation. The external recovery configuration (ERC) was designed with an external loop connected to an external bed adsorption (EBA) column and improved the (+)-zizaene titer 2.5-fold more than the LLPPC at shake flask scale. The internal recovery configuration (IRC) with adsorbers inside the reactor further improved the (+)-zizaene titers 2.2-fold more when compared to that of the ERC. An additional test by the internal recovery configuration with gas stripping (IRC+GS) confirmed an efficient product recovery from the IRC, and the gas stripping was considered unnecessary for

the bioprocess due to the contribution of less than 1% to the total (+)-zizaene amount. Consequently, the IRC improved the (+)-zizaene titer 8.4-fold and productivity 3-fold when compared to the highest result from chapter 2 (25 mg L⁻¹), and achieved the highest (+)-zizaene production (211 mg L⁻¹) reported so far. Finally, the in situ recovery configurations tested in this study are suitable methods for the recovery of (+)-zizaene and provide new insights for other bioprocesses towards the microbial production of fragrant sesquiterpenes.

Article

Improved Production and In Situ Recovery of Sesquiterpene (+)-Zizaene from Metabolically-Engineered *E. coli*

Francisco Aguilar , Thomas Scheper and Sascha Beutel *

Institute of Technical Chemistry, Leibniz University of Hannover, Callinstr. 5, 30167 Hannover, Germany; aguilar@iftc.uni-hannover.de (F.A.); scheper@iftc.uni-hannover.de (T.S.)

* Correspondence: beutel@iftc.uni-hannover.de; Tel.: +49-511-762-2867; Fax: +49-511-762-3004

Received: 17 August 2019; Accepted: 14 September 2019; Published: 15 September 2019



Abstract: The sesquiterpene (+)-zizaene is the direct precursor of khusimol, the main fragrant compound of the vetiver essential oil from *Chrysopogon zizanioides* and used in nearly 20% of men's fine perfumery. The biotechnological production of such fragrant sesquiterpenes is a promising alternative towards sustainability; nevertheless, product recovery from fermentation is one of the main constraints. In an effort to improve the (+)-zizaene recovery from a metabolically-engineered *Escherichia coli*, we developed an integrated bioprocess by coupling fermentation and (+)-zizaene recovery using adsorber extractants. Initially, (+)-zizaene volatilization was confirmed from cultivations with no extractants but application of liquid–liquid phase partitioning cultivation (LLPPC) improved (+)-zizaene recovery nearly 4-fold. Furthermore, solid–liquid phase partitioning cultivation (SLPPC) was evaluated by screening polymeric adsorbers, where Diaion HP20 reached the highest recovery. Bioprocess was scaled up to 2 L bioreactors and in situ recovery configurations integrated to fermentation were evaluated. External recovery configuration was performed with an expanded bed adsorption column and improved (+)-zizaene titers 2.5-fold higher than LLPPC. Moreover, internal recovery configuration (IRC) further enhanced the (+)-zizaene titers 2.2-fold, whereas adsorption velocity was determined as critical parameter for recovery efficiency. Consequently, IRC improved the (+)-zizaene titer 8.4-fold and productivity 3-fold from our last report, achieving a (+)-zizaene titer of 211.13 mg L⁻¹ and productivity of 3.2 mg L⁻¹ h⁻¹. This study provides further knowledge for integration of terpene bioprocesses by in situ product recovery, which could be applied for many terpene studies towards the industrialization of fragrant molecules.

Keywords: (+)-zizaene; khusimene; khusimol; vetiver essential oil; in situ product recovery; expanded bed adsorption; sesquiterpenes; terpenes; *Chrysopogon zizanioides*

1. Introduction

The biotechnological production of chemicals by engineered microorganisms is a potential alternative for the production of terpenes from renewable resources [1]. Recent advances in metabolic engineering have made possible the production of terpenes by microbial platforms at economically-feasible titers (over grams of terpene per liter of broth), reaching the industrial scale, such as artemisinin, β -farnesene, and squalane [2–4]. Fragrant sesquiterpenes used in the cosmetic industry are potential candidates to be produced by biotechnological systems, such as the sesquiterpenes contained in the vetiver essential oil (VEO) from the grass *Ch. zizanioides*. VEO is an important component for the formulation of cosmetics and it has been used in nearly 36% of Western perfumes and 20% of men's fragrances [5] with a total world production of 300–350 tons per year [6]. VEO is composed of a mixture of sesquiterpenes and their hydroxylated derivatives, with a characteristic

dark woody scent granted principally by khusimol, its main fragrant component [7,8]. Moreover, the biotechnological production of khusimol could lead to a reliable supply for the cosmetic industry and to avoid the shortages from the traditional supply of VEO (extracted from the vetiver roots) due to natural disasters such as earthquakes and floods [6,7].

An important step towards the microbial production of khusimol was the whole-cell bioproduction of (+)-zizaene (syn. khusimene), the direct precursor of khusimol, by a metabolically-engineered strain of *E. coli* [9]. This was demonstrated by engineering the mevalonate (MEV) pathway to increase the levels of the natural sesquiterpene precursor E,E-farnesyl diphosphate (FDP) and overexpressing the (+)-zizaene synthase (ZS) [9]. The latter terpene synthase catalyzes the substrate FDP through a complex reaction by carbocation rearrangements and cyclizations to yield the tricyclic (+)-zizaene with a product specificity over 90% [10].

Further development of the (+)-zizaene bioprocess would comprise the scale-up of the fermentation to bioreactors (upstream process) and the product recovery (downstream process). As usually, the scale-up of the fermentation is performed by optimizing the bioreactor variables such as pH, oxygen supply, and stirring [11]. Additionally, scale-up studies can be performed using fed-batch fermentation by feeding of a carbon source, such as glucose, to reach high cell density cultures (HCDC), as is the case with the production of farnesene, santalene, cucurbitadienol, and (-)- α -bisabolol [12–14].

The downstream process is one of the main challenges towards the industrialization of terpenes because of their inherent physicochemical properties such as hydrophobicity and volatility [15]. Such bioprocesses often suffer cell toxicity, product inhibition, product volatilization, and product degradation, which can be devastating for the bioprocess productivity [16]. As an alternative, in situ product recovery (ISPR) has been applied for the downstreaming of terpenes, defined as the removal of product during its formation in the reactor [17].

The liquid–liquid phase partitioning cultivation (LLPPC) is the most used ISPR technique for terpene recovery, in which the fermentation is carried out with a liquid extractant, forming two immiscible phases [15]. The liquid extractants are usually bio-compatible organic solvents with a high log P value that do not partition into the microbial membrane and sequester the terpenes from the aqueous phase [18,19]. Because of the ease of LLPPC, it is the first choice for ISPR of terpenes and it has been applied in the recovery of many terpenes such as limonene [20], taxadiene [21], α -santalene [22], and amorpho-4,11-diene [23].

Another ISPR alternative is the solid–liquid phase partitioning cultivation (SLPPC), in which a solid extractant is in contact with the fermentation, such as polymeric adsorbents, porous resins, zeolites, or activated charcoal [24]. Due to their high affinity to hydrophobic compounds, these extractants can selectively adsorb terpenes and can be applied in numerous configurations because of their mechanical stability [15], as implemented for the production of perillylic alcohol [25], epi-cedrol [26], and linalool oxides [27].

The mechanisms for ISPR of terpenes in *E. coli* are described in Figure 1 for both LLPPC and SLPPC. Accordingly, terpenes are synthesized in the cell cytosol and exported to the fermentation broth by solvent-resistant tripartite efflux pumps such as *AcrAB-TolC* and *MdtEF-TolC* [28,29]. For the LLPPC, terpenes are extracted into the organic solvent by the principle of hydrophobic interactions, in which non-polar hydrocarbons form aggregates together and separate from the aqueous phase [30]. In the case of SLPPC, terpenes are adsorbed to the porous surface of the solid extractant whether by physisorption or chemisorption, forming a film in the porous surface of the extractant, without altering the terpene structure [31]. Eventually, factors such as the chemical structure of the adsorbent, pore size, particle size, and specific surface area will affect the adsorption efficiency [32].

Regardless of whether LLPPC or SLPPC is used, the configurations for ISPR of terpenes can be applied internally or externally in a direct or indirect approach [33]. Internal recovery configuration (IRC) is based on the extractant phase inside the reactor vessel, whereas in the external recovery configuration (ERC), the fermentation broth is recirculated towards an external loop to an extractant unit, such as an expanded bed adsorption (EBA) column [16]. In consequence, the choices for ISPR of

terpenes are vast, whereas commercial processes employ a single or a combination of ISPR techniques, including adsorption recovery and/or gas phase recovery (gas stripping) [34]. However, the choice of configuration depends greatly on the downstream cost, which is determined by several factors such as the cost of extractant, number of phases, and recovery process, which will be related to the properties of the target molecule [33,35]. Moreover, ISPR provides numerous advantages when compared to the traditional extraction of terpenes and contribute towards a greener chemistry by reducing the recovery stages, amounts of solvents, and extracting products under milder conditions, which results in the reduction of the downstream costs [36].

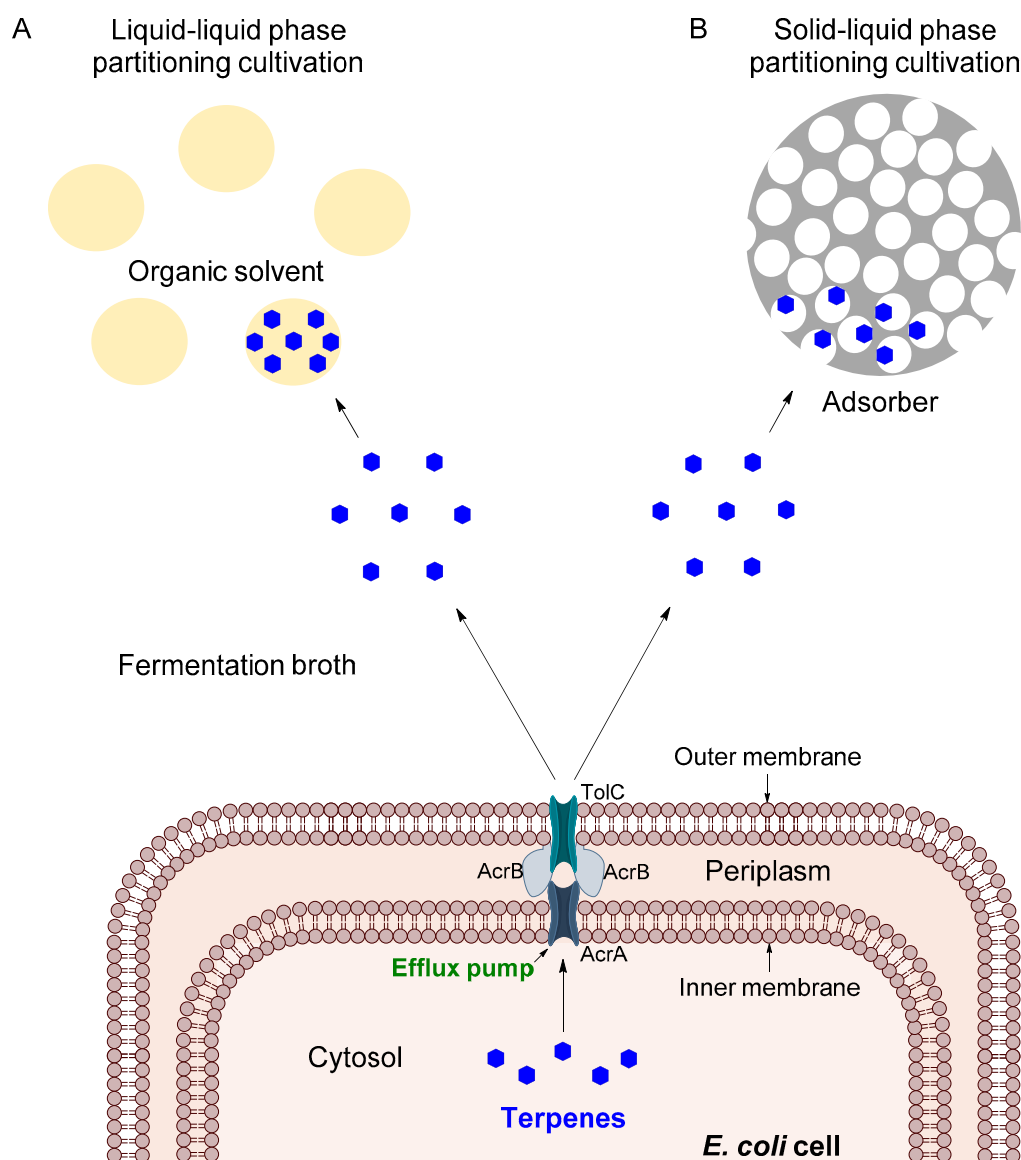


Figure 1. The mechanism for the in situ recovery of terpenes produced from metabolically engineered *E. coli*. (A) Liquid-liquid phase partitioning cultivation is carried out by liquid extractants (organic solvents), which extract the terpenes by hydrophobic interactions. (B) Solid-liquid phase partitioning cultivation utilizes solid extractants (adsorbers) and recovers the terpenes by adsorption. The tripartite efflux pump *AcrAB-TolC* is used as an example of a secretion system for hydrophobic molecules and its components are properly described.

In our previous report, we demonstrated the production of (+)-zizaene by a metabolically-engineered *E. coli* and optimized the fermentation conditions at shake flask scale, comprising the

induction, media, pH, and growth temperature, reaching a (+)-zizaene titer of 25.09 mg L⁻¹ and a productivity of 1.05 mg L⁻¹ [10]. However, the scale-up for the bioprocess of (+)-zizaene requires a suitable ISPR configuration to circumvent product loss and further improve the recovery of (+)-zizaene.

In this study, we developed an integrated ISPR configuration for the microbial production of (+)-zizaene at a 2 L bioreactor scale with adsorber extractants in order to improve the (+)-zizaene recovery. For that, the product loss by volatilization was analyzed and the (+)-zizaene recovery was improved by using LLPPC at shake flask scale. Furthermore, distinct polymeric adsorbers were evaluated, in terms of selectivity and recovery ratio, as potential extractants to be applied at bioreactor scale. The desorption process was studied by a comparative assessment of organic solvents. The bioprocess was scaled up to 2 L bioreactors using the fed-batch culture technique and three ISPR configurations by direct contact mode were tested: ERC, IRC, and IRC with gas stripping. As a result, the (+)-zizaene titers and productivity were improved significantly.

2. Results

2.1. Product Volatilization Measurements and (+)-Zizaene Recovery by LLPPC

In our previous report, we demonstrated the microbial production of (+)-zizaene by engineering the MEV pathway and the ZS synthase in a multi-plasmid *E. coli* strain [9]. To further improve the production of (+)-zizaene, the bioprocess development requires the scale-up to stirred-tank bioreactors to reach HCDC, and an efficient downstream procedure. However, the recovery of terpenes involves special considerations due to their physicochemical properties. For the production of (+)-zizaene, loss of product could be expected during cultivation due to volatilization or microbial degradation. Moreover, toxicity to the *E. coli* cells could occur because of (+)-zizaene accumulation in the fermentation.

Initially, we analyzed the loss of (+)-zizaene at shake flask scale without extractants by cultivating an induced *E. coli* TZS+MevZS strain, grown for 24 h. After removing the cells from the culture broth, (+)-zizaene measurements were taken time-wise from cell-free media. As a result, half of the (+)-zizaene amount was volatilized after 1 h and only traces were detected after 4 h (Figure 2). This demonstrates that, as for most terpenes, volatilization is a major constraint for the (+)-zizaene production. Eventually, the application of ISPR could provide solutions for these shortcomings, taking advantage of the hydrophobicity of (+)-zizaene (log P = 5.10), which could be extracted simultaneously during cultivation whether by liquid- or solid-phase recovery.

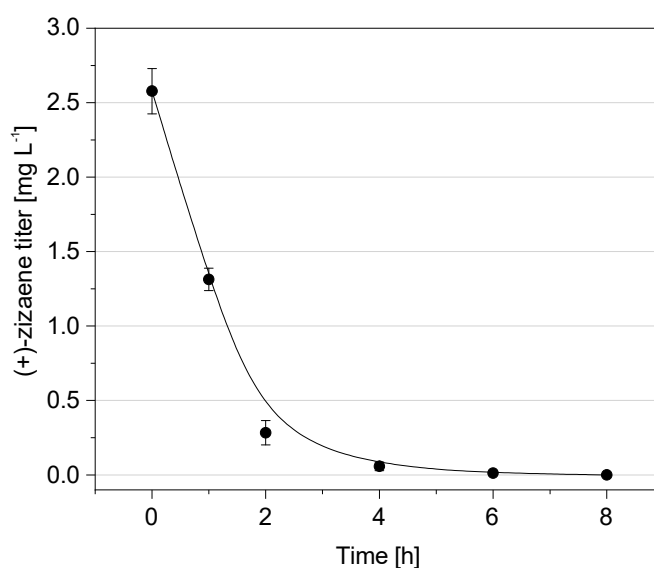


Figure 2. Loss of (+)-zizaene by volatilization on cell-free media at shake flask scale. Data are the mean of three replicates with error bars representing the standard deviation (SD).

To prove these hypotheses, a comparative test comprising a LLPPC with a solvent overlay and a negative control (without extractant) was performed with the *E. coli* TZS+MevZS strain at shake flask scale. As shown in Figure 3A, the (+)-zizaene production on the LLPPC and negative control tests followed similar kinetics, reaching the maximum peak at 48 h and dropping afterward. The LLPPC was nearly 4-fold higher when compared to that of the negative control at the highest production peak. Therefore, the loss of (+)-zizaene was estimated at nearly 27 mg L⁻¹ due to volatilization at 48 h. Similarly, cell growth was higher on the LLPPC (OD₆₀₀ 5.7 and biomass 2.1 g_{DCW} L⁻¹) than the negative control (OD₆₀₀ 5.1 and biomass 1.7 g_{DCW} L⁻¹) at 48 h, suggesting a toxic effect due to (+)-zizaene accumulation in the control tests (Figure 3B).

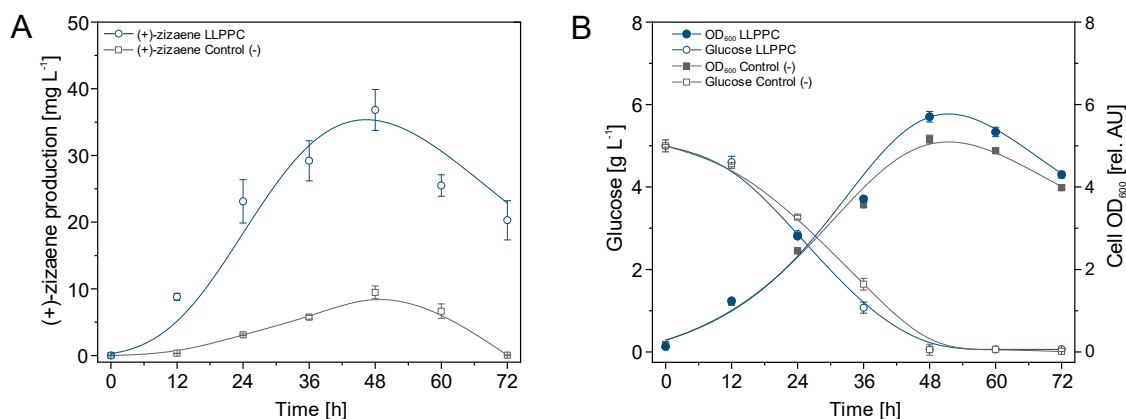


Figure 3. Comparison of the (+)-zizaene production (A) and growth kinetics (B) between the liquid-liquid phase partitioning cultivation (LLPPC) and the control (-) without extractant from the *E. coli* TZS+MevZS strain. Plots correspond to the mean of three independent experiments with error bars as SD.

2.2. Screening of Polymeric Adsorbers for SLPPC

Although LLPPC has been used widely for isoprenoid recovery, SLPPC with solid extractants can be advantageous towards the scale-up of bioprocesses due to the following features: reusability, bio-compatibility, cost reduction of organic solvents, non-emulsion formation, and simple separation from the aqueous phase [15,37,38]. Thus, an *in vivo* adsorber screening analysis was carried out based on Halka [11] at shake flask scale. The tested polymeric adsorbers were chosen according to their affinity to adsorb hydrophobic molecules, as demonstrated in previous terpene recovery studies [25,39]. A negative control without extractants and a LLPPC control were also included.

As a result, the adsorbers showed similar product selectivity, where the terpene profile for all the tested adsorbers by GC-MS showed approximately a product ratio of 90% of (+)-zizaene, 9.5% of β -acoradiene, and traces of hydrocarbons (Figures S1 and S2).

The tested adsorbers presented significant recovery differences, where the Diaion HP20 test achieved the highest (+)-zizaene titer from all the tested resins, followed by Amberlite XAD4, Amberlite XAD16N, Lewatit 1064MD and Amberlite IRA400 Cl tests (Figure 4A). Moreover, the (+)-zizaene recovery ratio from Diaion HP20 was similar to that obtained by the LLPPC control (92.5% vs. 94.4%, respectively) (Table S2).

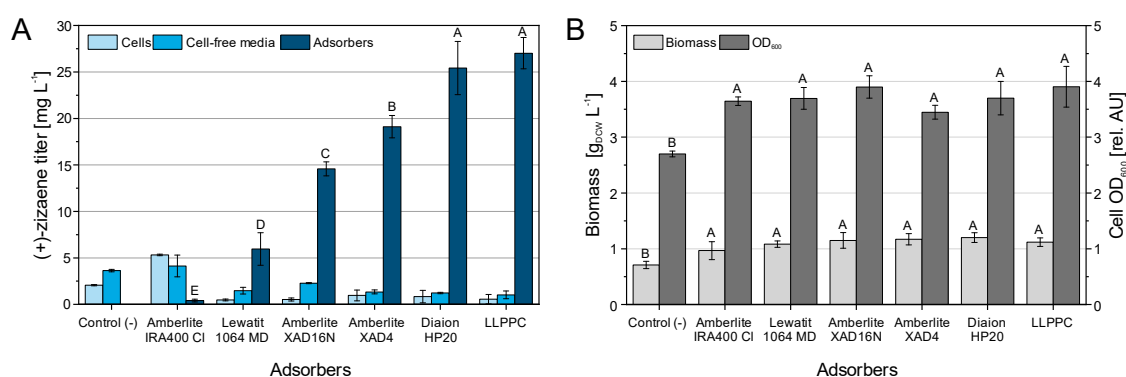


Figure 4. Screening of distinct polymeric adsorbers for the recovery of (+)-zizaene. **(A)** (+)-zizaene titers recovered from cells, cell-free media, and adsorbers. **(B)** Cell growth expressed by biomass and cell optical density. The negative control corresponds to culture without extractants. Data are the mean of three replicates with error bars as SD. Variables analyzed by ANOVA ($\alpha = 0.05$), letters that differ are significantly different.

Besides the Amberlite IRA400 Cl test, the rest of the adsorber tests recovered most of the (+)-zizaene amounts from the adsorbers (75.2%–92.5%), followed by the cell-free media (4.5%–18.7%) and in lower amounts from the cells (3.1%–6.1%; Table S2). As expected, only low (+)-zizaene amounts were measured from cell-free media by the negative control, confirming a loss of (+)-zizaene by volatilization. Besides, the highest amount of insoluble (+)-zizaene protein (inclusion bodies) was observed on the negative control, whereas most of the tested adsorbers and LLPPC showed low amounts of inclusion bodies (Figure S3).

All of the tested adsorbers obtained similar cell growth between OD₆₀₀ 3.4–3.9 and biomass 0.96–1.17 g_{DCW} L⁻¹ from the *E. coli* TZS+MevZS strain (Figure 4B). On the other hand, the negative control (without extractant) had a lower cell growth when compared to all the other tests, with an OD₆₀₀ of 2.7 and biomass of 0.7 g_{DCW} L⁻¹, suggesting a toxic effect from the (+)-zizaene amounts in the culture broth. Because of the high recovery performance from the Diaion HP20 between adsorbers and comparable results with the LLPPC control, the Diaion HP20 was selected for further cultivations.

2.3. Assessment of Organic Solvents for the Desorption of (+)-Zizaene

After the screening of adsorbers for the SLPPC, an evaluation was done to analyze the elution performance of different organic solvents, which ideally should have a high partition coefficient and high selectivity towards (+)-zizaene [19]. Consequently, distinct solvents with high log P values were tested comprising decane, dodecane, pentane, ethyl acetate, isopropanol, isooctane, and acetonitrile (Table S1).

As evidenced in Figure 5, the organic solvent tests displayed significant desorption differences, with (+)-zizaene titers between 15–25 mg L⁻¹ approximately. The eluents isooctane, decane, and ethyl acetate recovered the highest (+)-zizaene titers (25.7, 24.7, and 24.0 mg L⁻¹, respectively), followed by dodecane, pentane, acetonitrile, and isopropanol. As a consequence, isooctane was selected as the elution solvent and further used for scale-up tests.

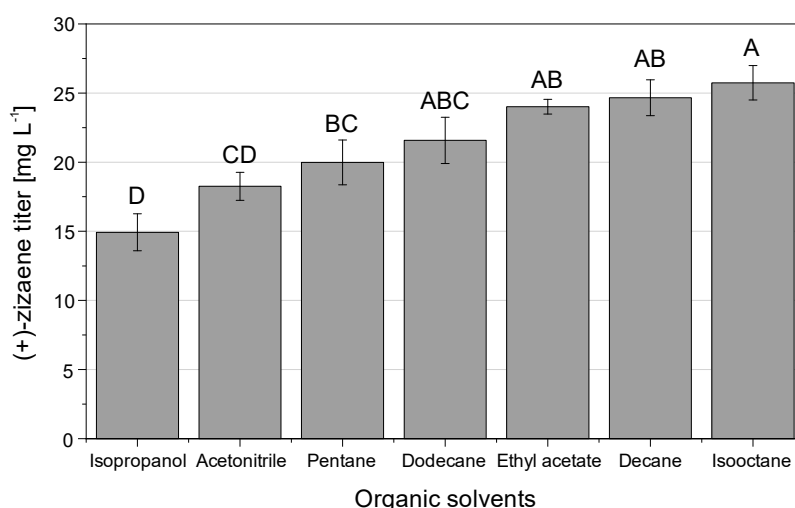


Figure 5. Elution performance of distinct organic solvents for the desorption of (+)-zizaene from the adsorber Diaion HP20. Data correspond to the mean of three independent experiments with error bars as SD. Data analyzed by ANOVA ($\alpha = 0.05$), letters that differ are significantly different.

2.4. Integration of In Situ Recovery of (+)-Zizaene to Fermentation at Bioreactor Scale

The fermentation was scaled up to 2 L stirred-tank bioreactors using the fed-batch cultivation method by feeding glucose continuously to reach HCDC. Because the use of liquid extractants is challenging for industrial-scale bioreactors [15,33], we tested the (+)-zizaene recovery with solid extractants. Thus, the external, internal, and internal with gas stripping in situ recovery configurations (Figure 6) were integrated to the fermentation with the best performing adsorber (Diaion HP20) and eluent (isooctane), in order to maximize product recovery and avoid cell toxicity, which could be more problematic at bioreactor scale due to the higher production of (+)-zizaene.

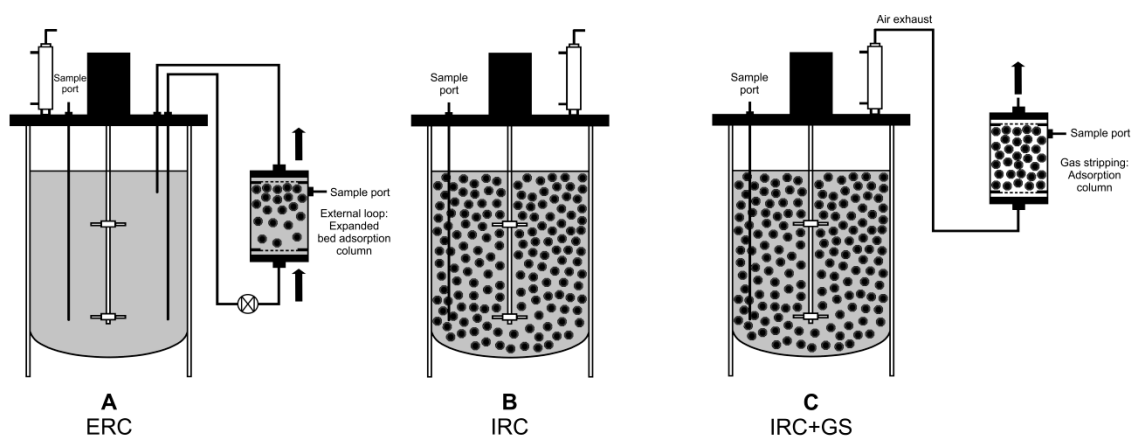


Figure 6. Diagram with the distinct bioreactor configurations used for the in situ recovery of (+)-zizaene. (A) External recovery: Adsorbers in expanded bed adsorption (EBA) column by an external loop. (B) Internal removal: Adsorbers inside the bioreactor vessel. (C) Internal removal with gas stripping: Adsorbers inside the bioreactor vessel and adsorption column coupled to the off-gas. Sample ports for adsorbers are indicated.

The Diaion HP20 adsorber was used at 50 g L^{-1} , whereas higher amounts resulted in mixing problems and reading disturbances from the probes of the bioreactors. The optimal fermentation conditions for (+)-zizaene production at shake flask scale were previously determined [9] and used as the initial point for the bioreactor cultivations (ADM, pH 7.0), including induction at $20 \text{ }^\circ\text{C}$ to avoid formation of inclusion bodies from the ZS protein and to reduce volatilization of (+)-zizaene.

Early induction was applied in all cultivations (OD_{600} 5–7) because late induction ($OD_{600} > 15$) was proven deleterious for the (+)-zizaene production, where most of the ZS protein was overexpressed as inclusion bodies (data not shown).

2.5. Bioreactor Cultivation with an Integrated ERC

The ERC was analyzed because external loops can facilitate product removal from large bioreactors and enable semi-continuous product recovery [15,38]. Moreover, the EBA chromatography was preferred as the extractant unit over the conventional packed-bed adsorption chromatography, because it allows operations at higher flow rates [40]. For this purpose, a stainless steel EBA column was built with the feature of a sampling port to ease the process monitoring and adsorber renovation (Figure 6A). The EBA was loaded with 75 g of Diaion HP20 and exchanged with 75 g of fresh resin every 24 h of operation.

The fed-batch stage started at 7 h of growth by lowering the temperature to 20 °C, and after 1 h the culture was induced with 0.5 mM IPTG (Figure 7B). Afterwards, the recirculation through the external loop (EBA) was initiated at a flow rate of 150 ml min⁻¹. Thereafter, the production of (+)-zizaene and cell growth increased proportionally from 12 to 72 h of culture (Figure 7A), showing a coupling between both variables with a Pearson coefficient (PI) of 0.99. After 72 h of growth, the maximum production peak was observed, reaching a (+)-zizaene titer of 93.4 mg L⁻¹ and an OD_{600} of 43.0. Therefore, the bioprocess improved the (+)-zizaene titer 2.5-fold and the cell growth 7.5-fold when compared to that of the LLPPC at shake flask scale. At the end of the cultivation (72 h), the recovery ratio (94.6%) from the adsorbers was similar to that obtained from the LLPPC test from Section 2.2 (94.4%), followed from the cell-free media (3.0%) and from the cells (2.4%).

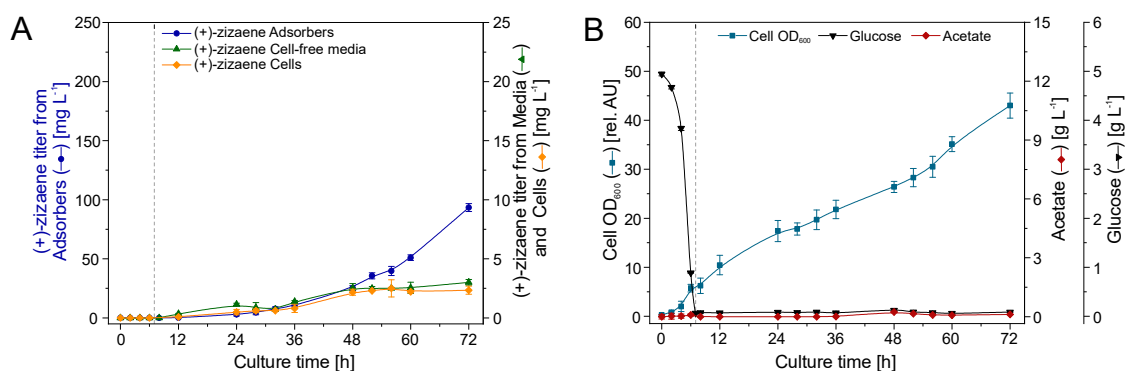


Figure 7. Production of (+)-zizaene (A) and growth kinetics (B) in 2 L bioreactor with external recovery configuration (ERC). Dotted line indicates division between batch and fed-batch stages.

2.6. Bioreactor Cultivation with an Integrated IRC

The IRC was evaluated as an alternative to improve the (+)-zizaene recovery further, whereas the configuration was designed to recover (+)-zizaene directly from the culture broth and improve the adsorption velocity (Figure 6B). To maintain the same amount of resin as the ERC, the bioreactor was loaded with 75 g of adsorbers.

Similar to the ERC, a positive correlation between (+)-zizaene levels and cell growth was observed from 12 to 72 h (PI = 0.98) (Figure 8B). Moreover, the production of (+)-zizaene increased after 24 h, achieving the highest (+)-zizaene titer of 207.8 mg L⁻¹ and cell growth (OD_{600} 48.9 and biomass 10.3 g_{DCW} L⁻¹) at the end of the fermentation (Figure 8A). Thus, the IRC improved the (+)-zizaene titers 2.2-fold when compared to that of the ERC. In addition, the (+)-zizaene recovery ratio from adsorbers was improved to 98.4% when compared to the ERC and reduced the amounts of (+)-zizaene from cell-free media (0.9%) and cells (0.7%).

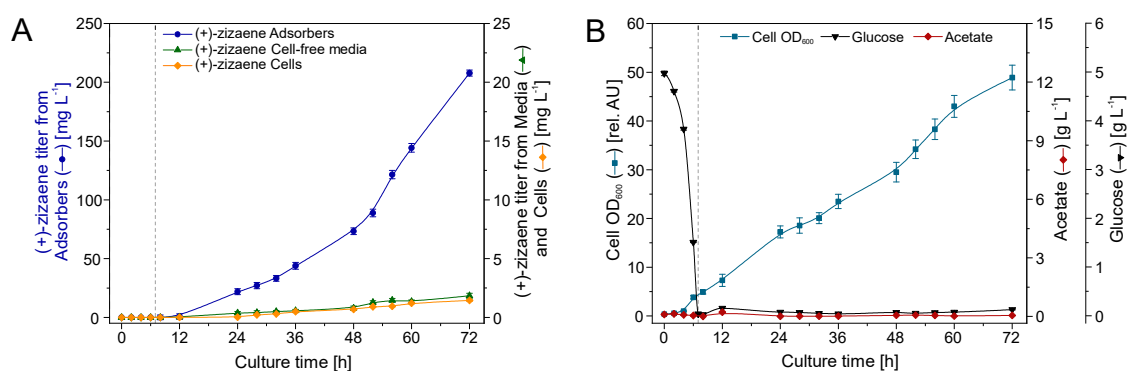


Figure 8. Production of (+)-zizaene (A) and growth kinetics (B) in 2 L bioreactor with internal recovery configuration (IRC). Dotted line indicates division between batch and fed-batch stages.

2.7. Bioreactor Cultivation with an Integrated IRC+GS

As discussed in Section 2.1, there was a loss of (+)-zizaene by volatilization at shake flask scale, which could be even higher at bioreactor scale due to the gassing of air through the bioreactor vessel. Therefore, the (+)-zizaene recovery from the off-gas of the bioreactor could be considered as an additional recovery source to enhance the accumulative (+)-zizaene recovery from the fermentation. For that, a variant from the IRC was performed with the addition of a column loaded with 75 g L⁻¹ of adsorbers and installed in the off-gas of the bioreactor (Figure 6C).

Similar to the other bioreactor configurations, the correlation between cell growth and (+)-zizaene production on the IRC+GS was positive with PI = 95%, indicating a coupling between both variables. The results were similar to the IRC test, where after 72 h of culture, the maximum cell growth (OD₆₀₀ 45.3 and biomass 9.7 g_{DCW} L⁻¹) and (+)-zizaene production (203.4 mg L⁻¹) were reached (Figure 9A,B). The (+)-zizaene amounts were not detected on the ethanol trap, demonstrating efficient adsorption of (+)-zizaene from the resins in the off-gas column with a (+)-zizaene recovery ratio of 0.6%. These low amounts of (+)-zizaene detected on the off-gas suggest an efficient (+)-zizaene trapping from the adsorbers in the culture broth, showing a recovery ratio from adsorbers of 97.6% and a low recovery ratio of 0.9% from both cell-free media and cells, similar to the IRC.

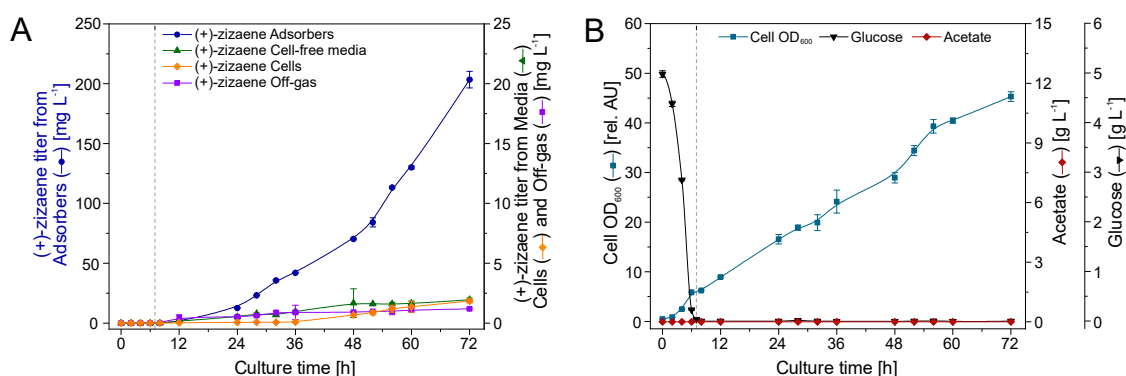


Figure 9. Production of (+)-zizaene (A) and growth kinetics (B) in 2 L bioreactor with internal recovery configuration with gas stripping (IRC+GS). Dotted line indicates division between batch and fed-batch stages.

2.8. Accumulative (+)-Zizaene Production from the Bioreactor Configurations

The contribution to the accumulative (+)-zizaene amount from the IRC+GS was low (less than 1%). In consequence, the IRC and the IRC+GS showed similar accumulative (+)-zizaene levels during the course of the fermentation, whereas the difference between the ERC and both IRCs increased after 12 h of cultivation (Figure 10).

The comparison of performance between bioreactor configurations is summarized in Table 1. The accumulative (+)-zizaene titer and productivity between the IRC and IRC+GS were more than 2-fold higher than the ERC at 72 h of cultivation. Although differences between cell growth and product yield ($Y_{X/S}$) were not so drastic between IRCs and ERC, the production of soluble ZS protein from the IRCs was roughly 4-fold higher when compared to the ERC, suggesting a relation between the soluble ZS protein and the (+)-zizaene levels. In consequence, the best configuration for the in situ recovery of (+)-zizaene at bioreactor scale was the IRC; achieving an accumulative (+)-zizaene titer of 211.13 mg L⁻¹ and productivity of 3.2 mg L⁻¹ h⁻¹. Moreover, these results improved the (+)-zizaene titers 8.4-fold and productivity 3-fold when compared to those from our last report [10].

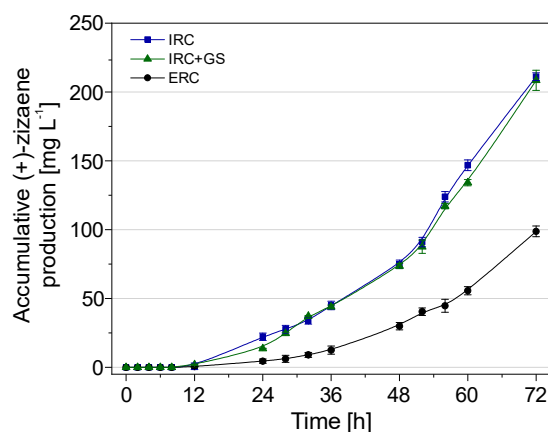


Figure 10. Accumulative production of (+)-zizaene at 2 L bioreactors by distinct in situ recovery configurations: External extraction (ERC), internal extraction (IRC), and internal extraction with gas stripping (IRC+GS). Data are the means of three sample replicates with error bars as SD.

Table 1. Comparison of the bioprocess-performance variables between distinct bioreactor configurations for the in situ recovery of (+)-zizaene after 72 h of growth.

Variable	ERC	IRC	IRC+GS
Accumulative titer (mg L ⁻¹)	98.78 ± 3.87	211.13 ± 1.97	208.41 ± 7.29
Titer from adsorbers (mg L ⁻¹)	93.42 ± 3.30	207.84 ± 1.68	203.44 ± 6.89
Productivity (mg L ⁻¹ h ⁻¹)	1.50 ± 0.06	3.20 ± 0.03	3.16 ± 0.11
$Y_{P/X}$ ¹ (mg _{zizaene} g _{DWCW} ⁻¹)	12.32 ± 0.56	20.45 ± 6.98	21.41 ± 2.29
$Y_{X/S}$ ² (g _{DWCW} g _{glucose} ⁻¹)	0.22 ± 0.003	0.28 ± 0.11	0.30 ± 0.02
$Y_{P/S}$ ³ (mg _{zizaene} g _{glucose} ⁻¹)	2.69 ± 0.08	5.82 ± 0.09	6.52 ± 0.18
Soluble ZS protein (mg L ⁻¹)	35.42 ± 3.20	143.20 ± 2.95	129.80 ± 6.51
Adsorber recovery ratio (%)	94.60 ± 0.14	98.40 ± 0.21	97.60 ± 0.12

¹ $Y_{P/X}$: product/biomass yield. $Y_{X/S}$: ² Biomass/substrate yield. ³ $Y_{P/S}$: product/substrate yield. Data correspond to the mean of three sample replicates with ± SD.

3. Discussion

For the microbial production of (+)-zizaene, significant product volatilization was observed when the recombinant *E. coli* strain was cultured without extractants, similar to that observed with the sesquiterpenes α -humulene [41]. Regardless of the low vapor pressure (5.1 kPa at 20 °C) and boiling point (288 °C) of (+)-zizaene, the volatilization of (+)-zizaene could be explained due to its low aqueous solubility (0.1289 mg L⁻¹ [42]), which practically remains immiscible in the aqueous broth and tends to volatilize. As a solution, we tested the LLPPC at shake flask scale and improved the (+)-zizaene recovery and cell growth, reducing then the cell toxicity. Similar results were shown for the recovery of amorpha-4,11-diene, where the titers from the LLPPC tests were 8.5-fold higher than the controls without extractants [43]. Such improvements can be explained because the organic solvents extract the

isoprenoids during culture due to hydrophobic interactions, and partition from the aqueous phase (culture broth) as demonstrated in many terpene studies [1,44,45].

Accordingly, the Diaion HP20 obtained the highest (+)-zizaene recovery ratio from all tested adsorbers. In comparison with the other adsorbers, Diaion HP20 has the largest pore size (290 Å) and pore volume (1.3 mL g⁻¹) and it is used commonly for the adsorption of relatively large molecules such as small proteins. Although the sesquiterpene (+)-zizaene is not considered a large molecule (204.35 g mol⁻¹), the large pores from the Diaion HP20 could possibly favor the (+)-zizaene adsorption. This idea could be supported due to the low recovery from the Lewatit 1064 MD, which has the lowest pore size of all the tested adsorbers (50 Å). Similar to our findings, the Diaion HP20 resin obtained the highest recovery ratio for the fragrant benzaldehyde (106.12 g mol⁻¹) and L-phenylalanine (165.19 g mol⁻¹) in bioreactor cultivations of *Pycnoporus cinnabarinus* [46], as well as for the prodigiosin-like red pigment (323 Da) from *Serratia sp.* KH-95 [47], whereas the Amberlite XAD16 adsorber (pore size 200 Å) showed the lowest recovery for both cases.

Additionally, all of the tested adsorbers demonstrated higher cell growth when compared to the negative control without extractants. Such results were expected since it is known that most of the adsorbers do not affect cell growth due to their synthetic polymeric composition [37,48]. In addition, the low cell growth from the negative control suggests a toxic effect due to (+)-zizaene accumulation, similar to the toxic effect of linalool and linalool oxides accumulation on the fermentation of *Corynespora cassiicola* [27]. Eventually, further tests are required to measure the toxicity threshold of (+)-zizaene in fermentations.

Concerning the screening of solvents for the desorption of (+)-zizaene, the results were as expected, where solvents with log P values higher than 0.73 eluted the highest sesquiterpene amounts due to their capability to trap hydrophobic compounds [15,19]. Although many studies used ethyl acetate [11,25] for terpene desorption, in our case we chose isooctane (log P = 3.80) because of the similar product recovery when compared to ethyl acetate but at a lower cost. In addition, isooctane has been proven suitable for the recovery of other terpenes such as limonene-1,2-diol produced by *Rhodococcus erythropolis* DCL14 [49]. Moreover, isooctane was used successfully for the extraction of (+)-zizaene on in vitro biotransformation reactions, as shown in our previous report [10].

To recover efficiently the (+)-zizaene at bioreactor scale, distinct ISPR configurations were integrated into the fermentation, using Diaion HP20 as adsorber and isooctane as elution solvent. Although these were chosen due to their recovery performance, other factors such as their low cost and ease for implementation were considered for the selection criteria.

Initially, the ERC improved the (+)-zizaene production 2.5-fold when compared to that of the LLPPC at shake flask tests. Eventually, the minimal growth by feeding glucose maintained the acetate levels at a minimum, allowing the fermentation to reach a higher cell growth (OD₆₀₀ of 43.0), and avoiding an overflow metabolism. Similar cell growth was also achieved by fed-batch fermentation of a metabolically-engineered *E. coli* strain for the production of (-)- α -bisabolol, fed with glycerol after 72 h of culture [14]. Besides, the external loop of the ERC allowed the semi-continuous product recovery, reaching (+)-zizaene titers of 93.4 mg L⁻¹. Such improvements have also been obtained by the use of ERC in other terpenes studies, such as monoterpene carvone (225 mg L⁻¹) [37] and diterpene cembratriene-ol (78.9 mg L⁻¹) [50].

The (+)-zizaene production was enhanced 2.2-fold further by the use of the IRC when compared to the ERC. Besides, the (+)-zizaene amounts from cell-free media from the IRC were lower than the ERC. This demonstrates a higher (+)-zizaene recovery ratio from the IRC (98.4%) than the ERC (94.6%), which resulted in higher cell growth and soluble ZS protein synthesis, suggesting cell toxicity from (+)-zizaene accumulation in the culture broth of the ERC. This could be explained due to the residence time of the adsorbers on the culture broth, whereas in the ERC, the adsorbers have less time in contact with the culture broth (recirculation rate 6 h⁻¹) than in the IRC, in which it resides constantly. Similar results were obtained for the production of prodigiosin-like red pigment from *Serratia sp.* KH-95, where the ERC obtained lower amounts than the IRC due to the lower contact of the adsorbers in the

culture broth [51]. Consequently, terpenes need to be recovered rapidly from the culture broth before becoming volatilized. This was confirmed by the IRC+GS, in which less than 1% of the (+)-zizaene amount was volatilized due to the efficient (+)-zizaene recovery from the adsorbers inside the vessel (97.6%). Hence, the adsorption velocity plays an important role in the ISPR of terpenes.

The IRC showed lower (+)-zizaene amounts from the cells than the ERC; demonstrating no correlation between cell growth and (+)-zizaene amount from cells. Possibly, the constant contact of the *E. coli* cells with the Diaion HP20 adsorbers from the IRC could improve the secretion and trapping of (+)-zizaene by an adsorption mechanism (chemisorption) as described in Figure 1. Similar behavior was observed in the production of a prodigiosin-like red pigment, where the compound was bound to the cell wall from *Serratia sp.* KH-95 and it was adsorbed towards the Diaion HP20 adsorbers, dispersed in the culture broth [51].

The contribution of the (+)-zizaene recovery from the adsorbers on the off-gas was lower than 1%, which demonstrates an efficient (+)-zizaene recovery from the adsorbers. For further scale-up studies of sesquiterpenes, the gas stripping recovery could be unnecessary when the IRC is used. Thus, the accumulative (+)-zizaene recovery from the IRC achieved titers of 211.1 mg L⁻¹ and productivities of 3.2 mg L⁻¹ h⁻¹, which are similar to other IRC terpene bioprocesses, such as fusicocca-2,10(14)-diene (43 mg L⁻¹, 0.6 mg L⁻¹ h⁻¹) [11], α -humulene (60.2 mg L⁻¹, 2.5 mg L⁻¹ h⁻¹) [41], and carvone (198 mg L⁻¹, 2.9 mg L⁻¹ h⁻¹) [37]. Moreover, our study demonstrated higher titers and productivities when compared to other LLPPC terpene bioprocesses, such as patchoulol (50 mg L⁻¹, 0.65 mg L⁻¹ h⁻¹) [52] valerenadiene (62 mg L⁻¹, 1.3 mg L⁻¹ h⁻¹) [53], and farnesol (135.5 mg L⁻¹, 2.8 mg L⁻¹ h⁻¹) [54]. Consequently, the use of IRC with solid extractants is a promising alternative towards the scale-up of the microbial production of terpenes.

4. Materials and Methods

4.1. Materials and Chemicals

Chemicals used in this study were of analytical grade. Polymeric adsorbers were Amberlite® IRA400 Cl, XAD4, XAD16N (Supelco, Bellefonte, PA, USA), Lewatit® 1064 MD (Lanxess, Cologne, Germany), and Diaion HP20 (Mitsubishi Chemicals, Tokyo, Japan).

4.2. Strain and Pre-Cultures

The metabolically-engineered strain used in all the experiments of this research was the multi-plasmid *E. coli* Tuner TZS+MevZS strain, as described in our previous report [9].

All pre-cultures were prepared in 5 mL LB broth with 30 mg L⁻¹ kanamycin and 34 mg L⁻¹ chloramphenicol from glycerol stocks, and cultivated at 37 °C in a rotatory incubator at 150 rpm. For shake flask experiments, pre-cultures were grown overnight and inoculated to main cultures consisting of 35 mL of a modified Aparicio defined medium (ADM, [9]) with 5 g L⁻¹ glucose in sealed glass-baffled shake flasks, to initiate at an OD₆₀₀ of 0.1, and grown with the same conditions as mentioned before. Induction was performed when cultures reached OD₆₀₀ 0.6–0.8 by lowering the temperature to 20 °C and adding isopropyl- β -D-thiogalactoside (IPTG) to a final concentration of 0.5 mM.

4.3. Product Volatilization and LLPPC Experiments

Shake flask cultures without extractants and induced for 24 h were centrifuged for 20 min (10,000 \times g at 4 °C) and the supernatant was filtered through a 0.2 μ m filter. Cell-free broth was transferred to sterile shake flasks and incubated at 20 °C and 150 rpm. Samples were taken from the cell-free broth, further extracted and terpene products were measured via gas chromatography coupled with a flame ionization detector (GC-FID).

For the LLPPC evaluation, cultures were prepared as in Section 4.2 and 10% isooctane (v/v) was added promptly after the addition of IPTG. No extractant was added to the negative control. Cultures were grown for 72 h and every 12 h samples were taken for growth kinetics and terpene analytics.

4.4. Screening of Polymeric Adsorbers

The testing of adsorbers was performed using an in vivo method as described by Halka [11]. For that, distinct polymeric adsorbers (Table 2) were conditioned by washing them with water, isopropanol, isooctane, and finally water. After autoclaving shake flasks with 50 g L⁻¹ of the respective adsorbers, 35 mL of ADM was added and inoculated with pre-culture broth to an initial OD₆₀₀ of 0.1. Growth conditions and induction procedures were according to Section 4.2 and samples were analyzed after 24 h of induction. Terpene products were extracted from adsorbers, cell-free broth, and cells according to Section 4.7.3. A negative control without extractants was included, in which only cell-free broth and cells were analyzed. Identification of terpene products was carried out via gas chromatography with mass spectrometry (GC-MS) and quantification of (+)-zizaene was carried out via GC-FID. To measure the effect of the tested adsorbers on cell growth, the OD₆₀₀ and the dry cell weight (DCW) biomass were analyzed from the distinct resins. The (+)-zizaene recovery ratio from adsorbers was calculated as the (+)-zizaene titer from adsorbers between the accumulative (+)-zizaene titer (recovered from adsorbers, cells, and cell-free media). Data sets were analyzed by ANOVA according to Section 4.8.

Table 2. Main properties of the polymeric adsorbers used for the in situ recovery of (+)-zizaene ¹.

Properties	Amberlite IRA400 CI	Lewatit 1064 MD	Amberlite XAD16N	Amberlite XAD4	Diaion HP20
Particle size (μm)	600–750	440–540	560–710	490–690	250–800
Mean pore size (radius) (Å)	100	50	200	100	290
Surface area (m ² g ⁻¹)	-	800	800	750	590
Pore volume (mL g ⁻¹)	-	1.2	0.55	0.5	1.3
Particle density (mg L ⁻¹)	1.06–1.09	1.02	1.02	1.02	1.01
Functional groups	Dimethyl ethanol ammonium	-	-	-	-
Ionic form	Basic anion exchange	Non-ionic	Non-ionic	Non-ionic	Non-ionic

¹ Information obtained from supplier data sheets.

4.5. Evaluation of Organic Solvents for the (+)-Zizaene Desorption

Organic solvents with a high log P value were evaluated for the desorption of (+)-zizaene comprising decane, dodecane, isooctane, ethyl acetate, isopropanol, acetonitrile, and pentane (Table S1). The Diaion HP20 adsorbers were prepared as described in Section 4.4 and the tested organic solvents were used respectively for the conditioning of adsorbers.

Microbial cultures were prepared as described in Section 4.2 without extractants and after 48 h of cultivation, 2 mL of culture broth was transferred to sterile vials with 0.5 g of Diaion HP20 adsorbers. Afterwards, vials were incubated for 4 h at 20 °C and 150 rpm. Furthermore, the culture broth was discarded and adsorbers were extracted with the tested solvents as described in Section 4.7.3 (+)-Zizaene concentrations were measured via GC-FID and statistical analyses were carried out according to Section 4.8.

4.6. Bioreactor Cultivations with In Situ Recovery of (+)-Zizaene

Pre-cultures were prepared as described in Section 4.2, followed by a third pre-culture that consisted of a 100 mL ADM shake flask culture. After 12 h of cultivation, pre-cultures were inoculated to bioreactors to an OD₆₀₀ of 0.3–0.4.

2 L stirred-tank bioreactors (Biostat A+, Sartorius, Göttingen, Germany) were used for the cultivations, with 1.5 L working volume consisting of an ADM with 5 g L⁻¹ glucose and respective antibiotics. The pH was controlled automatically with 1 M HCl and 25% NH₄OH (v/v) solutions. The Diaion HP20 adsorbers were conditioned according to Section 4.4 with isooctane as the solvent.

4.6.1. IRC Bioreactor

The IRC was prepared with 50 g L⁻¹ of Diaion HP20 dispersed in the culture broth, inside the bioreactor vessel. The IRC with gas stripping (IRC+GS) was carried out similarly to the IRC and a 200 mL column was added to the off-gas line loaded with 75 g of Diaion HP20, followed by an ethanol trap cooled with dry ice and two 0.2 µm sterile filters.

4.6.2. ERC Bioreactor

The ERC was configured without extractants inside the bioreactor vessel, and the culture broth was recirculated to an external recovery loop through a stainless steel EBA column of 200 mL inner volume with 75 g of Diaion HP20 as the fluidized bed. For that, a silicone tubing of 4 mm inner diameter (i.d.) was connected to the EBA column (4.6 cm i.d., 12 cm length for inner chamber) with outlets of 4 mm i.d. and a sampling port on the lateral side. The EBA column had two stainless steel meshes (6 cm diameter of 500 µm) on both terminal sides, fixed with gaskets to recirculate cells and media through the resins while retaining the adsorbers inside the column. The external loop operated continuously at a flow rate of 150 mL min⁻¹ (recirculation rate = 6 h⁻¹) by a SciLog Expert peristaltic pump (Wisconsin, USA).

For all bioreactor configurations, the batch cultivation settings were dissolved oxygen >30%, agitation 400–700 rpm, temperature 37 °C, pH 7.0, and gas flow rate 1.0 vvm. When the glucose was exhausted, the fed-batch stage was initiated by dropping the temperature to 20 °C and initiating the feeding. The fed-batch medium was composed of glucose 100 g L⁻¹, NaCl 1.2 g L⁻¹, CaCl₂ 0.14 g L⁻¹, MgSO₄·7H₂O 0.6 g L⁻¹, FeSO₄·7H₂O 0.001 g L⁻¹, and CuSO₄·5H₂O 0.001 g L⁻¹ with respective antibiotics. The induction was performed after 1 h of feeding by adding 0.5 mM IPTG and in the case of the ERC, the recirculation towards the external loop was activated. Samples for growth kinetics, soluble ZS protein, and terpene analysis were properly taken, measured according to Section 4.7, and plotted with Origin 9.5.5. (Northampton, MA, USA).

4.7. Analytical procedures

4.7.1. Growth Kinetics Analysis

To assess the growth kinetics from cultivations, the cell growth was analyzed by measuring the optical density from fermentation samples at 600 nm using a Biochrom Libra S50 UV-Vis spectrophotometer (Cambridge, UK) and biomass by the dry cell weight method. Glucose consumption was measured from cell-free broth samples with the Biochemistry Analyzer YSI 2900 (Yellow Springs, Greene County, OH, USA). Acetate was measured via high-pressure liquid chromatography as described elsewhere [55].

4.7.2. Soluble ZS Protein Fraction Analysis

Broth samples were normalized to an OD₆₀₀ of 2.0 and extracted as described in our previous report [9]. Soluble ZS protein fractions were analyzed on a 10% sodium dodecyl sulfate polyacrylamide gel electrophoresis with a calibration curve of bovine serum albumin. Quantification of soluble ZS protein was performed by a densitometric method [56,57], measuring the intensity of the ZS protein bands at 78 kDa from stained gel images by the GelAnalyzer 2010 (developed by Istvan Lazar).

4.7.3. Sample extraction

Samples for terpene analyses were extracted from distinct sources during cultivations. Samples from cell-free media, known also as supernatant, were prepared by transferring 2 mL of culture broth to 10 mL glass vials. After centrifugation for 5 min at 10,000× g, the supernatant was transferred to other glass vials and extracted vigorously thrice with 0.5 mL of isooctane. Organic phases were obtained by centrifugation and transferred to GC vials for (+)-zizaene measurements via GC-FID.

Samples from cells were prepared similar to Section 4.7.2. After extracts were ultrasonicated, 300 μL of isooctane was added to 300 μL of cell extract and extracted vigorously. Organic phases were separated by centrifugation and transferred to GC vials for (+)-zizaene measurements via GC-FID.

Samples from adsorbers were extracted vigorously three times by transferring 300 mg of resins to 10 mL glass vials and adding 1 volume of isooctane (or tested solvent for Section 4.5). Organic phases were transferred to GC vials for further product identification via GC-MS and (+)-zizaene quantification via GC-FID.

4.7.4. GC-MS analysis

For the identification of terpene products from the adsorber screening test (Section 4.4), the extracted samples were analyzed by an Agilent 7890B GC-MS system (Santa Clara, CA, USA). Samples of 0.5 μL were injected into the GC-MS equipped with a VF-WAXms capillary column (0.25 mm i.d. \times 0.25 μm thickness \times 30 m length; Agilent, Santa Clara, CA, USA) by the on-column mode with helium 5.0 as the carrier gas at a constant gas flow of 1 mL min^{-1} and injector temperature of 230 $^{\circ}\text{C}$. The oven program comprised 3 steps: (1) 40 $^{\circ}\text{C}$, 3 min; (2) 40–230 $^{\circ}\text{C}$, 10 $^{\circ}\text{C min}^{-1}$; (3) 10 min hold. The scan range was set to 33–300 m/z and the ionization energy to 70.0 eV. Product identification was carried out by comparing mass spectra of samples with authentic standards obtained from the VEO and references from the mass spectral NIST 14 database.

4.7.5. GC-FID analysis

Quantification of (+)-zizaene was done with a GC-2010 plus Shimadzu system coupled with a flame ionization detector (Kyoto, Japan). Samples of 1 μL were injected to the GC-FID with an injector temperature of 240 $^{\circ}\text{C}$ on splitless mode. Oven program was set with the following steps: (1) 40 $^{\circ}\text{C}$, 20 s; (2) 40–200 $^{\circ}\text{C}$, 10 $^{\circ}\text{C min}^{-1}$; (3) 0.5 min hold; (4) 200–230 $^{\circ}\text{C}$, 30 $^{\circ}\text{C min}^{-1}$; (5) 2 min final hold. The quantification of (+)-zizaene was calculated as α -cedrene equivalents by a calibration curve of α -cedrene (standard grade) due to the lack of a commercial (+)-zizaene standard, as demonstrated in a previous report [10].

4.8. Statistical Analysis

Data from Sections 4.4 and 4.5 were analyzed by analysis of variance (ANOVA) and mean comparison tests to assess statistical differences. Adsorbers and organic solvents were used as factors respectively and (+)-zizaene titer was used as the response variable. Data sets were analyzed by Minitab 16 (Pennsylvania, USA) with the ANOVA module and the Bonferroni test was applied for mean comparison test with a 95% confidence level.

5. Conclusions

The results achieved in this study demonstrated the improvement of the microbial production of (+)-zizaene compared to previous studies by enhancing the recovery of (+)-zizaene. Initially, the loss of (+)-zizaene by volatilization was measured and further reduced by LLPPC at shake flask scale. Furthermore, the Diaion HP20 resin obtained the highest (+)-zizaene recovery after screening distinct adsorbers by SLPPC. After evaluating distinct solvents for the desorption process, the isooctane was selected as a suitable eluent and the SLPPC reached (+)-zizaene titers comparable to those obtained by the LLPPC. The scale-up to bioreactors by integrated product recovery configurations improved dramatically the (+)-zizaene production, whereas the IRC demonstrated higher (+)-zizaene titers (211.13 mg L^{-1}) and productivities (3.2 $\text{mg L}^{-1} \text{h}^{-1}$) than the ERC. Consequently, the successful application of ISPR proved a greener extraction method, which reutilizes the extractant material (polymeric adsorbers), reduces the number of extraction reagents (only one solvent is required), reduces the energy input and quantity of chemical wastes, and improves the recovery ratio of (+)-zizaene over 98%.

Supplementary Materials: The following are available online: Figure S1: Terpene profile between distinct polymeric adsorbers; Figure S2: Mass spectra of terpene products; Figure S3: Comparison of soluble and insoluble ZS protein amounts between distinct polymeric adsorbers; Figure S4: Off-line analytics from bioreactor configurations; Table S1: Physicochemical properties of the organic solvents used for the desorption of (+)-zizaene; Table S2: Recovery ratio of (+)-zizaene from distinct polymeric adsorbers.

Author Contributions: Funding acquisition and conceptualization, T.S. and S.B.; methodology, S.B. and F.A.; experimentation, data analysis, and manuscript draft preparation, F.A.; manuscript revision, T.S. and S.B. All authors agreed to the final version.

Funding: This research was funded by the PINN program from the Ministry of Science, Technology and Telecommunications of Costa Rica (MICITT), grant PED-058-2015-1, and by the Open Access Fund of the Leibniz Universität Hannover.

Acknowledgments: We thank Friedbert Gellermann for the development of the EBA column. We thank Kimia Ekramzadeh, Lukas Koch and Samuel Edward Hakim for the technical support for the cultivations.

Conflicts of Interest: The authors declare no conflicts of interest. The funders had no role in the design of the study; in the collection, analyses, or interpretation of data; in the writing of the manuscript, or in the decision to publish the results.

References

1. Peralta-Yahya, P.P.; Ouellet, M.; Chan, R.; Mukhopadhyay, A.; Keasling, J.D.; Lee, T.S. Identification and microbial production of a terpene-based advanced biofuel. *Nat. Commun.* **2011**, *2*, 483–488. [[CrossRef](#)] [[PubMed](#)]
2. Paddon, C.J.; Westfall, P.J.; Pitera, D.J.; Benjamin, K.; Fisher, K.; McPhee, D.; Leavell, M.D.; Tai, A.; Main, A.; Eng, D.; et al. High-level semi-synthetic production of the potent antimalarial artemisinin. *Nature* **2013**, *496*, 528–532. [[CrossRef](#)] [[PubMed](#)]
3. Westfall, P.J.; Gardner, T.S. Industrial fermentation of renewable diesel fuels. *Curr. Opin. Biotechnol.* **2011**, *22*, 344–350. [[CrossRef](#)]
4. Leavell, M.D.; McPhee, D.J.; Paddon, C.J. Developing fermentative terpenoid production for commercial usage. *Curr. Opin. Biotechnol.* **2016**, *37*, 114–119. [[CrossRef](#)] [[PubMed](#)]
5. Lavania, A.C. Other uses, and utilization of vetiver: Vetiver Oil. In *Proceedings of the Third International Conference on Vetiver*; The Vetiver Network International: Guangzhou, China, 2003; p. 486.
6. Sanganerla, P. *Essential Oils Market Report Summer 2018*; Report summer 2018; Ultra International B.V: Spijkenisse, The Netherlands, 2018; pp. 36–39.
7. Belhassen, E.; Filippi, J.J.; Brévard, H.; Joulain, D.; Baldovini, N. Volatile constituents of vetiver: A review. *Flavour Fragr. J.* **2015**, *30*, 26–82. [[CrossRef](#)]
8. Pripdeevech, P.; Wongpornchai, S.; Marriott, P.J. Comprehensive two-dimensional gas chromatography-mass spectrometry analysis of volatile constituents in Thai vetiver root oils obtained by using different extraction methods. *Phytochem. Anal.* **2010**, *163*–173. [[CrossRef](#)]
9. Aguilar, F.; Scheper, T.; Beutel, S. Modulating the precursor and terpene synthase supply for the whole-cell biocatalytic production of the sesquiterpene (+)-zizaene in a pathway engineered *E. coli*. *Genes* **2019**, *10*, 478. [[CrossRef](#)]
10. Aguilar, F.; Hartwig, S.; Scheper, T.; Beutel, S. Catalytic specificity, reaction mechanisms, and conformational changes during catalysis of the recombinant SUMO (+)-zizaene synthase from *Chrysopogon zizanioides*. *ACS Omega* **2019**, *4*, 6199–6209. [[CrossRef](#)]
11. Halka, L.; Wichmann, R. Enhanced production and in situ product recovery of fusicocca-2,10(14)-diene from yeast. *Fermentation* **2018**, *4*, 65. [[CrossRef](#)]
12. Tippmann, S.; Scalcinati, G.; Siewers, V.; Nielsen, J. Production of farnesene and santalene by *Saccharomyces cerevisiae* using fed-batch cultivations with RQ-controlled feed. *Biotechnol. Bioeng.* **2016**, *113*, 72–81. [[CrossRef](#)]
13. Qiao, J.; Luo, Z.; Cui, S.; Zhao, H.; Tang, Q.; Mo, C.; Ma, X.; Ding, Z. Modification of isoprene synthesis to enable production of curcubitadienol synthesis in *Saccharomyces cerevisiae*. *J. Ind. Microbiol. Biotechnol.* **2019**, *46*, 147–157. [[CrossRef](#)] [[PubMed](#)]
14. Han, G.H.; Kim, S.K.; Yoon, P.K.S.; Kang, Y.; Kim, B.S.; Fu, Y.; Sung, B.H.; Jung, H.C.; Lee, D.H.; Kim, S.W.; et al. Fermentative production and direct extraction of (–)- α -bisabolol in metabolically engineered *Escherichia coli*. *Microb. Cell Fact.* **2016**, *15*, 1–13. [[CrossRef](#)] [[PubMed](#)]

15. Schewe, H.; Mirata, M.A.; Schrader, J. Bioprocess engineering for microbial synthesis and conversion of isoprenoids. In *Biotechnology of Isoprenoids. Advances in Biochemical Engineering/Biotechnology*; Schrader, J., Bohlmann, J., Eds.; Springer: Cham, Switzerland, 2015; pp. 251–286.
16. Schügerl, K.; Hubbuch, J. Integrated bioprocesses. *Curr. Opin. Microbiol.* **2005**, *8*, 294–300. [[CrossRef](#)] [[PubMed](#)]
17. Buque-Taboada, E.M.; Straathof, A.J.J.; Heijnen, J.J.; Van Der Wielen, L.A.M. In situ product recovery (ISPR) by crystallization: Basic principles, design, and potential applications in whole-cell biocatalysis. *Appl. Microbiol. Biotechnol.* **2006**, *71*, 1–12. [[CrossRef](#)] [[PubMed](#)]
18. Sikkema, J.; Bont, J.; Poolman, B. Interactions of cyclic hydrocarbons with biological membranes. *J. Biol. Chem.* **1994**, *269*, 8022–8028. [[PubMed](#)]
19. Bruce, L.J.; Daugulis, A.J. Solvent selection strategies for extractive biocatalysis. *Biotechnol. Prog.* **1991**, *7*, 116–124. [[CrossRef](#)] [[PubMed](#)]
20. Willrodt, C.; David, C.; Cornelissen, S.; Bühler, B.; Julsing, M.K.; Schmid, A. Engineering the productivity of recombinant *Escherichia coli* for limonene formation from glycerol in minimal media. *Biotechnol. J.* **2014**, *9*, 1000–1012. [[CrossRef](#)] [[PubMed](#)]
21. Boghigian, B.A.; Myint, M.; Wu, J.; Pfeifer, B.A. Simultaneous production and partitioning of heterologous polyketide and isoprenoid natural products in an *Escherichia coli* two-phase bioprocess. *J. Ind. Microbiol. Biotechnol.* **2011**, *38*, 1809–1820. [[CrossRef](#)] [[PubMed](#)]
22. Gionata, S.; Scalcinati, G.; Partow, S.; Siewers, V.; Schalk, M.; Daviet, L.; Nielsen, J. Combined metabolic engineering of precursor and co-factor supply to increase α -santalene production by *Saccharomyces cerevisiae*. *Microb. Cell Fact.* **2012**, *11*, 117. [[CrossRef](#)]
23. Tsuruta, H.; Paddon, C.J.; Eng, D.; Lenihan, J.R.; Horning, T.; Anthony, L.C.; Regentin, R.; Keasling, J.D.; Renninger, N.S.; Newman, J.D. High-level production of amorpho-4,11-diene, a precursor of the antimalarial agent artemisinin, in *Escherichia coli*. *PLoS ONE* **2009**, *4*, e4489. [[CrossRef](#)]
24. Dafoe, J.T.; Daugulis, A.J. In situ product removal in fermentation systems: Improved process performance and rational extractant selection. *Biotechnol. Lett.* **2014**, *36*, 443–460. [[CrossRef](#)] [[PubMed](#)]
25. Alonso-Gutierrez, J.; Chan, R.; Batt, T.S.; Adams, P.D.; Keasling, J.D.; Petzold, C.J.; Lee, T.S.; Adams, P.D. Metabolic engineering of *Escherichia coli* for limonene and perillyl alcohol production. *Metab. Eng.* **2013**, *19*, 33–41. [[CrossRef](#)] [[PubMed](#)]
26. Jackson, B.E.; Hart-Wells, E.A.; Matsuda, S.P.T. Metabolic engineering to produce sesquiterpenes in yeast. *Org. Lett.* **2003**, *5*, 1629–1632. [[CrossRef](#)] [[PubMed](#)]
27. Bormann, S.; Etschmann, M.M.W.; Mirata, M.A.; Schrader, J. Integrated bioprocess for the stereospecific production of linalool oxides from linalool with *Corynespora cassicola* DSM 62475. *J. Ind. Microbiol. Biotechnol.* **2012**, *39*, 1761–1769. [[CrossRef](#)] [[PubMed](#)]
28. Dunlop, M.J.; Dossani, Z.Y.; Szmids, H.L.; Chu, H.C.; Lee, T.S.; Keasling, J.D.; Hadi, M.Z.; Mukhopadhyay, A. Engineering microbial biofuel tolerance and export using efflux pumps. *Mol. Syst. Biol.* **2011**, *7*, 1–7. [[CrossRef](#)] [[PubMed](#)]
29. Wang, J.F.; Xiong, Z.Q.; Li, S.Y.; Wang, Y. Enhancing isoprenoid production through systematically assembling and modulating efflux pumps in *Escherichia coli*. *Appl. Microbiol. Biotechnol.* **2013**, *97*, 8057–8067. [[CrossRef](#)] [[PubMed](#)]
30. Southall, N.T.; Dill, K.A.; Haymet, A.D.J. A view of the hydrophobic effect. *J. Phys. Chem. B* **2002**, *106*, 521–533. [[CrossRef](#)]
31. Butt, H.; Graf, K.; Kappl, M. *Physics and Chemistry of Interfaces*; Wiley-VCH Verlag GmbH & Co. KGaA: Heidelberg, Germany, 2003; pp. 177–205. [[CrossRef](#)]
32. Grozdev, L.; Kaiser, J.; Berensmeier, S. One-step purification of microbially produced hydrophobic terpenes via process chromatography. *Front. Bioeng. Biotechnol.* **2019**, *7*, 1–12. [[CrossRef](#)]
33. Freeman, A.; Woodley, J.M.; Lilly, M.D. In situ product removal as a tool for bioprocessing. *Nat. Biotechnol.* **1993**, *11*, 1007–1012. [[CrossRef](#)]
34. Schempp, F.M.; Drummond, L.; Buchhaupt, M.; Schrader, J. Microbial cell factories for the production of terpenoid flavor and fragrance compounds. *J. Agric. Food Chem.* **2018**, *66*, 2247–2258. [[CrossRef](#)]
35. Stark, D.; von Stockar, U. In situ product removal (ISPR) in whole cell biotechnology during the last twenty years. In *Process Integration in Biochemical Engineering*; Springer: Berlin/Heidelberg, Germany, 2007; Volume 80, pp. 149–175. [[CrossRef](#)]

36. Moser, S.; Pichler, H. Identifying and engineering the ideal microbial terpenoid production host. *Appl. Microbiol. Biotechnol.* **2019**, *103*, 5501–5516. [[CrossRef](#)] [[PubMed](#)]
37. Morrish, J.L.E.; Daugulis, A.J. Improved reactor performance and operability in the biotransformation of carveol to carvone using a solid-liquid two-phase partitioning bioreactor. *Biotechnol. Bioeng.* **2008**, *101*, 946–956. [[CrossRef](#)] [[PubMed](#)]
38. Cuellar, M.C.; Sraathof, A.J.J. Improving fermentation by product removal. In *Intensification of Biobased Processes*; Gorak, A., Stankiewicz, A., Eds.; Royal Society of Chemistry: London, UK, 2018; pp. 86–108.
39. Krings, U.; Berger, R.G. In situ recovery of the aroma compound perillene from stirred-tank cultured *Pleurotus ostreatus* using gas stripping and adsorption on polystyrene. *Biotechnol. Lett.* **2008**, *30*, 1347–1351. [[CrossRef](#)] [[PubMed](#)]
40. Tan, J.S.; Ling, T.C.; Mustafa, S.; Tam, Y.J.; Ramanan, R.N.; Ariff, A.B. An integrated bioreactor-expanded bed adsorption system for the removal of acetate to enhance the production of alpha-interferon-2b by *Escherichia coli*. *Process Biochem.* **2013**, *48*, 551–558. [[CrossRef](#)]
41. Alemdar, S.; König, J.C.; Hartwig, S.; Frister, T.; Scheper, T.; Beutel, S. Bioproduction of α -humulene in metabolically engineered *Escherichia coli* and application in zerumbone synthesis. *Eng. Life Sci.* **2017**, *17*, 900–907. [[CrossRef](#)]
42. The Good Scents Company Information System. Available online: <http://www.thegoodscentscompany.com/episys/ep1563221.html> (accessed on 20 June 2019).
43. Newman, J.D.; Marshall, J.; Chang, M.; Nowroozi, F.; Paradise, E.; Pitera, D.; Newman, K.L.; Keasling, J.D. High-level production of amorpha-4,11-diene in a two-phase partitioning bioreactor of metabolically engineered *Escherichia coli*. *Biotechnol. Bioeng.* **2006**, *95*, 684–691. [[CrossRef](#)] [[PubMed](#)]
44. Morrish, J.L.E.; Brennan, E.T.; Dry, H.C.; Daugulis, A.J. Enhanced bioproduction of carvone in a two-liquid-phase partitioning bioreactor with a highly hydrophobic biocatalyst. *Biotechnol. Bioeng.* **2008**, *101*, 768–775. [[CrossRef](#)]
45. Westfall, P.J.; Pitera, D.J.; Lenihan, J.R.; Eng, D.; Woolard, F.X.; Regentin, R.; Horning, T.; Tsuruta, H.; Melis, D.J.; Owens, A.; et al. Production of amorphadiene in yeast, and its conversion to dihydroartemisinin acid, precursor to the antimalarial agent artemisinin. *Proc. Natl. Acad. Sci. USA* **2012**, *109*, E111–E118. [[CrossRef](#)]
46. Lomascolo, A.; Lesage-Meessen, L.; Labat, M.; Navarro, D.; Delattre, M.; Asther, M. Enhanced benzaldehyde formation by a monokaryotic strain of *Pycnoporus cinnabarinus* using a selective solid adsorbent in the culture medium. *Can. J. Microbiol.* **1999**, *45*, 653–657. [[CrossRef](#)]
47. Kim, C.H.; Kim, S.W.; Hong, S.I. An integrated fermentation-separation process for the production of red pigment by *Serratia sp.* KH-95. *Process Biochem.* **1999**, *35*, 485–490. [[CrossRef](#)]
48. Amsden, B.G.; Bochansz, J.; Daugulis, A.J. Degradation of xenobiotics in a partitioning bioreactor in which the partitioning phase is a polymer. *Biotechnol. Bioeng.* **2003**, *84*, 399–405. [[CrossRef](#)] [[PubMed](#)]
49. De Carvalho, C.C.R.; Van Keulen, F.; Da Fonseca, M.M.R. Production and recovery of limonene-1,2-diol and simultaneous resolution of a diastereomeric mixture of limonene-1,2-epoxide with whole cells of *Rhodococcus erythropolis* DCL14. *Biocatal. Biotransform.* **2000**, *18*, 223–235. [[CrossRef](#)]
50. Mischko, W.; Hirte, M.; Roehrer, S.; Engelhardt, H.; Mehlmer, N.; Minceva, M.; Brück, T. Modular biomanufacturing for a sustainable production of terpenoid-based insect deterrents. *Green Chem.* **2018**, *20*, 2637–2650. [[CrossRef](#)]
51. Bae, J.; Moon, H.; Oh, K.K.; Kim, C.H.; Sil Lee, D.; Kim, S.W.; Hong, S.I. A novel bioreactor with an internal adsorbent for integrated fermentation and recovery of prodigiosin-like pigment produced from *Serratia sp.* KH-95. *Biotechnol. Lett.* **2001**, *23*, 1315–1319. [[CrossRef](#)]
52. Henke, N.A.; Wichmann, J.; Baier, T.; Frohwitter, J.; Lauersen, K.J.; Risse, J.M.; Peters-Wendisch, P.; Kruse, O.; Wendisch, V.F. Patchouliol production with metabolically engineered *Corynebacterium glutamicum*. *Genes* **2018**, *9*, 219. [[CrossRef](#)] [[PubMed](#)]
53. Nybo, S.E.; Saunder, J.; McCormick, S. Metabolic engineering of *Escherichia coli* for production of valerenadiene. *J. Biotechnol.* **2017**, *262*, 60–66. [[CrossRef](#)] [[PubMed](#)]
54. Wang, C.; Yoon, S.H.; Shah, A.A.; Chung, Y.R.; Kim, J.Y.; Choi, E.S.; Keasling, J.D.; Kim, S.W. Farnesol production from *Escherichia coli* by harnessing the exogenous mevalonate pathway. *Biotechnol. Bioeng.* **2010**, *107*, 421–429. [[CrossRef](#)] [[PubMed](#)]

55. Li, Z.; Kessler, W.; Van Den Heuvel, J.; Rinas, U. Simple defined autoinduction medium for high-level recombinant protein production using T7-based *Escherichia coli* expression systems. *Appl. Microbiol. Biotechnol.* **2011**, *91*, 1203–1213. [[CrossRef](#)]
56. Ude, C.; Ben-Dov, N.; Jochums, A.; Li, Z.; Segal, E.; Scheper, T.; Beutel, S. Online analysis of protein inclusion bodies produced in *E. coli* by monitoring alterations in scattered and reflected light. *Appl. Microbiol. Biotechnol.* **2016**, *100*, 4147–4159. [[CrossRef](#)]
57. Lamy, E.; Rodrigues, L.; Guerreiro, O.; Soldado, D.; Francisco, A.; Lima, M.; Silva, F.C.E.; Lopes, O.; Santos-Silva, J.; Jerónimo, E. Changes in salivary protein composition of lambs supplemented with aerial parts and condensed tannins: Extract from *Cistus ladanifer* L.—A preliminary study. *Agrofor. Syst.* **2019**, *4*, 1–9. [[CrossRef](#)]

Sample Availability: Samples of the compounds are not available from the authors.



© 2019 by the authors. Licensee MDPI, Basel, Switzerland. This article is an open access article distributed under the terms and conditions of the Creative Commons Attribution (CC BY) license (<http://creativecommons.org/licenses/by/4.0/>).

5. Concluding remarks

The microbial production of terpenes is a promising alternative towards a sustainable supply by renewable resources. Although much progress has been achieved in the metabolic engineering of many terpenes by the academic and industrial sector, few are the cases which have reached the industrial scale. The knowledge developed from this dissertation provides new insights in the biotechnological production of fragrant sesquiterpenes. The main concluding remarks of this research are summarized as follows:

Most plant-based TPS are expressed poorly in *E. coli*, leading to inclusion body formation. To circumvent such formation, the ZS is overexpressed with a fusion SUMO domain that increases solubility. Consequently, most of the ZS protein is produced in the soluble fraction and in an active form, demonstrating a high catalytical selectivity towards E,E-FDP, yielding 90% (+)-zizaene (main product) and 8.5% β -acoradiene (side product). The optimal reaction conditions are found to be pH 7.5 and 36 °C, showing a similar pH as found in the cytosol from plant cells. Interestingly, the ZS follows a substrate inhibition kinetic model, which is believed to play a role in the regulation of terpene biosynthesis in plants, triggered by abiotic factors.

Concerning the substrate specificity, ZS is a promiscuous TPS for monoterpenes substrates (GPP and NPP), leading to the formation of 8 distinct acyclic, cyclic and hydroxylated monoterpenes. On the contrary, ZS is a high-fidelity TPS for sesquiterpene isomer substrates (E,Z-FDP and Z,E-FDP), yielding only 1 acyclic and 3 acyclic/cyclic sesquiterpenes respectively.

The catalyzation of E,E-FDP by ZS is very stable at a broad range of pH values and temperatures, as demonstrated by the constant product ratio through the tested conditions. Further in silico docking models revealed that the residue composition from the J-K and A-C loops contributed to the stabilization of the closed conformation of ZS, capable of standing the pH and temperature variations.

The metabolic engineering of the (+)-zizaene biosynthetic pathway was performed in *E. coli* as host. As a proof of concept, (+)-zizaene can be produced by overexpressing the SUMO-fused ZS and utilizing the FDP supply from the endogenous MEP-pathway from *E. coli*, but at lower titers. Thus, the engineering of the exogenous MEV-pathway is necessary to increase the FDP supply. However, overexpression of the MEV-pathway and the ZS gene into a single polycistronic vector produces still low (+)-zizaene titers due to the decline of the ZS supply, in part because of the design of the MEV operon and the strength of the *lacUV5* promoter. After testing distinct promoters for the ZS gene with mono-cistronic plasmids, the T7 promoter was found to increase the ZS supply, which leads to the increase of the (+)-zizaene titers. At this point, the ZS is still the bottleneck of the biosynthetic pathway. This was demonstrated by increasing the ZS supply further by overexpressing a second copy of the ZS gene. In consequence, the overexpression of

the ZS gene into two distinct plasmids under the control of two promoters is an optimal alternative to improve the (+)-zizaene titer.

Optimization of the fermentation conditions by testing media, pH, temperature, induction and *E. coli* B strains further improves the (+)-zizaene titer. The most relevant factor is the nitrogen concentration in the media, which enhances the protein synthesis, resulting in a higher cell growth and soluble ZS protein amounts. Moreover, the use of the *E. coli* Tuner(DE3) B strain improves the (+)-zizaene production because it reduces the overexpression of unnecessary recombinant proteins, reducing the metabolic burden of the cells.

Further development of the (+)-zizaene bioprocess requires an efficient product recovery method integrated to fed-batch cultivations at bioreactor scale. Initially, the loss of (+)-zizaene by volatilization was confirmed in cultures without extractants, and the application of LLPPC improves the (+)-zizaene recovery 4-fold from culture broth. Furthermore, the Diaion HP20 is the best polymeric adsorber for SLPPC with similar recovery ratio as the LLPPC. Because of the ease of resin removal, reuse and non-emulsion formation, the SLPPC is preferred as ISPR of (+)-zizaene and evaluated by testing distinct bioreactor configurations. As a result, (+)-zizaene recovery from ERC enhances the (+)-zizaene titer 2.5-fold higher than the LLPPC. Application of IRC further improves the (+)-zizaene titer 2.2-fold and additional IRC+GS fermentation test confirmed the efficient (+)-zizaene recovery from IRC due to the low (+)-zizaene amount recovered from the off-gas. Moreover, the IRC demonstrated the highest (+)-zizaene recovery due to a higher adsorption velocity when compared to that of the ERC. In consequence, the IRC is the most suitable method for (+)-zizaene recovery in HCDC at bioreactor scale, reaching (+)-zizaene titers of 211.13 mg L⁻¹ and productivities of 3.2 mg L⁻¹ h⁻¹.

Finally, this thesis contributes towards the microbial production of the fragrant sesquiterpene khusimol by the characterization of the ZS, the metabolic engineering of (+)-zizaene and the enhanced (+)-zizaene production by integrating fermentation and product recovery. Overall, this study provides new insights in the bioprocess development for the microbial production of fragrant terpenes.

6. Outlook and recommendations

The microbial production of (+)-zizaene can be improved further by applying protein engineering to the ZS, which could augment its catalytical activity. Eventually, improved ZS variants can be developed by site-directed mutagenesis from residues in the active site, identified in chapter 1. Additionally, the application of other protein engineering methods such as directed evolution should also be considered.

Raising the ZS supply in combination with the increase of the FDP supply could boost the production of (+)-zizaene. This can be achieved by engineering the MEV-pathway by testing distinct FDP synthases from distinct organisms, as demonstrated for the metabolic engineering of the sesquiterpene longifolene in *E. coli* [60]. Eventually, other enzymes belonging to the MEV-pathway could also be considered for further tests. Engineering the (+)-zizaene biosynthetic pathway in yeasts could eventually boost the terpene production, as shown in other cases [31] and should be considered for further experiments.

Concerning the in situ recovery of (+)-zizaene, the ERC process could be improved further. Although the IRC showed higher recovery than the ERC, the latter holds a higher potential to be applied at larger scales. Therefore, the optimization of the EBA variables, such as recirculation rate, adsorber amount and degree of bed expansion (sedimented bed height) could considerably improve the recovery rate, as observed by the acetate recovery for the production of alpha-interferon-2b in *E. coli* [75]. On the other hand, the IRC could be improved by devising a fixed adsorption basket such as that described for the production of prodigiosin-like pigment from *Serratia* sp. KH-95 [71]. Among the advantages of this method are stabilizing the fermentation parameters (pH, pO₂ and stirring), avoiding clogging of valves and preventing damage of adsorbers due to shear forces.

Although the improvement of the (+)-zizaene production by metabolic engineering and product recovery is of interest, the production of the final compound, the fragrant khusimol, is of greater relevance. As a starting point, the enzymatic hydroxylation of (+)-zizaene towards khusimol should be addressed.

Currently, there is a patent that describes two cytochrome P450 monooxygenases capable of such hydroxylation [49]; however, our results overexpressing these P450 enzymes in *E. coli* and *Chlamydomonas* sp. demonstrated a different catalytical specificity (unpublished results). Consequently, the screening of other monooxygenases from the *Ch. zizanioides* is considered the recommended approach to fulfill this enzymatic hydroxylation. Taking into account the published transcriptomes from the vetiver grass [76,77], a bioinformatic approach could be used to screen RNA sequences from putative cytochrome P450 monooxygenases and test them experimentally by codon optimized synthetic genes, overexpressed in microbes.

Furthermore, *in vitro* hydroxylation assays can be applied to confirm the catalyzation to khusimol by the P450 enzyme candidates. Once the positive hydroxylating enzymes are obtained, the bioprocess can be developed by the following alternatives:

6.1. Whole-cell biocatalytical system:

Positive cytochrome P450 monooxygenases for khusimol formation could be engineered into the microbial platform developed in this thesis and could be constructed a whole-cell biocatalytical *E. coli* strain able to produce khusimol from a carbon source. This could be engineered by cloning the P450 gene downstream the *ZS* gene in the pETZS plasmid with an IRES in between and co-transforming it with the pMev plasmid into the Tuner *E. coli* strain. Alternatively, cloning the P450 gene and the *ZS* gene into a single vector with two promoters, such as the pETDuet (Novagen), should provide a stronger overexpression.

Once the proof of concept for the khusimol production is reached, the bioprocess could follow a similar strategy as chapter 3, to test distinct ISPR configurations for the *in situ* recovery of khusimol in fed-batch bioreactors.

6.2. *In vitro* biotransformations:

Because of the low titers reported from the microbial production of hydroxylated sesquiterpenes [78,79], an alternative could be the *in vitro* biotransformation of (+)-zizaene to khusimol in reactors. For this method, the substrate (+)-zizaene would be produced by using the bioprocess developed in this thesis. Afterwards, the cytochrome P450 monooxygenases would be produced and purified similar to the procedure of the *ZS*. After the purification of both (+)-zizaene and P450 enzyme, the *in vitro* biotransformation reactions could be carried out by incubating both under controlled conditions into a reactor to yield khusimol and further extract and purify it via flash chromatography.

7. References

1. Lavania, A.C. Other uses, and utilization of vetiver: vetiver oil. In Proceedings of the Third International Conference on Vetiver; The Vetiver Network International: Guangzhou, 2003; pp. 486. [[CrossRef](#)]
2. Morris, E.T. *Vetiver: Gift of India*; Dragoco Report; Holzminden, Germany, 1983; pp. 158–165.
3. Merfort, I. Review of the analytical techniques for sesquiterpenes and sesquiterpene lactones. *J. Chromatogr. A* **2002**, *967*, 115–130. [[CrossRef](#)]
4. Tholl, D. Biosynthesis and biological functions of terpenoids in plants. In *Advances in Biochemical Engineering/Biotechnology*; Schrader, J., Bohlmann, J., Eds.; Springer International: Switzerland, **2015**; pp. 63–106. [[CrossRef](#)]
5. Morrow, G.W. *Bioorganic synthesis: An introduction*; Oxford University Press: New York, USA, **2016**; pp. 1-429. [[CrossRef](#)]
6. Cane, D.E. Isoprenoid biosynthesis. stereochemistry of the cyclization of allylic pyrophosphates. *Acc. Chem. Res.* **1985**, *18*, 220–226. [[CrossRef](#)]
7. Dewick, P.M. The mevalonate and methylerythritol phosphate pathways: Terpenoids and steroids. In *Medicinal Natural Products*; Dewick, P.M., Ed.; John Wiley and Sons, Ltd., Publication: Chichester, UK, **2009**; pp. 167–289. [[CrossRef](#)]
8. Ashour, M.; Wink, M.; Gershenzon, J. Biochemistry of terpenoids: monoterpenes, sesquiterpenes and diterpenes. In *Annual plant reviews, Volume 40 Biochemistry of plant secondary metabolism*; Wink, M., Ed.; Blackwell Publishing Ltd: Heidelberg, Germany; 2nd Edition, **2010**; Vol. 40, pp. 258–303. [[CrossRef](#)]
9. Wang, C.; Liwei, M.; Park, J. Bin; Jeong, S.H.; Wei, G.; Wang, Y.; Kim, S.W. Microbial platform for terpenoid production: *Escherichia coli* and yeast. *Front. Microbiol.* **2018**, *9*, 1–8. [[CrossRef](#)]
10. Liao, P.; Hemmerlin, A.; Bach, T.J.; Chye, M.L. The potential of the mevalonate pathway for enhanced isoprenoid production. *Biotechnol. Adv.* **2016**, *34*, 697–713. [[CrossRef](#)]
11. Rohmer, M.; Knani, M.; Simonin, P.; Sutter, B.; Sahm, H. Isoprenoid biosynthesis in bacteria: A novel pathway for the early steps leading to isopentenyl diphosphate. *Biochem. J.* **1993**, *295*, 517–524. [[CrossRef](#)]
12. Frank, A.; Groll, M. The methylerythritol phosphate pathway to isoprenoids. *Chem. Rev.* **2017**, *117*, 5675–5703. [[CrossRef](#)]
13. Schempp, F.M.; Drummond, L.; Buchhaupt, M.; Schrader, J. Microbial cell factories for the production of terpenoid flavor and fragrance compounds. *J. Agric. Food Chem.* **2018**, *66*, 2247–2258. [[CrossRef](#)]
14. Tholl, D. Terpene synthases and the regulation, diversity and biological roles of terpene metabolism. *Curr. Opin. Plant Biol.* **2006**, *9*, 297–304. [[CrossRef](#)]
15. Christianson, D.W. Structural biology and chemistry of the terpenoid cyclases. *Chem. Rev.* **2006**, *106*, 3412–3442. [[CrossRef](#)]
16. Dougherty, D.A. Cation- π interactions in chemistry and biology: A new view of benzene, Phe, Tyr, and Trp. *Science* **1996**, *271*, 163–168. [[CrossRef](#)]

7. References

17. Wendt, K.U.; Schulz, G.E. Isoprenoid biosynthesis: Manifold chemistry catalyzed by similar enzymes. *Structure* **1998**, *6*, 127–133. [[CrossRef](#)]
18. Christianson, D.W. Structural and chemical biology of terpenoid cyclases. *Chem. Rev.* **2017**, *117*, 11570–11648. [[CrossRef](#)]
19. Pateraki, I.; Heskes, A.M.; Hamberger, B. Cytochromes P450 for terpene functionalisation and metabolic engineering. In *Biotechnology of Isoprenoids*; Schrader, J., Bohlmann, J., Eds.; Springer International: Heidelberg, **2015**; pp. 107–139. [[CrossRef](#)]
20. Buchanan, B.B.; Grisse, W.; Jones, R.L. *Biochemistry and Molecular Biology of Plants*; Buchanan, B.B., Grisse, W., Jones, R.L., Eds.; 2nd Ed.; Wiley Blackwell: New York, **2015**; pp. 1-1280. [[CrossRef](#)]
21. Vickers, C.E.; Possell, M.; Cojocariu, C.I.; Velikova, V.B.; Laothawornkitkul, J.; Ryan, A.; Mullineaux, P.M.; Nicholas Hewitt, C. Isoprene synthesis protects transgenic tobacco plants from oxidative stress. *Plant, Cell Environ.* **2009**, *32*, 520–531. [[CrossRef](#)]
22. Kim, S.; Keasling, J.D. Metabolic engineering of the nonmevalonate isopentenyl diphosphate synthesis pathway in *Escherichia coli* enhances lycopene production. *Biotechnol. Bioeng.* **2001**, *72*, 408–415. [[CrossRef](#)]
23. Vickers, C.E.; Bongers, M.; Liu, Q.; Delatte, T.; Bouwmeester, H. Metabolic engineering of volatile isoprenoids in plants and microbes. *Plant, Cell Environ.* **2014**, *37*, 1753–1775. [[CrossRef](#)]
24. Young, A.J. The photoprotective role of carotenoids in higher plants. *Physiol. Plant.* **1991**, *83*, 702–708. [[CrossRef](#)]
25. Rohloff, J. Monoterpene composition of essential oil from peppermint (*Mentha x piperita* L.) with regard to leaf position using solid-phase microextraction and gas chromatography/mass spectrometry analysis. *J. Agric. Food Chem.* **1999**, *47*, 3782–3786. [[CrossRef](#)]
26. Vaughan, M.M.; Wang, Q.; Webster, F.X.; Kiemle, D.; Hong, Y.J.; Tantillo, D.J.; Coates, R.M.; Wray, A.T.; Askew, W.; O'Donnell, C.; et al. Formation of the unusual semivolatile diterpene rhizathalene by the *Arabidopsis* class I terpene synthase TPS08 in the root stele is involved in defense against belowground herbivory. *Plant Cell* **2013**, *25*, 1108–1125. [[CrossRef](#)]
27. Huang, M.; Sanchez-Moreiras, A.M.; Abel, C.; Sohrabi, R.; Lee, S.; Gershenzon, J.; Tholl, D. The major volatile organic compound emitted from *Arabidopsis thaliana* flowers, the sesquiterpene (E)-beta-caryophyllene, is a defense against a bacterial pathogen. *New Phytol.* **2012**, *193*, 997–1008. [[CrossRef](#)]
28. Rai, M.K.; Qureshi, S.; Pandey, A.K. In vitro susceptibility of opportunistic *Fusarium* spp. to essential oils. *Mycoses* **1999**, *42*, 97–101. [[CrossRef](#)]
29. Beale, M.H.; Birkett, M.A.; Bruce, T.J.A.; Chamberlain, K.; Field, L.M.; Huttly, A.K.; Martin, J.L.; Parker, R.; Phillips, A.L.; Pickett, J.A.; et al. Aphid alarm pheromone produced by transgenic plants affects aphid and parasitoid behavior. *Proc. Natl. Acad. Sci. U. S. A.* **2006**, *103*, 10509–10513. [[CrossRef](#)]
30. Aharoni, A.; Giri, A.P.; Deuerlein, S.; Griepink, F.; Kogel, W. De; Verstappen, F.W.A.; Verhoeven, H.A.; Jongsma, M.A.; Schwab, W.; Bouwmeester, H.J. Terpenoid metabolism in wild-type and transgenic *Arabidopsis* plants. *Plant Cell* **2003**, *15*, 2866–2884. [[CrossRef](#)]
31. Davidovich-Rikanati, R.; Sitrit, Y.; Tadmor, Y.; Iijima, Y.; Bilenko, N.; Bar, E.; Carmona, B.; Fallik, E.; Dudai, N.; Simon, J.E.; et al. Enrichment of tomato flavor by diversion of the early plastidial terpenoid pathway. *Nat. Biotechnol.* **2007**, *25*, 899–901. [[CrossRef](#)]

7. References

32. Lewinsohn, E.; Schalechet, F.; Wilkinson, J.; Matsui, K.; Tadmor, Y.; Nam, K.; Amar, O.; Lastochkin, E.; Larkov, O.; Ravid, U.; et al. Enhanced levels of the aroma and flavor compound. *Plant Physiol.* **2001**, *127*, 1256–1265. [[CrossRef](#)]
33. Westfall, P.J.; Gardner, T.S. Industrial fermentation of renewable diesel fuels. *Curr. Opin. Biotechnol.* **2011**, *22*, 344–350. [[CrossRef](#)]
34. Cosmetics industry worldwide. Available online: <https://www.statista.com/study/38765/cosmetics-industry-worldwide-statista-dossier/> (accessed on August 20, 2019). [[CrossRef](#)]
35. Barbieri, C.; Borsotto, P. Essential oils: Market and legislation. In *Potential of Essential Oils*; El-Shemy, H., Ed.; IntechOpen: London, United Kingdom, **2018**; pp. 107–127. [[CrossRef](#)]
36. Grand View Research. *Essential oils market size, share & trends analysis report by application*; Grand View Research, San Francisco, USA, **2019**. [[CrossRef](#)]
37. Sarkic, A.; Stappen, I. Essential oils and their single compounds in cosmetics—A critical review. *Cosmetics* **2018**, *5*, 11. [[CrossRef](#)]
38. Vankar, P.S. Essential oils and fragrances from natural sources. *Resonance* **2004**, *9*, 30–41. [[CrossRef](#)]
39. Gnansounou, E.; Alves, C.M.; Raman, J.K. Multiple applications of vetiver grass – a review. *Int. J. Environ. Sci.* **2017**, *2*, 125–141. [[CrossRef](#)]
40. Sanganerria, P. *Essential oils market report, Summer 2018*; Report Summer 2018; Ultra International B.V: Spijkenisse, The Netherlands, **2018**; pp. 36–39. [[CrossRef](#)]
41. Vetiver oil market expected to reach \$169.5 million by 2022. Available online: <https://www.grandviewresearch.com/press-release/global-vetiver-oil-market> (accessed on Apr 22, 2019). [[CrossRef](#)]
42. Belhassen, E.; Filippi, J.J.; Brévard, H.; Joulain, D.; Baldovini, N. Volatile constituents of vetiver: A review. *Flavour Fragr. J.* **2015**, *30*, 26–82. [[CrossRef](#)]
43. Maffei, M. Introduction to the genus *Vetiveria*. In *Vetiveria: The Genus Vetiveria*; Maffei, M., Ed.; Taylor & Francis: London, United Kingdom, **2002**; pp. 3–21. [[CrossRef](#)]
44. Talansier, E.; Braga, M.E.M.; Rosa, P.T.V.; Paolucci-Jeanjean, D.; Meireles, M.A.A. Supercritical fluid extraction of vetiver roots: A study of SFE kinetics. *J. Supercrit. Fluids* **2008**, *47*, 200–208. [[CrossRef](#)]
45. Sanganerria, P. *Essential oils market report, Spring 2019*; Report Spring 2019; Ultra International B.V: Spijkenisse, The Netherlands, **2019**; pp. 1–39. [[CrossRef](#)]
46. Surburg, H.; Panten, J. *Common fragrance and flavor materials*; 5th ed.; Wiley-VCH Verlag GmbH & Co: Weinheim, **2006**; pp. 236-237. [[CrossRef](#)]
47. Belhassen, E.; Baldovini, N.; Brevard, H.; Meierhenrich, U.J.; Filippi, J.J. Unravelling the scent of vetiver: Identification of character-impact compounds. *Chem. Biodivers.* **2014**, *11*, 1821–1842. [[CrossRef](#)]
48. Mallavarapu, G.R.; Syamasundar, K. V.; Rameshc, S.; Rajeswara Rao, B.R. Constituents of South Indian vetiver oils. *Nat. Prod. Commun.* **2012**, *7*, 223–225. [[CrossRef](#)]
49. Schalk, M.; Deguerry, F. Cytochrome P450 and use thereof for the enzymatic oxidation of terpenes. **2015**, 1–33. [[CrossRef](#)]

7. References

50. Coates, R.M.; Sowerby, R.L. Stereoselective total synthesis of (+)-zizaene. *J. Am. Chem. Soc.* **1972**, *94*, 5386–5396. [[CrossRef](#)]
51. Piers, E.; Banville, J.; Kun Lau, C.; Nagakura, I. Five-membered ring annulation via thermal rearrangement of β -cyclopropyl α,β -unsaturated ketones. A formal total synthesis of the sesquiterpenoid (\pm)-zizaene. *Environ. Sci.* **1999**, *12*, 51–69. [[CrossRef](#)]
52. Chandra Pati, L.; Roy, A.; Mukherjee, D. A stereocontrolled total synthesis of (\pm)-zizaene. *Tetrahedron* **2002**, *58*, 1773–1778. [[CrossRef](#)]
53. Schalk, M.; Deguerry, F. Method for producing (+)-zizaene 2014, 1–20. [[CrossRef](#)]
54. Hartwig, S.; Frister, T.; Alemdar, S.; Li, Z.; Scheper, T.; Beutel, S. SUMO-fusion, purification, and characterization of a (+)-zizaene synthase from *Chrysopogon zizanioides*. *Biochem. Biophys. Res. Commun.* **2015**, *458*, 883–889. [[CrossRef](#)]
55. Peralta-Yahya, P.P.; Ouellet, M.; Chan, R.; Mukhopadhyay, A.; Keasling, J.D.; Lee, T.S. Identification and microbial production of a terpene-based advanced biofuel. *Nat. Commun.* **2011**, *2*, 483–488. [[CrossRef](#)]
56. Wu, W.; Liu, F.; Davis, R.W. Engineering *Escherichia coli* for the production of terpene mixture enriched in caryophyllene and caryophyllene alcohol as potential aviation fuel compounds. *Metab. Eng. Commun.* **2018**, *6*, 13–21. [[CrossRef](#)]
57. Meadows, C.W.; Kang, A.; Lee, T.S. Metabolic engineering for advanced biofuels production and recent advances toward commercialization. *Biotechnol. J.* **2018**, *13*, 1–14. [[CrossRef](#)]
58. Pyne, M.E.; Narcross, L.; Martin, V.J.J. Engineering plant secondary metabolism in microbial systems. *Plant Physiol.* **2019**, *179*, 844–861. [[CrossRef](#)]
59. Vincent JJ Martin; Douglas J Pitera; Sydnor T Withers; Jack D Newman; Jay D Keasling Engineering a mevalonate pathway in *Escherichia coli* for production of terpenoids. *Nat. Biotechnol.* **2003**, *21*, 796–802. [[CrossRef](#)]
60. Cao, Y.; Zhang, R.; Liu, W.; Zhao, G.; Niu, W.; Guo, J.; Xian, M.; Liu, H. Manipulation of the precursor supply for high-level production of longifolene by metabolically engineered *Escherichia coli*. *Sci. Rep.* **2019**, *9*, 1–10. [[CrossRef](#)]
61. Nybo, S.E.; Saunder, J.; McCormick, S. Metabolic engineering of *Escherichia coli* for production of valerenadiene. *J. Biotechnol.* **2017**, *262*, 60–66. [[CrossRef](#)]
62. Degenhardt, J.; Köllner, T.G.; Gershenzon, J. Monoterpene and sesquiterpene synthases and the origin of terpene skeletal diversity in plants. *Phytochemistry* **2009**, *70*, 1621–1637. [[CrossRef](#)]
63. Schewe, H.; Mirata, M.A.; Schrader, J. Bioprocess engineering for microbial synthesis and conversion of isoprenoids. In *Biotechnology of Isoprenoids. Advances in Biochemical Engineering/Biotechnology*; Schrader, J., Bohlmann, J., Eds.; Springer: Cham, **2015**; pp. 251–286. [[CrossRef](#)]
64. Sikkema, J.; Bont, J.; Poolman, B. Interactions of cyclic hydrocarbons with biological membranes. *J. Biol. Chem.* **1994**, *269*, 8022–8028. [[CrossRef](#)]
65. Schügerl, K.; Hubbuch, J. Integrated bioprocesses. *Curr. Opin. Microbiol.* **2005**, *8*, 294–300. [[CrossRef](#)]

7. References

66. Bruce, L.J.; Daugulis, A.J. Solvent selection strategies for extractive biocatalysis. *Biotechnol. Prog.* **1991**, *7*, 116–124. [[CrossRef](#)]
67. Dafoe, J.T.; Daugulis, A.J. In situ product removal in fermentation systems: Improved process performance and rational extractant selection. *Biotechnol. Lett.* **2014**, *36*, 443–460. [[CrossRef](#)]
68. Buque-Taboada, E.M.; Straathof, A.J.J.; Heijnen, J.J.; Van Der Wielen, L.A.M. In situ product recovery (ISPR) by crystallization: Basic principles, design, and potential applications in whole-cell biocatalysis. *Appl. Microbiol. Biotechnol.* **2006**, *71*, 1–12. [[CrossRef](#)]
69. Freeman, A.; Woodley, J.M.; Lilly, M.D. In situ product removal as a tool for bioprocessing. *Nat. Biotechnol.* **1993**, *11*, 1007–1012. [[CrossRef](#)]
70. Morrish, J.L.E.; Daugulis, A.J. Improved reactor performance and operability in the biotransformation of carveol to carvone using a solid-liquid two-phase partitioning bioreactor. *Biotechnol. Bioeng.* **2008**, *101*, 946–956. [[CrossRef](#)]
71. Bae, J.; Moon, H.; Oh, K.K.; Kim, C.H.; Sil Lee, D.; Kim, S.W.; Hong, S.I. A novel bioreactor with an internal adsorbent for integrated fermentation and recovery of prodigiosin-like pigment produced from *Serratia* sp. KH-95. *Biotechnol. Lett.* **2001**, *23*, 1315–1319. [[CrossRef](#)]
72. Mischko, W.; Hirte, M.; Roehrer, S.; Engelhardt, H.; Mehlmer, N.; Minceva, M.; Brück, T. Modular biomanufacturing for a sustainable production of terpenoid-based insect deterrents. *Green Chem.* **2018**, *20*, 2637–2650. [[CrossRef](#)]
73. Leavell, M.D.; McPhee, D.J.; Paddon, C.J. Developing fermentative terpenoid production for commercial usage. *Curr. Opin. Biotechnol.* **2016**, *37*, 114–119. [[CrossRef](#)]
74. Paddon, C.J.; Westfall, P.J.; Pitera, D.J.; Benjamin, K.; Fisher, K.; McPhee, D.; Leavell, M.D.; Tai, A.; Main, A.; Eng, D.; et al. High-level semi-synthetic production of the potent antimalarial artemisinin. *Nature* **2013**, *496*, 528–532. [[CrossRef](#)]
75. Tan, J.S.; Ling, T.C.; Mustafa, S.; Tam, Y.J.; Ramanan, R.N.; Ariff, A.B. An integrated bioreactor-expanded bed adsorption system for the removal of acetate to enhance the production of alpha-interferon-2b by *Escherichia coli*. *Process Biochem.* **2013**, *48*, 551–558. [[CrossRef](#)]
76. Chakrabarty, D.; Chauhan, P.S.; Chauhan, A.S.; Indoliya, Y.; Lavania, U.C.; Nautiyal, C.S. De novo assembly and characterization of root transcriptome in two distinct morphotypes of vetiver, *Chrysopogon zizanioides* (L.) Roberty. *Sci. Rep.* **2015**, *5*, 1–13. [[CrossRef](#)]
77. Das, P.; Sarkar, D.; Datta, R. Proteomic profiling of vetiver grass (*Chrysopogon zizanioides*) under 2,4,6-trinitrotoluene (TNT) stress. *GeoHealth* **2017**, *1*, 66–74. [[CrossRef](#)]
78. Henke, N.A.; Wichmann, J.; Baier, T.; Frohwitter, J.; Lauersen, K.J.; Risse, J.M.; Peters-Wendisch, P.; Kruse, O.; Wendisch, V.F. Patchoulol production with metabolically engineered *Corynebacterium glutamicum*. *Genes*. **2018**, *9*, 1–15. [[CrossRef](#)]
79. Alonso-Gutierrez, J.; Chan, R.; Batt, T.S.; Adams, P.D.; Keasling, J.D.; Petzold, C.J.; Lee, T.S.; Adams, P.D. Metabolic engineering of *Escherichia coli* for limonene and perillyl alcohol production. *Metab. Eng.* **2013**, *19*, 33–41. [[CrossRef](#)]

Appendix

I. Publications and academic activities

Articles:

- **Aguilar, F.** (90%); Hartwig, S. (5%); Scheper, T.; Beutel, S (5%). Catalytical specificity, reaction mechanisms, and conformational changes during catalysis of the recombinant SUMO (+)-zizaene synthase from *Chrysopogon zizanioides*. ACS Omega 2019, 4, 6199–6209. DOI:10.1021/acsomega.9b00242
- **Aguilar, F.** (95%); Scheper, T.; Beutel, S (5%). Modulating the precursor and terpene synthase supply for the whole-cell biocatalytic production of the sesquiterpene (+)-zizaene in a pathway engineered *E. coli*. Genes 2019, 10, 478. DOI:10.3390/genes10060478
- **Aguilar, F.** (95%); Scheper, T.; Beutel, S (5%). Improved Production and In Situ Recovery of Sesquiterpene (+)-Zizaene from Metabolically-Engineered *E. coli*. Molecules 2019, 24, 3356. DOI: 10.3390/molecules24183356

Conferences:

- **Aguilar, F.**; Hartwig, S.; Scheper, T.; Beutel, S. Characterization of the recombinant SUMO-fusion zizaene synthase from *Chrysopogon zizanioides*, a novel terpene cyclase for the production of a variety of monoterpenes and sesquiterpenes. Bioflavour 2018 - Biotechnology of Flavours, Fragrances and Functional Ingredients, Frankfurt am Main, 2018.

Research proposals:

- Biotechnological production of terpenes originating from endemic plant species of Costa Rica for the control of *Fusarium oxysporum* f. sp. *Cubense*, the causal agent of the Panama disease in banana (*Musa* sp.) plantations. Call: Joint Networking and Research Projects, BMBF–MICITT, 2017.

Posters:

- **Aguilar, F.** Hartwig, S., Alemdar, S., Frister, T., Scheper, T., Beutel, S. Scale-up of the production and purification of the novel recombinant zizaene synthase for the biotransformation of the khusimol precursor (+)-zizaene. 8th International Congress on Biocatalysis, Hamburg-Harburg 2016. [[CrossRef](#)]
- **Aguilar, F.** Scheper, T., Beutel, S. Product specificity and reaction mechanisms of the recombinant SUMO (+)-zizaene synthase from *Chrysopogon zizanioides* with substrate analogues. 9th International Congress on Biocatalysis, Hamburg-Harburg 2018. [[CrossRef](#)]

Supervised research thesis

- **Kai Pandera:** Untersuchung zum Produktionsverhalten einer rekombinanten Zizaensynthase. Bachelor thesis for Life Sciences, LUH, December 2016. Results in section 4.1.
- **Daniela Santamaría-Muñoz:** Evaluación de la producción de citocromo P450 de *Chrysopogon zizanioides* (L.) Nash. en *Escherichia coli* para la posterior obtención de khusimol. Bachelor thesis for Biotechnology Engineering, Institute of Technology of Costa Rica, December 2017. Results not included in this dissertation.
- **Lukas Koch:** Optimierung der Produktion von Patchoulol und (+)-Zizaene in *Escherichia coli*. Bachelor thesis for Bioverfahrenstechnik, Hochschule Aalen, February 2019. Results in section 4.2, 4.3.

II. Curriculum Vitae

Personal details

Name	Francisco José Aguilar Cascante
Place of birth	San José, Costa Rica
Nationality	Costarrican
E-mail	aguilar.fran@gmail.com

Working experience

2014–2015	Scientific Group Leader , Bioprocess Unit, National Center for Biotechnological Innovations of Costa Rica - CENIBiot
2009–2013	Bioprocess Specialist , Plant Biotechnology Unit, National Center for Biotechnological Innovations of Costa Rica - CENIBiot
2005–2006	Production Leader , Industrial micropropagation facility at Microplantas S.A., Costa Rica
2001–2005	R&D Leader , Industrial micropropagation facility at Microplantas S.A., Costa Rica

Education

2015–2019	Doctor in Natural Sciences , Institute of Technical Chemistry, Leibniz University of Hannover
2009–2012	Master in Industrial Engineering , Major in Manufacture and Control Quality, University of Costa Rica
2006–2008	Master in Sciences in International Horticulture , Major in Plant Biotechnology, Leibniz University of Hannover
1997–2001	Bachelor in Biotechnology , Institute of Technology of Costa Rica